Development of Optical Tools to Control Biological Processes

by

Trevor Horst

B.A. Chemistry, College of Wooster, 2016

Submitted to the Graduate Faculty of the

Dietrich School of Arts and Sciences in partial fulfillment

of the requirements for the degree of

Master of Science

University of Pittsburgh

2019

UNIVERSITY OF PITTSBURGH

Dietrich School of Arts and Sciences

This thesis was presented

by

Trevor Horst

It was defended on

March 26, 2019

and approved by

Dr. Paul Floreancig, Professor, Department of Chemistry

Dr. Kabirul Islam, Assistant Professor, Department of Chemistry

Committee Chair: Dr. Alexander Deiters, Professor, Department of Chemistry

Development of Optical Tools to Control Biological Processes

Trevor Horst, M.S.

University of Pittsburgh, 2019

Optical control of protein function has garnered considerable interest in chemical biology. The use of light to modulate protein function allows for higher spatial and temporal control than small molecule control. Rapamycin is a natural product that can be used to induce the dimerization of FKBP and FRB proteins and has been used as a small molecule to control a wide range of dimerization-based protein functions. We synthesized several light sensitive analogs of rapamycin to allow for optical control of protein dimerization. A visible light-activated rapamycin analog was synthesized and its ability to effectively photocage rapamycin *in vivo* was demonstrated. A light-deactivated rapamycin analog was synthesized through the conjugation of a reactive oxygen species generating chromophore to rapamycin in an adaption of chromophore-assisted light inactivation of proteins. The ability of this conjugate to reverse protein dimerization was demonstrated *in vivo* as well. Several analogs of rapamycin conjugated to arylazopyrazole and spiropyran photoswitches were synthesized and the difference in dimerization activity of the two states was determined. Optical control of protein function was also explored through the incorporation of photoswitching amino acids through unnatural amino acid mutagenesis. Two novel photoswitching amino acids containing arylazopyrazole and phenazopyridine photoswitches were synthesized, and incorporation in proteins was demonstrated.

Optically active materials have been a focus of researchers developing robotics, information storage methods, and light-activated drug delivery. Commonly, azobenzene is used in these materials. We synthesized an arylazopyrazole-containing monomer capable of being incorporated into a polymer. Analysis of that polymer showed an unexpectedly lesser macroscopic response to irradiation than an azobenzene containing material.

Table of Contents

List of Tables

List of Figures

List of Schemes

List of Abbreviations

9-AJ – 9-azajulolidine

ACN – acetonitrile

AcOH – acetic acid

ANBP – aminonitrobiphenyl

BIST – bisstyrylthiophene

BnOH – benzyl alcohol

Boc – butoxycarbonyl

BODIPY – boron dipyrromethene

CALI – Chromophore- Assisted Light Inactivation

CID – Chemical Inducer of Dimerization

DABCO – 1,4-diazabicyclo[2.2.2]octane

DCM – dichloromethane

DDQ – 2,3-dichloro-5,6-dicyano-1,4-benzoquinone

DIPEA – diisopropylethylamine

DMAP – 4-dimethylaminopyridine

DMF – dimethylformamide

DMSO – dimethyl sulfoxide

DSC – disuccinimidyl carbonate

EDC – 1-ethyl-3-(3-dimethylaminopropyl)carbodiimide

EtOH – ethanol

Fmoc – fluorenylmethoxycarbonyl

HOBT – hydroxybenzotriazole

ISC – intersystem crossing

MeOH – methanol

mCPBA – 3-chloroperoxybenzoic acid

mRNA – messenger RNA

NCS – *N*-chlorosuccinimide

NIS – *N*-iodosuccinimide

ONB – *ortho*-nitrobenzyl

PylRS – pyrrolysine tRNA synthetase

ROS – reactive oxygen species

TBAB – tetrabutylammonium bromide

TBACl – tetrabutylammonium chloride

TBAF – tetrabutylammonium fluoride

TBSCl – *tert*-butyldimethylsilyl chloride

THF – tetrahydrofuran

TFA – trifluoroacetic acid

TPGS-750-M – DL-α-Tocopherol methoxypolyethylene glycol succinate solution

tRNA – transfer RNA

TsCl – tosyl chloride

UAA – unnatural amino acid

TBTA – Tris[(1-benzyl-1H-1,2,3-triazol-4yl)methyl]amine

t-BuOH – *tert*-butanol

TEA – triethylamine

1.0 Optical Control of Rapamycin Dimerization

1.1 Introduction

1.1.1 Introduction to Chemical Inducers of Dimerization

Chemical inducers of dimerization (CID) are small molecules that are able to bind two proteins simultaneously to form a ternary complex with the two proteins in close proximity. This provides a useful way for researchers to conditionally control protein activity, dependent upon addition of the CID. The proximities of proteins to one another play a role in many cellular processes, thus, artificially being able to control proximity allows researchers to probe the role of these interactions. Depending on the CID used, the dimerization can either form a homo or heterodimer. CIDs have been used to control cellular processes such as transcription[1], protein localization[2,3], protein degradation[4–6], cell death[7], and signaling processes[8,9].

1.1.2 Rapamycin as a Dimerizer

Rapamycin is a macrolide natural product that was first reported in 1975 by Suren Sehgal while working for Ayerst Laboratories.[10] The bacteria (*Streptomyces hygroscopicus*) from which rapamycin was isolated was found on the island of Rapa Nui (Easter Island). It was discovered to have antibacterial, antifungal, and immunosuppressive properties. The function of rapamycin in *S. hygroscopicus* has not been elucidated, though the complexity and high regulation of its biosynthesis indicate an important role.[11] The biosynthesis gene cluster of rapamycin contains 5 known regulatory genes, the biosynthesis itself incorporates several metabolites including shikimate derivatives and pipecolate, and following the cyclization concluding its polyketide synthase formation, more than 5 additional modifications are made to generate the final rapamycin product.[12,13]

Rapamycin was approved by the FDA in 1999 for use in organ transplantation procedures to help prevent organ rejection. Analogs of rapamycin have since been approved and its medicinal use has been expanded to aid in the treatment of cancer.[14,15] Research with rapamycin is

ubiquitous at the University of Pittsburgh. The Thomson group focuses on its role in regulating immune response[16,17] while the Monga and Oertel groups have collaborated to investigate its use in treating hepatic cancers.[18] Rapamycin has demonstrated inhibition of cell growth in a variety of eukaryotes through its ability to inhibit the kinase activity of a highly conserved class of proteins known as the TOR proteins.[19] Rapamycin's mechanism of action in human cells is driven by its strong association with both mTOR (mammalian target of rapamycin) and FKBP12 (FK506 binding protein).

Rapamycin's FKBP12 binding partner belongs to the FKBP family of proteins. These proteins can function as chaperones in protein folding and peptidyl prolyl *cis*/*trans* isomerases, though not all proteins function as both.[20] The mammalian FKBP73 and wheat FKBP52 proteins have been identified as FK506 and rapamycin insensitive chaperones, yet their isomerase activity is sensitive to those compounds. However, FKBP12, rapamycin's binding partner, only acts as an isomerase naturally.

Rapamycin's other binding partner, mTOR, forms two complexes (mTORC1 and mTORc2) that is sensitive to several factors essential to cell survival (**Figure 1.1**).[21] Rapamycin has a pronounced effect on mTORC1. The binding of FKBP-rapamycin to mTORC1 is a potent inhibitor of its kinase activity, slowing cell division. Rapamycin was not initially thought to have an effect on mTORC2 since FKBP-rapamycin does not bind to mTORC2, but studies have shown that prolonged exposure to rapamycin is capable of lowering mTORC2 activation of Akt, an oncogenic protein downstream of mTORC2, in some cell types.[22] Sabatini *et al*. determined that rapamycin achieves this through FKBP-rapamcyin binding free mTOR before it forms mTORC2. As existing mTORC2 is degraded, it is not replenished, leading to a slow decline in Akt activation.
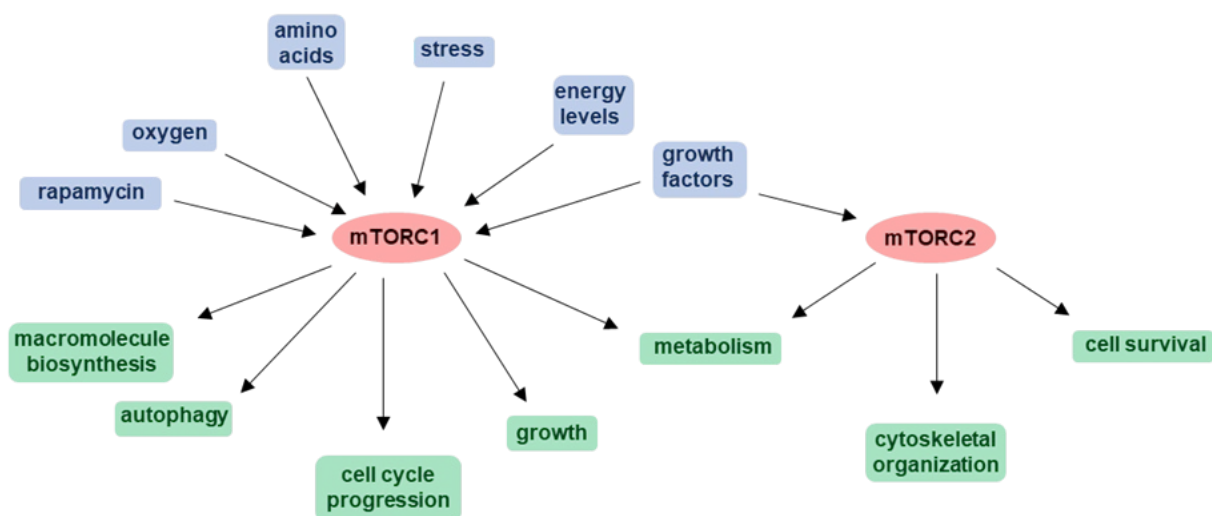
Figure 1.1 - A simplified representation of inputs and outputs of the mTOR complexes 1 and 2.

Schreiber discovered that the 289 kD mTOR binding partner could be reduced to the 11 kD FRB (FK506-Rapamycin Binding) domain while retaining the ability to form a ternary complex with rapamycin and FKBP.[23] This gave rapamycin more utility as a heterodimerizer by minimizing the size of its binding partners to 11 kD (FRB) and 12 kD (FKBP). Proteins of interest could be expressed as fusion proteins with FKBP and FRB and then conditionally dimerized with the addition of rapamycin. Since larger proteins are more likely to alter the function of the protein they are fused to, it is essential to use the significantly smaller FRB rather than mTOR in this context.

The FRB domain, shown in red in **Figure 1.2C**, binds rapamycin throughout the triene region (**Figure 1.2A**). An alpha helix allows for a strong hydrophobic interaction. The FKBP domain shown in blue in **Figure 1.2C** binds an oxygen rich face of rapamycin via a beta sheet and unfolded segments. Wandless *et al*. determined that rapamycin first binds FKBP with a K_d of 0.2 nM, then binds FRB with a K_D of 12 nM (**Figure 1.2B**). The rapamycin-FRB interaction is not nearly as strong as the interaction of FRB with the FKBP-rapamycin dimer. This suggests that interactions between the two proteins are likely stabilizing the ternary complex more than the rapamycin-FRB interface.
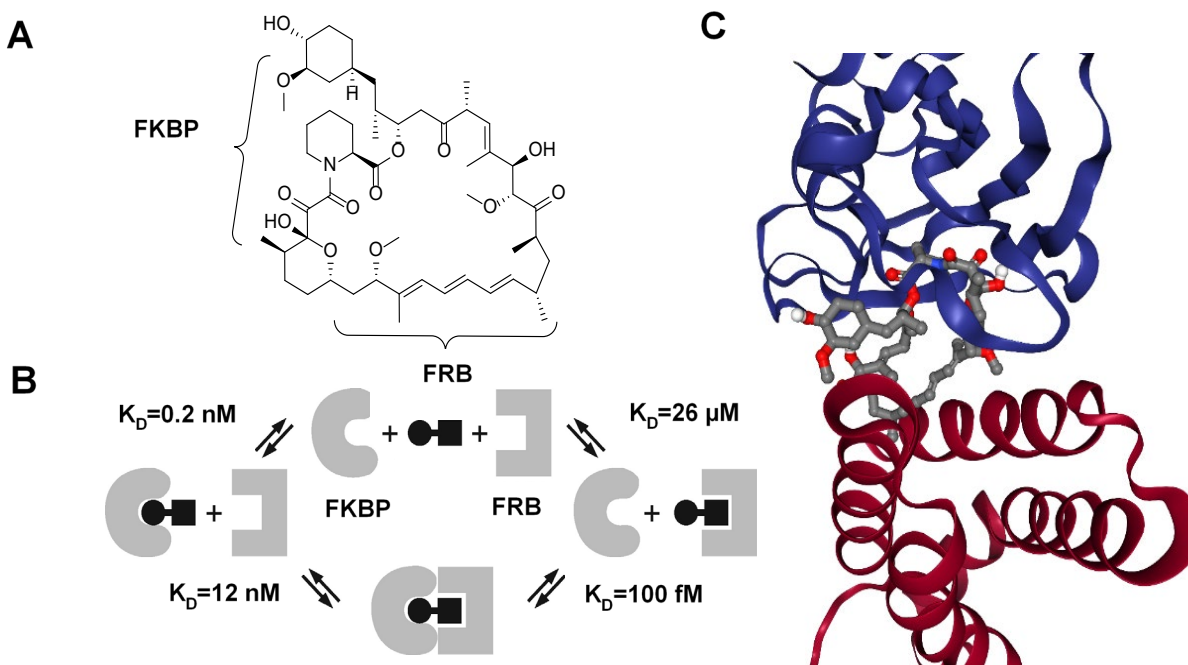
Figure 1.2 - A) Structure of rapamycin with the portions interacting with FKBP and FRB indicated. B) The mechanism of binding and ternary complex formation.[24] Adapted with permission from Banaszynski *et al*. Characterization of the FKBP·Rapamycin·FRB Ternary Complex. Journal of the American Chemical Society 2005, 127 (13), 4715–4721. Copyright 2005 American Chemical Society. C) Crystal structure of rapamycin bound to FKBP and FRB obtained by the Schreiber lab (PDB ID: 1FAP).[25]

The ability of rapamycin to act as a CID has expanded its role in controlling biological processes beyond inhibiting mTOR. A key application that researchers have used rapamycin for is the conditional control of protein localization in cellular compartments. The Gestwicki lab has demonstrated that rapamycin can be used to conditionally localize proteins to the nucleus (**Figure 1.3A**).[26] By expressing both a protein of interest as a fusion with FRB and FKBP with a nuclear localization tag, the addition of rapamycin allows for localization of the otherwise cytosolic FRB-protein of interest fusion to the nucleus. This same principle has been used to induce localization to the cellular[27] and mitochondrial[28] membranes. Conditional control of localization allows researchers to activate protein function simply through small molecule addition. This can allow for control of gene transcription, cell signaling, and other processes.
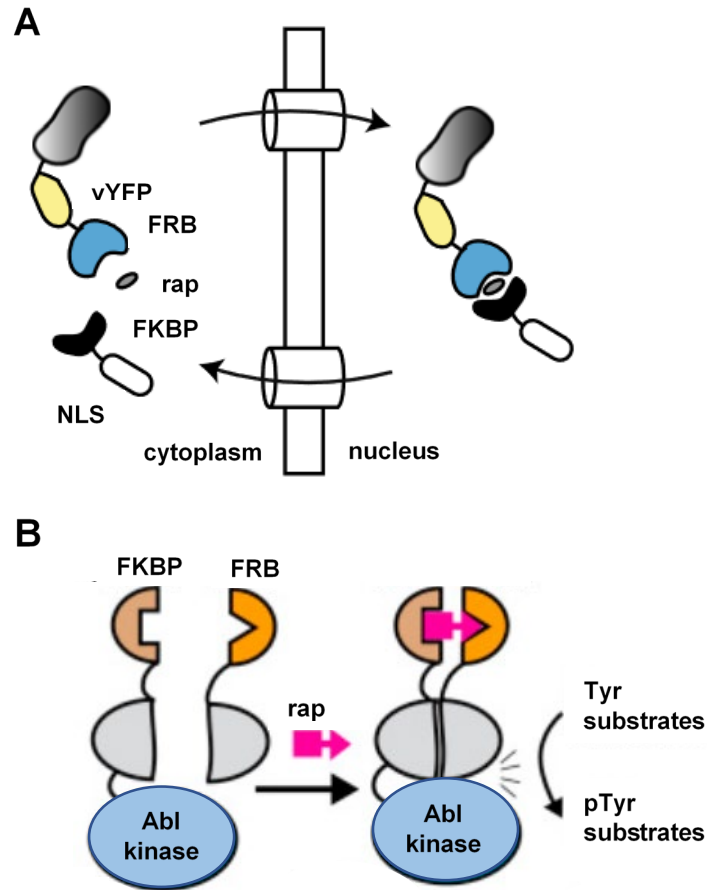
Figure 1.3 - A) Design of a rapamycin-induced nuclear localization system reported by the Gestwicki group.[26] Cytosolic FRB is transported to the nucleus by nuclear localized of FKBP upon additions of rapamycin. Adapted with permission from Patury, *et al*. Conditional Nuclear Import and Export of Yeast Proteins Using a Chemical Inducer of Dimerization. Cell Biochemistry and Biophysics 2009, 53 (3), 127–134. Copyright 2009 Springer Nature. B) Design of a split Abl kinase developed by the Wells group.[29] Addition of rapamycin dimerizes the FRB and FKBP fused portions of Abl kinase to activate the enzyme. Adapted with permission from Diaz *et al*. A Split-Abl Kinase for Direct Activation in Cells. Cell Chemical Biology 2017, 24 (10), 1250-1258.e4. Copyright 2017 Elsevier.

Cell signaling and enzyme activity can also be controlled through the use of split proteins. The Wells group demonstrated that a protein, Abl kinase in this case, could be split into two parts, one as a fusion with FKBP and one as a fusion with FRB. Upon addition of rapamycin, the FKBP-rapamyin-FRB ternary complex formed and the two Abl kinase parts were brought into close proximity, forming an active kinase (**Figure 1.3B**).[29] The split protein system allows for the conditional activation of nearly any protein, given a split version is able to be optimized. The development of split protein systems for horseradish peroxidase,[30] TEV protease,[31] and Cas9[32] suggest a general applicability.

These processes have become essential tools for investigating the roles and targets of proteins, but the use of rapamycin as a dimerizer has limitations. The dimerization induced by rapamycin is not localized. Once rapamycin is added to a culture, its activation will be present throughout all cells as it diffuses. Additionally, there is little temporal control over activation. In the context of developmental biology, this is a significant limitation, since proteins may be active for only a certain period of development.[33]

1.2 Optical Activation of Rapamycin

1.2.1 Optical Activation of CID

To address the problem of limited control of CID, researchers have developed photocaged analogs of CIDs to allow for spatiotemporal control of protein dimerization. These caged CID analogs are capable of being added to cells at any time, but should only become active once irradiated (**Figure 1.4A**). One photocaged CID that has been published is an *ortho*-nitrobenzyl (ONB) caged abscisic acid **1** (**Figure 1.4B**).[34] When added, **1** will not induce dimerization until irradiated with UV light. Though an ester is used to link the abscisic acid and caging group, it does not appear to be sensitive to esterases. Incubation for 24 hours in cells did not show background activation. Once irradiated with 365 nm light, abscisic acid is generated and GID1 and GA1 form a strong interaction with either side of the abscisic acid. A second CID that has been published is a photocaged form is gibberellic acid.[35] Wombacher published an ONB-caged analog as well as the red-shifted caged analog **2**. Though the methyl ester of gibberellic acid is known to be cleaved in cells, **2** demonstrated stability in cells for up to 3 hours, suggesting it is not an optimal substrate for cellular esterases. Wombacher *et al*. also decided to use an aminonitrobiphenyl (ANBP)

caging group rather than ONB. The introduction of the second phenyl group increases the conjugation within the caging group inducing a bathochromic shift of the absorption maximum.[36] The ANBP caging group is discussed in further detail in **1.2.3**. When irradiated with 412 nm light, gibberellic acid is released. Gibberellic acid then binds the protein GID and induces a conformational change that allows for interaction with the protein GAI.
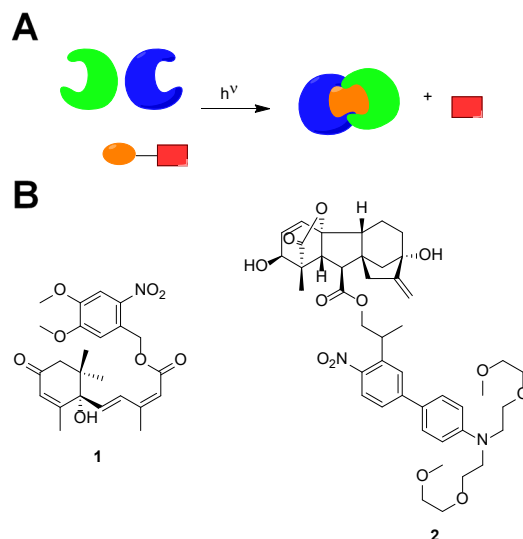
Figure 1.4 - A) Principle of a general photocaged CID. The orange dimerizer is inactive until irradiation releases the red caging group, allowing for ternary complex formation. B) Photocaged analogs of abscisic acid and gibberellic acid reported by the Liang and Wombacher groups, respectively.[34,35]

1.2.2 UV-Activated Caged Rapamycin

The introduction of caged rapamycin analogs has also been used to allow for spatiotemporal control of protein dimerization. However, all the published analogs to date have required the use of UV light to release rapamycin since the caging groups used were ONB alcohol derivatives. The ONB alcohol group is one of the best understood and most commonly used photocages.[37]
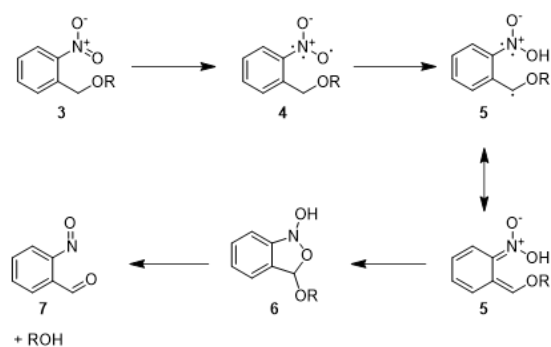
Scheme 1.1 - The decaging mechanism for a generic nitrobenzyl alcohol compound.

Mechanistically, the photolysis of the ONB alcohol **3** begins with the UV mediated homolytic cleavage of the NO double bond of the nitro group to yield **4**. The oxygen radical of **4** then abstracts a proton from the benzylic position to give **5**, which can be shown as two relevant resonance structures. The lower resonance structure of **Scheme 1.1** helps show the nitro oxyanion is able to attack the benzylic position to create the benzoxazole derivative **6**. Finally, the lone pair of **6**'s exocyclic alcohol can form a protonated nitroso group, forcing the endocyclic oxygen to form the aldehyde, which forces the OR group to leave where it will pick up the proton from the nitroso to generate the final ROH and nitrosobenzaldehyde **7**. Many ONB derivatives with extended conjugation that will be discussed later undergo similar decaging mechanisms.
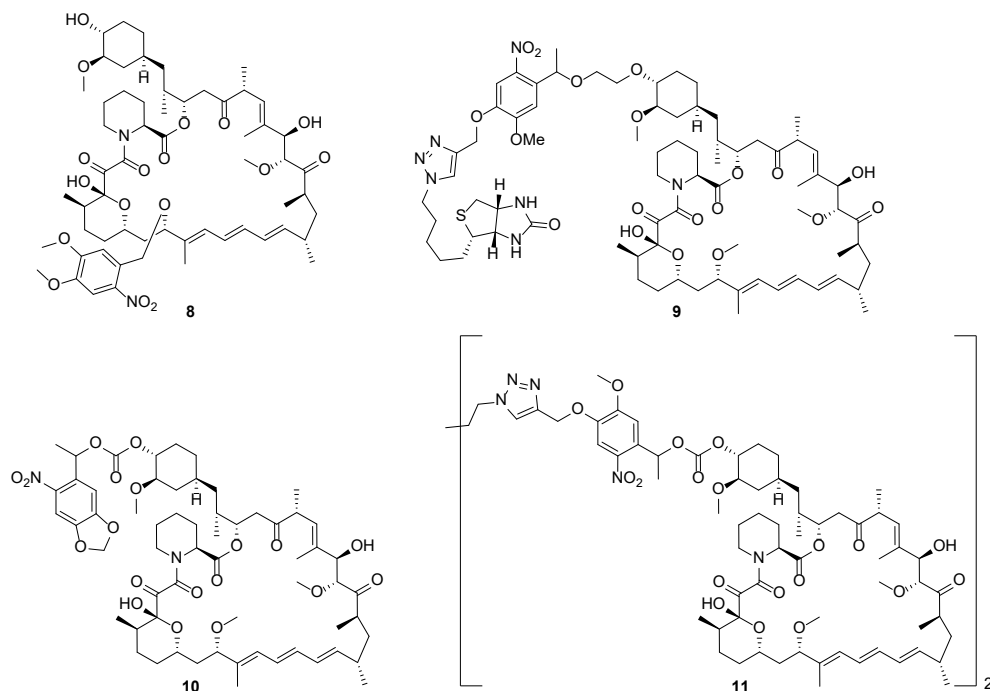
Figure 1.5 - The structures of four published rapamycin analogs with nitrobenzyl caging groups. Compound **8** cages the C_{16} methoxy, compound **9** cages the primary alcohol of everolimus, compound **10** is a nitrobenzyl caging of the C_{40} hydroxyl, and compound **11** is a dimerized version of **10**.

Woolley's lab first demonstrated the potential of caging of rapamycin by introducing an ONB group to the C_{16} position of **8** in April 2010 (**Figure 1.5**).[38] Compound **8** was theorized to be an effective caged rapamycin compound since the C_{16} oxygen being caged is within rapamycin's binding interface with FRB. Though decaging does not release native rapamycin (what is usually the C_{16} methoxy is a hydroxyl upon decaging), this analog retains near native dimerizing capability. The efficacy of the caging was tested in HELA cells by examining the phosphorylation of S6 and S6K, proteins regulated by the mTOR complex.

The caged rapamycin analog **9** was published by the Inoue group in December of 2010.[39] To aid in the synthesis, everolimus (rapamycin with a C_{40} ethyl alcohol) was used. The primary alcohol of everolimus gives greater selectivity for alcohol couplings than native rapamycin's C_{40} secondary alcohol. Inoue *et al*. coupled biotin to everolimus through a photocleavable linker. Incubating the everolimus-biotin conjugate **9** with avidin yielded a conjugate of **9** with avidin that could not enter cells. Upon irradiation, everolimus was released and was able to diffuse into cells, dimerizing FKBP and FRB.

9

Compound **10** was a first generation caged rapamycin published by the Deiters lab in December of 2010.[40] Rapamycin analog **10** was used with a truncated form of FKBP known as iFKBP. The Deiters lab had previously demonstrated that iFKBP could be inserted into the FAK protein to destabilize it due to iFKBP lack of conformational rigidity.[41] Upon binding of rapamycin, iFKBP became more structurally rigid, which in turn allowed for the FAK protein to fold properly and become active. Compound **10** was used in a similar system. It was shown that **10** would not activate the FAK-iFKBP protein until it was irradiated with UV light, indicating that decaging was necessary for activity of the rapamycin analog. The second generation caged rapamycin published by the Deiters lab in 2015, compound **11**, utilized a similar ONB alcohol caging group, but linked two rapamycin moieties together as a dimer.[42] As shown earlier (**Figure 1.2B**), rapamycin binds FKBP with a 0.2 nM K_D, then FRB binds and the ternary complex is formed with a K_D of 12 nM. The higher affinity for FKBP likely leads to both rapamycin moieties of the dimer binding FKBP and FRB being sterically excluded from forming the ternary complex. Upon release of native rapamycin with UV light the FKBP-rapamycin-FRB complex is able to form. This was demonstrated both by the light activation of mTOR inhibition by **11**, as well as a light activation of a split TEV protease.

1.2.3 ANBP Caged Rapamycin

As described above, rapamycin was effectively caged through various methods. However, a drawback of the ONB caging group used in compounds **8**-**11** is that it uses UV light to release native rapamycin. UV light is known to be toxic to cells during long exposures.[43] UV light is also known to alter the expression levels of several proteins.[44] It would be advantageous to use a caging group that can be decaged with a longer wavelength of light to avoid these undesired effects. To achieve this, several caging groups were explored as potential targets.
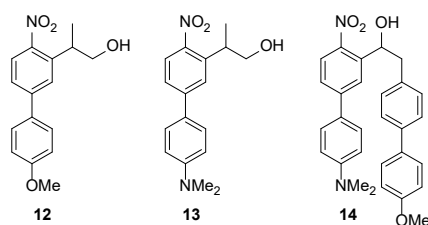
Figure 1.6 - The structures of three ANBP caging groups developed by the Specht group.[36,45,46]

The Specht lab has published three versions of the ANBP chromophore. The first (**12**) was published in 2008 and used a propyl linker that forced a beta-elimination decaging pathway upon irradiation.[36] Though not technically an ANBP caging group because it has a methoxy instead of dimethylamino, it is still in the same class of caging group. This was improved upon in 2012 with the ANBP **13** which has superior photolytic efficiency due to the greater electron donating effect of the dimethylamino group.[36] The third ANBP caging group **14** was published in 2018 and used an ethyl linker.[46] Interestingly, the decaging product of **14** favors the enol over the carbonyl that is normally generated (**Scheme 1.1**), allowing for fluorescent tracking of decaging. The decaging mechanism of the ethyl linked **14** is analogous to that of nitrobenzyl alcohols shown in **Scheme 1.1**. The only difference between ANBP and ONB decaging is that the extended conjugation into the biphenyl forces a bathochromic shift of the initial excitation that induces homolytic cleavage of the NO bond.
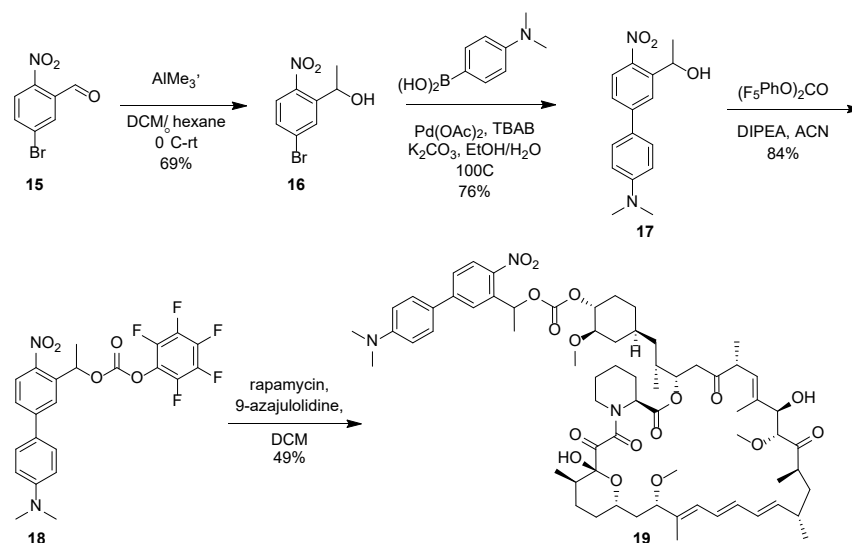
Scheme 1.2 - Synthesis of an ANBP caged rapamycin analog.

The synthesis of the ANBP caged rapamycin **19** is shown in **Scheme 1.2**. The initial formation of the secondary alcohol **16** is achieved through methylation of the commercially available nitrobenzaldehyde **15** by trimethylaluminum.[47] The subsequent Suzuki coupling with 4-

(dimethylamino)phenylboronic acid run in a microwave reactor for 15 minutes at constant temperature with air flow cooling to allow for higher microwave power forms the biphenyl core of the caging group with **17**.[36] Activation of the alcohol **17** was achieved with bis-(pentafluorophenyl) carbonate, and the resultant pentafluorophenyl carbonate **18** was reacted with rapamycin in the presence of 9-azajulolidine (9-AJ) to give the ANBP caged rapamycin **19**.

A small comparative study was performed in the synthesis of **19**. Pentafluorophenyl carbonates had not previously been reported as potential coupling partners for the rapamycin C40 hydroxyl group, but they have been used with success in other carbonate formations.[48] Additionally, 9-AJ has been shown to give higher yields than DMAP when acylating bulky alcohols.[49] We believed the superior acylation catalysis would translate to an increased yield in the similar mechanism of the rapamycin conjugation to activated carbonates. When synthesizing **19**, the 9-AJ/pentafluorophenylcarbonate combination gave 10-15% higher yields than the analogous DMAP/NHS carbonate pairing based on conditions described in Yan Zou's thesis. The 9-AJ/pentafluorophenyl carbonate system has proven more effective in many, but not all other cases tested.
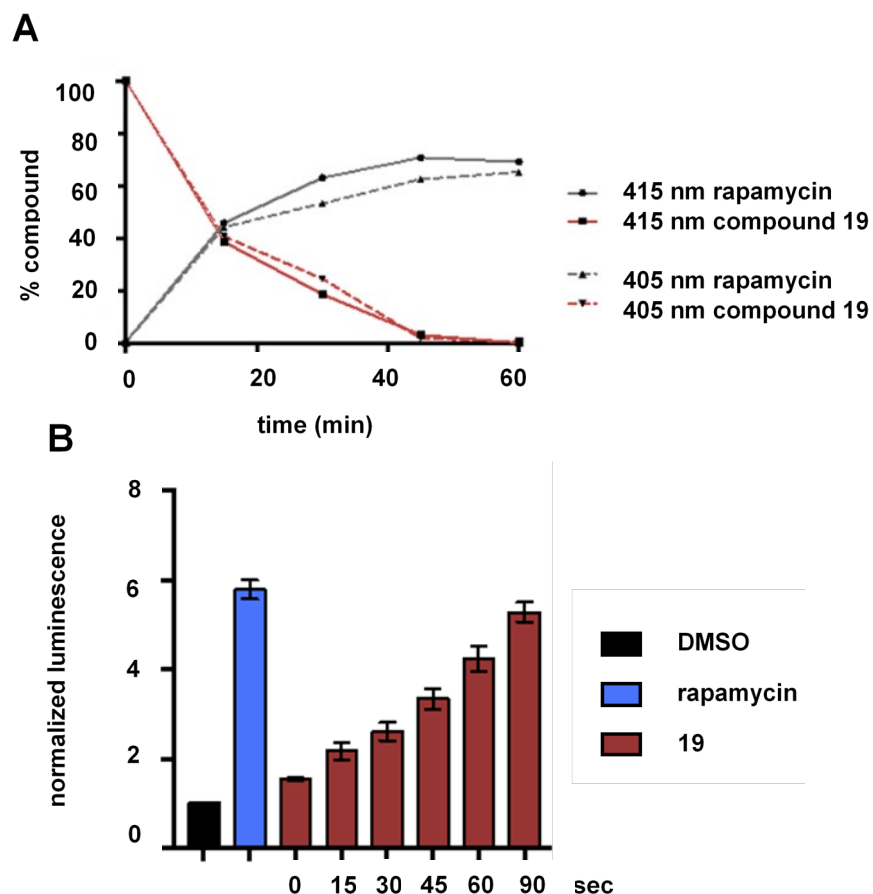
Figure 1.7 - Experiments performed by Taylor Courtney. A) HPLC analysis of **19** decaging with 405 and 415 nm light. B) Split luciferase assay in HEK293T cells demonstrating formation of rapamycin from **19** upon irradiation with 415 nm light.

The ANBP group has a max absorbance of 410 nm.[46] We did not have a 410 nm LED to perform irradiations, so Taylor Courtney compared the effectiveness of both a 405 and 415 nm LED by irradiating with 250 W/cm^2 light and tracking formation of rapamycin by HPLC (**Figure 1.7A**). By following the loss of **19** and formation of rapamycin, it was shown that 415 nm light is marginally better, so it was used by Taylor in further cellular experiments. One representative experiment performed by Taylor was a split luciferase assay (**Figure 1.7**).[50] As mentioned in **1.1.2**, it has been reported that enzymes can be split into two parts, with each part expressed as a fusion protein with either FKBP or FRB. Upon addition of rapamycin, the two luciferase parts are brought into close proximity and form an active enzyme. The luminescence generated from processing of luciferin upon addition of rapamycin or **19** was assayed. Compound **19** showed good response to irradiation with a 415 nm LED at an intensity of 250 mW/cm^2. At 90 seconds irradiation, nearly full

decaging of **19** was observed, as indicated by luciferase activity comparable to that of rapamycin, while a dose-response curve was also visible with varying irradiation times.

Though the ANBP caged rapamycin analog **19** demonstrated less than 2-fold activation over DMSO control in the absence of light exposure, a dimer would still have the potential to exhibit even lower background. The planned synthesis of an ANBP caged rapamycin dimer **25** is shown in **Scheme 1.3**. The synthesis began with the Suzuki coupling of the aryl bromide **15** and 4-(dimethylamino)phenylboronic acid.[46] A Barbier propargylation of **20** was then performed.[51] In the synthesis of **19**, the aldehyde was alkylated first followed by a Suzuki reaction. The reaction sequence is inverted here because attempting the Suzuki reaction in the presence of an alkyne led to a substantial loss in yield, likely due to a Zn-catalyzed Negishi reaction taking place.[52] In addition to a Negishi reaction occurring, there is the potential that the aryl bromide may have been activated by Zn to help facilitate a Barbier type reaction with the aldehyde in competition with the propargyl bromide. This is unlikely due to the superior activity of alkyl halides in Barbier reactions, but there is evidence of aryl halides undergoing Barbier reactions with aldehydes in the presence of a Rh catalyst.[53]

With the propargylated ANBP **21** successfully generated, the alcohol was activated as the pentafluorophenylcarbonate **22** and coupled to rapamycin with 9-AJ to give the alkyne-modified ANBP-rapamycin analog **23** in 40% yield. Taylor Courtney provided previously synthesized 1,4-diazidobutane to be used in the click reaction coupling two equivalences of **21**. Following conditions used by Yan Zou in her synthesis of the ONB caged rapamycin dimer **11**, a mixture of several compounds resulted from the reaction, none of which were the ANBP dimer **24**. NMR spectra of the 4 collected compounds revealed starting material as well as three unidentified products, none of which exhibited the expected triazole protons suggesting the reactants degraded rather than participate in the click reaction. An additional complication could be the presence of multiple stereoisomers. The Barbier reaction forming **21** generates a racemic product, so coupling to rapamycin generates two diastereomers. The click reaction, forming a dimer, would therefore generate three diastereomers. Alternative conditions could be tried. In past experiments, a mixture of CuI, DCM, and DIPEA was successful in rapamycin-based click reactions based on reported anhydrous conditions.[54]
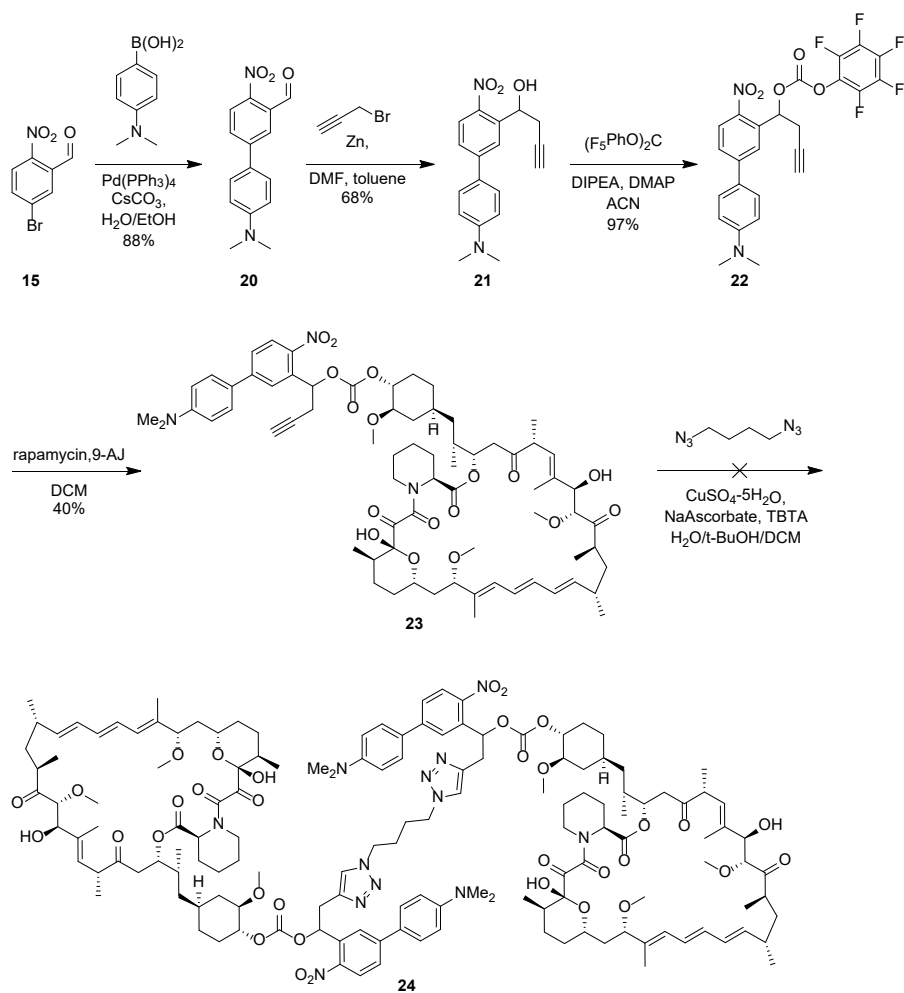
Scheme 1.3 - Attempted synthesis of the ANBP-caged rapamycin dimer **24**.

1.2.4 BIST Caged Rapamycin

The bisstyrylthiophene (BIST) caging group was published initially by the Ellis-Davies group in 2016.[55] The Ellis-Davies group developed BIST as a new long wavelength caging group and demonstrated its utility in caging Ca^{2+} ions. The BIST group absorbs blue light very effectively with an extinction coefficient of 66,000 M^{-1} cm^{-1} at 440 nm, comparable to fluorescein's extinction coefficient of approximately 77,000 M^{-1} cm^{-1}. The BIST group decages at a wavelength further red shifted than ANBP and can be activated via two-photon irradiation, a technique using light approximately twice the wavelength of the absorbance otherwise used to decage. Upon absorbance of two photons, the caging group is at the excited state required for decaging. This gives greater spatial control since the intensity of the irradiation must be very high.

The initial attempt at a BIST-caged rapamycin analog is shown in **Scheme 1.4**. Taylor Courtney had made a di-NHS carbonate BIST compound previously, but was unable to couple two rapamycin molecules to it. We speculated that click chemistry could be used to more effectively synthesize the BIST rapamycin dimer. Rapamycin carbonate formations are generally low yielding (30-50%),[40,42,56] so a reaction coupling two rapamycin molecules was likely to be low yielding. Two rapamycin dimers had been synthesized previously through click chemistry in good yield, both in Yan Zou's thesis and the published rapamycin dimer **11**. Though the target rapamycin dimer **31** in **Scheme 1.4** would not produce rapamycin upon photolysis, we thought there was the possibility it could still be active. The rapamycin analog everolimus has an ethyl alcohol in the same position that is well tolerated.[39] However, since the triazole and carbonate are not precedented modifications for rapamycin analogs demonstrating similar activity to rapamycin, the photolysis product **29** was also synthesized to investigate the expected activity of **31** upon irradiation.
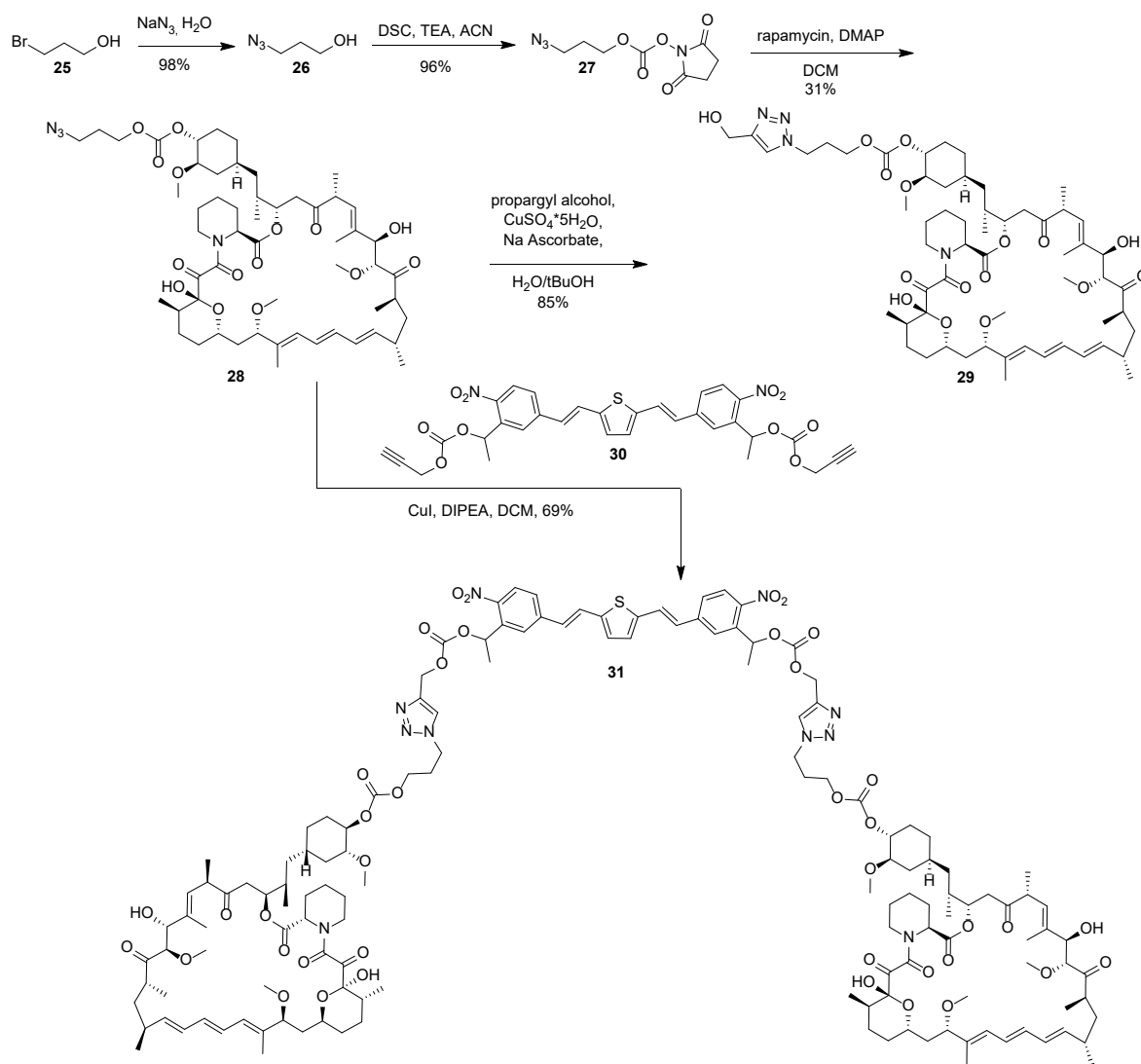
Scheme 1.4 - The synthesis of a BIST caged rapamycin dimer **31** and its photolysis product **29**.

The syntheses of **29** and **31** began with an azide substitution onto **25** to form the azidopropanol **26** via an S_N2 reaction in 98% yield.[57] This was followed by the generation of the NHS carbonate **27** in 96% yield. The subsequent coupling with DMAP to generate azido-modified rapamycin **27** proceeded in 31% yield, but this is common for NHS carbonate couplings with rapamycin. The 9-AJ/pentafluorophenyl carbonate conditions would likely work well with this reaction, but had not yet been tested at the time. A subsequent click reaction allowed formation of the triazole containing photolysis product **29** in 85% yield. Initial attempts at synthesis using a copper iodide/DIPEA/DCM mixture resulted in a pale yellow aggregate. Based on literature reports, this was likely a copper-alkyne aggregate forming that irreversibly stops the click reaction.[58] Switching to a more polar solvent system was a suggested method to limit this aggregation, so the reaction was attempted with the more polar *tert*-butanol/water solvent system with 10-fold excess of propargyl alcohol to yield **29**. Taylor had previously synthesized the BIST alkyne **30** used in the synthesis of the rapamycin dimer. Due to poor solubility of **30** in *tert*-butanol/water, a solution using copper iodide in DCM with DIPEA was used to synthesize **31** in 69% yield.[54]
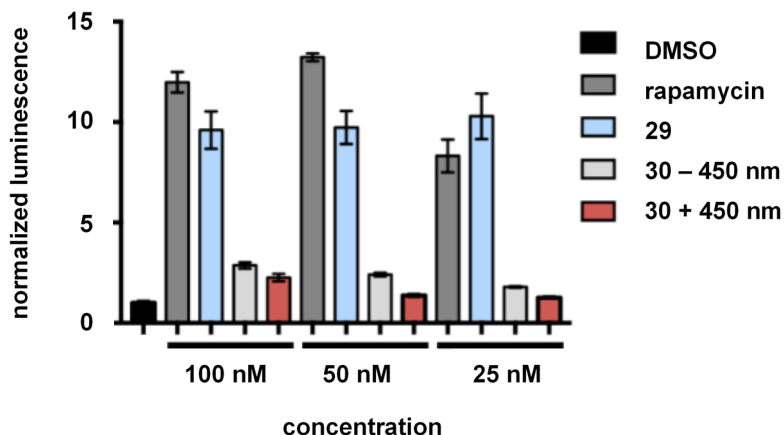
Figure 1.8 - Experiment performed by Taylor Courtney. Split luciferase assay in HEK293T cells with rapamycin, the caged rapamycin dimer **31**, and its photolysis product **29**. Irradiations were performed a with 450 nm LED.

Once the BIST rapamycin dimer **31** and its photolysis product **29** were obtained, they were tested in cells by Taylor Courtney. Testing in a split luciferase assay as was done with ANBP rapamycin analog **19** did not yield active rapamycin (**Figure 1.8**). Attempts to generate the

decaged rapamycin analog **29** from a 0.1 mM solution of **31** irradiated with a 447.5 nm LED at an intensity of 300 mW/cm^2 for 1 minute were unsuccessful. The photolysis product **29** in this experiment showed comparable activity to rapamycin, but its activity was variable over multiple assays. Most commonly it showed about half the activity of rapamycin with the most pronounced decrease in activity at lower concentrations. Compound **31** showed no activation after irradiation. In fact, the activity of the dimer **31** showed a slight decrease upon irradiation. This minor loss of activity was seen across multiple experiments. Due to the lower activity of the photolysis product and the apparent loss of activity rather than gain upon irradiation, we targeted a BIST analog that released native rapamycin.
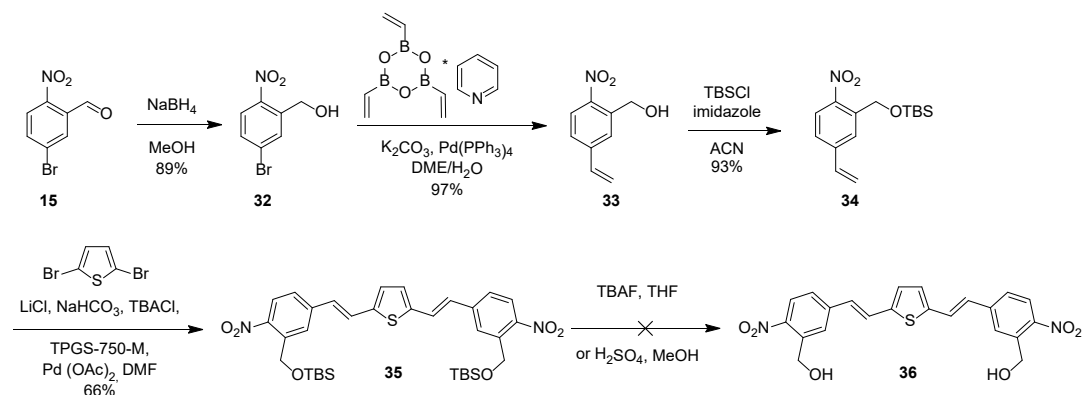
Scheme 1.5 - Attempted synthesis of a BIST caged rapamycin dimer releasing native rapamycin.

Initial attempts at forming the BIST dimer that would release native rapamycin focused first on creating the BIST dialcohol **36**, converting the alcohols to activated carbonates and then reacting both carbonates with rapamycin. Taylor had made the analog of **36** with the benzyl positions methylated, but was unable to get two molecules of rapamycin to substitute on the corresponding double NHS carbonate. We theorized that the steric bulk of the methyl groups may have played a role in preventing double substitution, so we targeted the nonmethylated version (**Scheme 1.5**).

Synthesis of the new BIST diol began with reduction of **15** with sodium borohydride.[59] The aryl bromide **32** was coupled to vinylboronic acid in a Suzuki reaction to give **33**.[55] Attempts to run the double Heck reaction to form the BIST chromophore at this stage showed reaction

progress on TLC, but the product was unstable to column purification. TBS protection of the alcohol yielded **34**, which was able to be used for the formation of a stable BIST product **35**, but conditions could not be found for the desilylation. When attempting a fluoride deprotection with either 1 equivalence or excess TBAF, compound **35** degraded to form a black baseline spot. A similar degradation occurred when attempting acid deprotection, both with a 0.5 M H_2SO_4 solution for 1 hour and with a 0.01 M H_2SO_4 solution overnight. When Taylor had made the analog of **36** that was methylated at the benzyl positions, she did not observe similar instability of the BIST diol, though her yield was only 29%. It appears the benzylic methyl groups were contributing to the chromophore stability through either steric or electronic effects. Since the methyl groups should have only minor electronic effects on the system, a steric explanation seems more likely. In acidic conditions, protonation of the alcohols may lead to the benzyl positions being somewhat electrophilic, leading to undesired substitution reactions, or if the alcohol were to leave generating the carbocation, other degradation pathways could ensue. The acid instability may be inherent to the BIST group as the Ellis-Davies group only used basic conditions in reactions with the BIST chromophore.[55] To see if the BIST chromophore in general is unstable to acidic/fluoride containing conditions, the methylated analog could be tested for stability in those conditions, but that was not tested at this time.
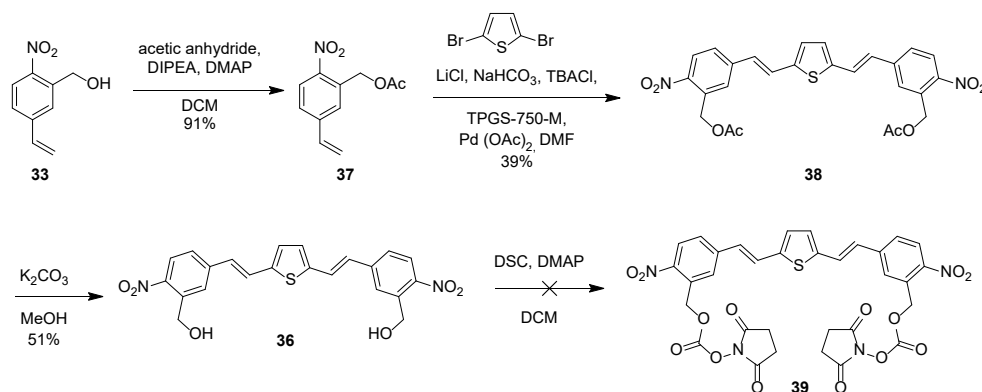
Scheme 1.6 - Alternate attempted route to synthesize BIST caged rapamycin dimer.

Instead, a basic deprotection was attempted with the synthesis of the acetyl protected BIST chromophore **38** (**Scheme 1.6**). Benzyl alcohol **33** was acetylated with acetic anhydride to yield **37**.[60] The acetyl styrene **37** was used in a subsequent double Heck reaction to form BIST diester **38** in 39% yield.[55] Using basic conditions, the diol **36** was isolated in 51% yield, lower than

expected for a acetyl hydrolysis. During the reaction, **36** precipitated as an orange solid. It had poor solubility in varying solvents such as DCM, methanol, and DMF. A baseline degradation spot had also formed during the reaction requiring column purification, and the low solubility in column chromatography eluents led to poor yields. The low solubility could be a result of the benzyl position being deprotonated under basic acetyl deprotection conditions, leading to a stable salt that would not be observed in the acidic or fluoride based deprotection of **35**. The benzyl protons of **36** could be acidic due to its extended conjugation in an electron poor aromatic system. The formation of a salt may also explain the differential stability when forming **36** in basic rather than acidic conditions. Attempted activation of **36** as the di-NHS carbonate **39** was unsuccessful, potentially as a result of its poor solubility. No reaction was observed by TLC, leading us to attempt an alternative route again.
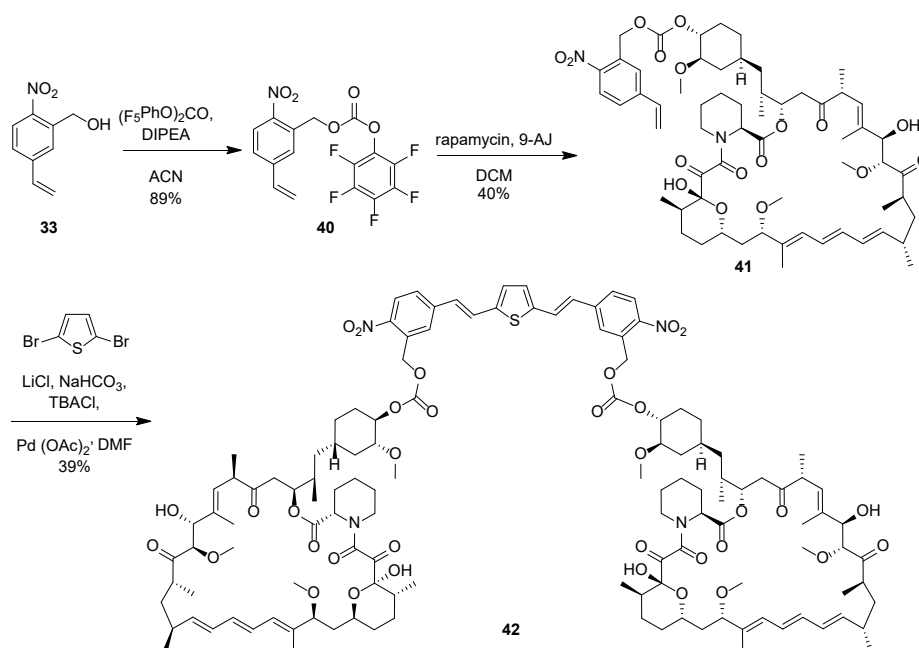
Scheme 1.7 - The synthesis of a BIST caged rapamycin dimer that produces native rapamycin upon decaging.

Our alternative route avoided the BIST diol **36** by adding rapamycin to the styrene prior to the double Heck reaction that forms the BIST chromophore (**Scheme 1.7**). One concern with this approach was the 110 °C temperature called for in the double Heck reaction because rapamycin is unstable at high temperatures.[61] To determine how long rapamycin was stable at 110 °C, a

solution of rapamycin in DMF was prepared and heated to 110 °C with TLC of the solution taken periodically. No degradation was observed by TLC over 120 minutes, but degradation began to be observed at 150 minutes. With the possibility of rapamycin being stable throughout the double Heck reaction, the benzyl alcohol **31** was activated as the pentafluorophenylcarbonate **40** and coupled to rapamycin with 9-AJ in 40% yield to give the styrene-rapamycin conjugate **41**. To ensure rapamycin didn't degrade, the subsequent double Heck reaction was only heated for 90 minutes instead of the 3 hours I had been previously using in similar reactions. This gave the BIST rapamycin dimer **42** in 39% yield.
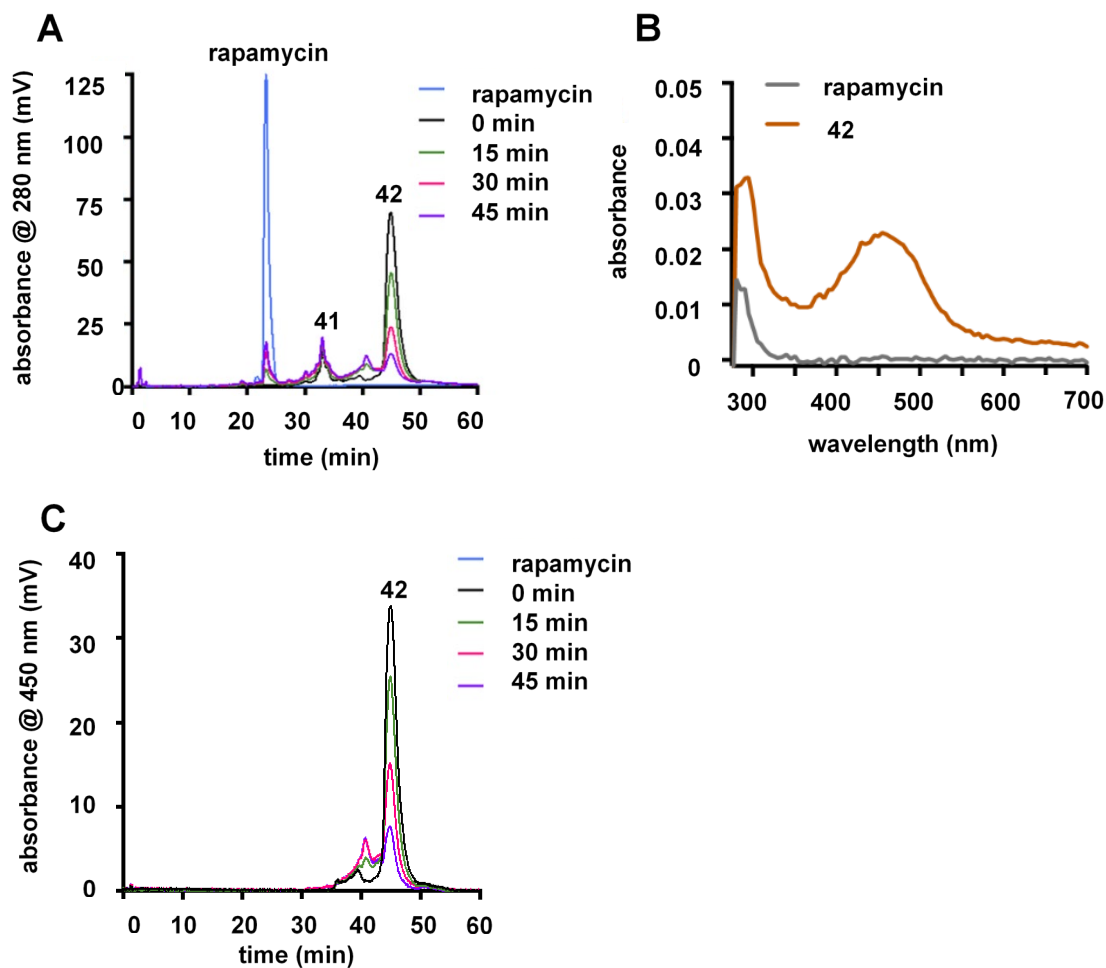
Figure 1.9 - Experiments performed by Taylor Courtney. A) HPLC testing of the decaging of **42** monitored at 280 nm. Loss of **42** is observed with little formation of rapamycin. B) Absorbance scan comparing 50 µm rapamycin and 50 µm **42**. C) HPLC testing of the decaging of **42** monitored at 450 nm.

Attempts to decage the BIST rapamycin dimer **42** proved unsuccessful with both 405 and 447.5 nm light, as seen before with the BIST rapamycin dimer **31** (**Figure 1.9A**). Taylor Courtney used a sample of **42** containing a small impurity of **41** that was later repurified. This sample was irradiated with either 405 or 447.5 nm LEDs as a 0.1 mM solution with an intensity of 250 mW/cm^2. HPLC analysis of the 405 nm irradiation showed minor formation of rapamycin (retention time 22 min) following irradiation, but not enough was generated to account for the loss of **42** absorbance (retention time 46 min). Since the wavelength monitored is in the UV region, only the rapamycin triene should be seen, meaning the full BIST signal integration should be converted to the peak for rapamycin. This was confirmed by comparing the 50 µM absorbance spectra of rapamycin and **42** (**Figure 1.9B**). The absorbance at 300 nm of **42** being approximately twice the absorbance of rapamycin indicates the major absorbing group at that wavelength is rapamycin. The loss of the BIST rapamycin dimer **42** signal in **Figure 1.9A** indicates that rapamycin is somehow being degraded upon irradiation which is consistent with the loss of activity seen upon irradiation of **31** as well (**Figure 1.8**). Rapamycin alone did not show degradation when irradiated by Taylor (HPLC chromatogram not shown) Taylor also showed that the BIST chromophore was degrading by monitoring 450 nm absorbance by HPLC throughout irradiation with 405 nm light (**Figure 1.9C**).

The triene of rapamycin has been shown to react with nitroso compounds in heteroatomic Diels-Alder reactions.[62,63] Upon decaging, a BIST nitroso would be formed that could potentially react with rapamycin, with the reaction possibly being facilitated by the BIST chromophore being in an electronic excited state due to the prolonged irradiation. Taylor tested this by irradiating in the presence of a 1000-fold excess of 1,4-butadiene. Any nitroso should react with the butadiene instead of rapamycin's triene. However, HPLC still showed loss of the rapamycin triene absorbance of **42** indicating the decaged rapamycin was not being consumed in a Diels-Alder type reaction (data not shown).
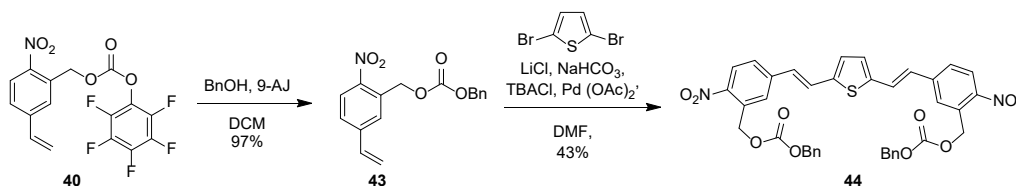
Scheme 1.8 - The synthesis of BIST caged benzyl alcohol **44**.

To determine if the caging group or rapamycin was the reason for the lack of decaging, the benzyl alcohol BIST dimer **44** was synthesized. The BIST analog would release an alkyl carbonate making it a good electronic model system, though the alcohol formed upon carbonate decomposition is primary rather than secondary. The UV activity of the benzyl alcohol aided in analysis by HPLC while simultaneously mimicking the rapamycin triene. A noteworthy difference between the rapamycin triene and benzyl moiety is that the aromatic character of the phenyl portion would be lower energy than that of the triene, and therefore less reactive. The synthesis was completed in analogous fashion to previous BIST syntheses. One notable difference is that the double Heck reaction coupling **43** to dibromothiophene was run overnight at 60 °C instead of 110 °C for 3 hours since the BIST carbonate **44** was unstable at high reaction temperatures. These same conditions could be used in the double Heck to synthesize the BIST rapamycin dimer **42** to potentially improve yield through a longer reaction time.
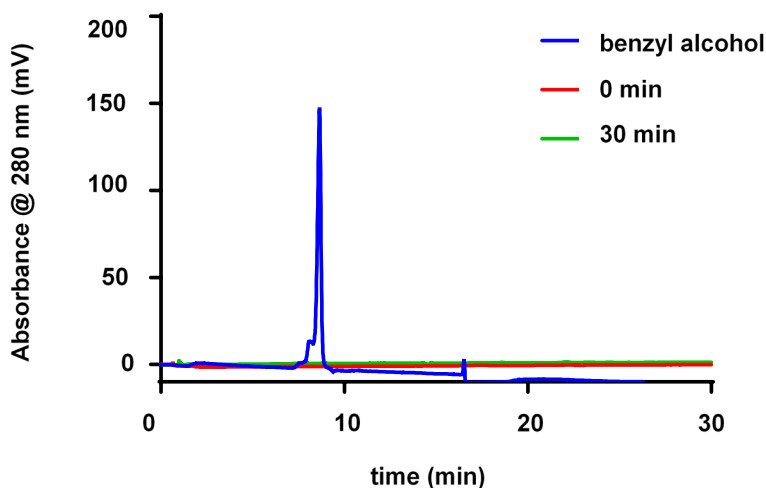
Figure 1.10 - Decaging of benzyl alcohol dimer **44**. Compound **44** was irradiated as a 0.25 mM solution in ACN with 415 nm light for 30 minutes at an intensity of 300 mW/cm^2.

Attempts to decage the BIST dimer **44** did not yield benzyl alcohol. When irradiated as a 0.25 mM solution in ACN with 415 nm light for 30 minutes at an intensity of 300 mW/cm^2, no product photolysis was observed. The dimer **44** was too nonpolar to be visualized via HPLC, but benzyl alcohol showed a retention time of 8.5 minutes (**Figure 1.10**). This result was replicated in

TLC experiments; **43** disappeared as irradiation progressed, while no corresponding benzyl alcohol formed.

Taking into account the three attempted decaging experiments, we thought it may be worth attempting an asymmetric BIST caged rapamycin. The lack of decaging across two rapamycin dimers and a benzyl alcohol dimer led us to believe that the chromophore could have been the problem rather than the substituent being released. Anirban Bardhan, a fellow Deiters lab member, had used an asymmetric BIST chromophore in the caging of thymidine. We believed the asymmetric BIST may alter the decaging efficiency to allow for release of rapamycin. When Anir synthesized a BIST caged thymidine, he tested decaging by HPLC. However, he only monitored for the loss of BIST absorbance, and he has not tested decaging in cells to see a gain of function.

Anirban provided BIST alcohol **45** for the synthesis of an asymmetric BIST caged rapamycin (**Scheme 1.9**). This was activated as the pentafluorophenylcarbonate **46**, then coupled to rapamycin to yield the asymmetric BIST rapamycin analog **47** in 21% yield.
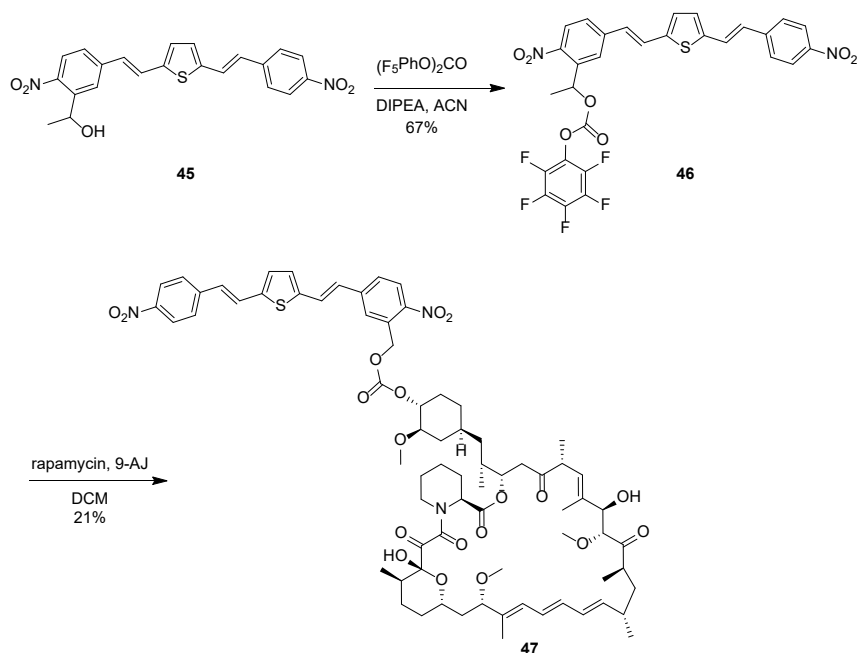
Scheme 1.9 - Synthesis of asymmetric BIST rapamycin analog **47**.

Testing the decaging of **47** as a 0.25 mM solution in ACN via HPLC after irradiation with 415 nm LED at an intensity of 300 mW/cm^2 still did not show any decaging (**Figure 1.11**) indicating that the issue was not the dimeric nature of the caging group. I believe there are two potential reasons the photolysis isn't working. The first is the use of one-photon irradiation. In Ellis-Davies' publication, he primarily uses two-photon irradiation for decaging.[55] In one cell-based experiment, he demonstrated the use of one-photon irradiation, but we have demonstrated only minimal decaging with one-photon irradiation (**Figure 1.9**). It could be that his one-photon irradiation was inefficient, but that inefficient decaging still produced a signal in the assay used.
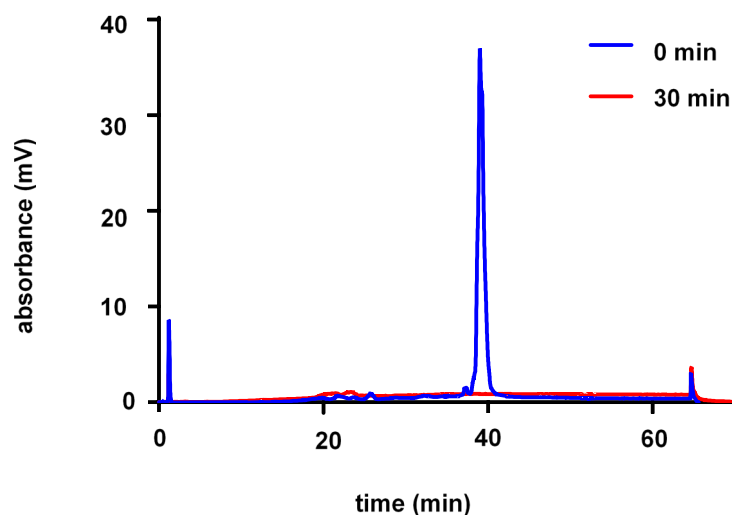
Figure 1.11 - HPLC decaging of **47** upon irradiation with 415 nm light. Compound **47** was irradiated as a 0.25 mM solution in ACN with 415 nm light for 30 minutes at an intensity of 300 mW/cm^2.

A second option is that aromatic and unsaturated compounds are incompatible with the BIST caging group. Ellis-Davies releases a caged calcium ion that is coordinated by groups not containing any unsaturated C-C bonds. It is possible that the BIST group is somehow interacting with the unsaturated compounds (rapamycin or benzyl alcohol) in a way that causes decomposition of both.

27

1.2.5 BODIPY Caged Rapamycin

We also attempted to synthesize a boron dipyrromethene (BODIPY) caged rapamycin conjugate. Two variations of boron dipyrromethene chromophores as caging groups were published by the Urano group in 2014 (**48**)[64] and the Winter group in 2015 (**49a**).[65] The Urano group synthesized the BODIPY caged histamine **48**. The caged histamine was attached to the BODIPY through a phenoxy linker attached directly to the boron that, when decaged, will undergo an immolative elimination to release the histamine. With **49a**, the Winter group conjugated a dinitrobenzoic acid to the mesomethyl hydroxy group of the BODIPY chromophore. The dinitrobenzoic acid acted as a quencher of BODIPY fluorescence. They demonstrated an increase in fluorescence upon irradiation, indicating that the fluorescence quencher had been released from the BODIPY fluorophore.
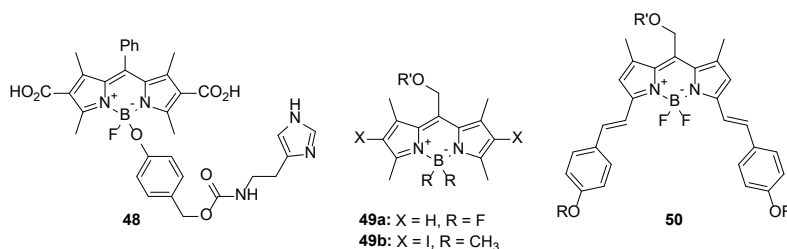
Figure 1.12 - Select published BODIPY caging groups.[64–67] Compounds **49a**, **49b**, and **50** showed release of acetate (R' = Ac) in addition to other groups.

The Winter group subsequently published an improved BODIPY photocage that has the pyrrole C-H positions from **49b** iodinated and the BF_2 exchanged for a $B(CH_3)_2$, demonstrating it's photolytic efficacy with groups such as acetate and benzoic acid released.[66] The rationale for these modifications is that, through the heavy atom effect, the iodination prolongs the electronic excited state by facilitating intersystem crossing to the triplet state.[68] A drawback of this is that the triplet state is capable of being quenched by oxygen, generating singlet oxygen, which is toxic to cells.[69] The methylation of the boron also increased decaging efficiency. As shown in **Scheme 1.10**, a cation is produced upon decaging.[66] The electron withdrawing nature of the fluorines increases the energy of cationic **51**, slowing down the release of the photolysis product RO⁻. Methylation increases the electron density relative to the fluorinated version, lowering the energy

of the methylated analog of **51**. In conditions containing a water or alcohol, the R'OH will react with the cation giving **52**. Other nucleophiles would theoretically be able to attack the cationic methylene, but have not been tested. The Winter group has since described a BODIPY photocaging group that decages in the near-IR region.[67] The extended conjugation of the BODIPY chromophore of **50** via styrene moieties where there are commonly methyl groups induces a bathochromic shift into the near-IR. By releasing a fluorescence quencher from the BODIPY compound, decaging was confirmed with single-photon irradiation.
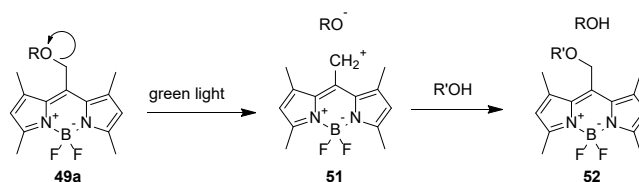
Scheme 1.10 - Decaging mechanism of BODIPY **49a**, **49b**, or **50**. It has been reported that carboxylates and carbonates can be released as R groups. R' can be either H or alkyl depending on if aqueous or an alcohol solvent is used.

Since the triazole containing rapamycin analog **29** showed some loss of dimerizing ability, and the ANBP rapamycin analog **19** showed less than that, we reasoned that adding an even bulkier BODIPY group to rapamycin should further reduce background. To this end, synthesis of a BODIPY caged rapamycin analog was planned (**Scheme 1.11**). Following the procedure by the Winter group, dimethylpyrrole **53** was coupled to acid chloride **54** in 15% yield.[66] However 10-40% yields are common for syntheses of similar BODIPY compounds.[66,70,71] The BODIPY is prone to degradation, as evidenced by a black baseline TLC spot forming in many BODIPY reactions conducted. Hydrolysis of the acetyl ester **55** proved problematic, however. In Winter's and others' protocols, LiOH in a THF/water mixture is used, but this produced substantial degradation in my hands.[66,72,73] Stirring **55** in the basic, aqueous mixture produced a degradation product, while literature protocols report clean conversion and a lack of column purification in some cases. I also tried potassium carbonate in methanol/DCM, and this worked better but still produced substantial degradation. The highest yield obtained was 59% on a small scale, but when scaling up above 10 mg, the yield dropped precipitously to 18%. The alcohol **56** I managed to isolate was converted to the pentafluorophenylcarbonate **57** in 15% yield with substantial degradation observed again.

Rapamycin conjugate **58** could not be isolated as no product was observed by TLC in a small scale reaction.
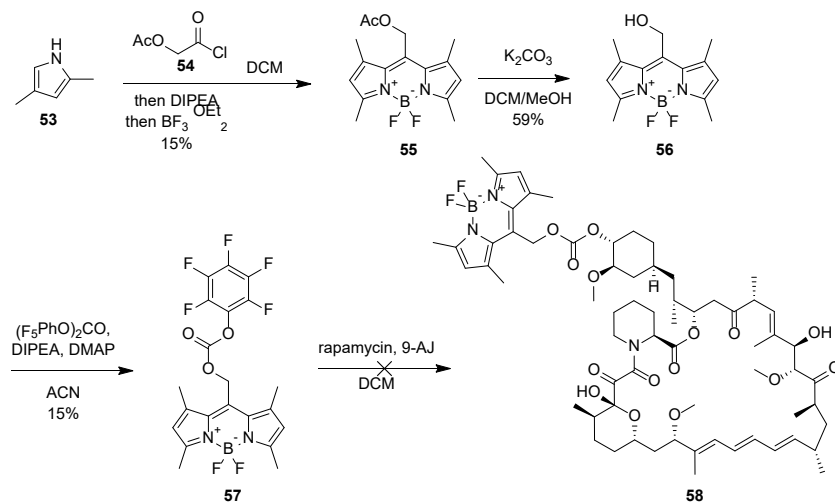
Scheme 1.11 - The attempted synthesis of BODIPY caged rapamycin **58**.

In work shown later (**Section 1.3.3**), I discovered that iodination of the pyrrole C-H positions, such as those seen on BODIPY **49b** in **Figure 1.12**, conferred much greater stability to a different BODIPY chromophore. To this end, I explored what groups could be added to that C-H position. Iodination would not be ideal because the ROS generation ability resulting from iodination in addition to decaging is not desired. However, there have been many reports of BODIPY analogs ethylated at this position.[66,72,74] A synthesis of the ethylated BODIPY rapamycin conjugate **63** can be seen in **Scheme 1.12**. It follows the same conditions as those described in **Scheme 1.11**, but the ethylated version showed better stability. The initial chromophore formation between pyrrole **59** and acyl chloride **54** proceeded in 30% yield, a two-fold improvement over that of **55**. The hydrolysis of **60** to yield alcohol **61** was completed in 40% yield which is lower than listed above. However, this yield was achieved on a larger scale, whereas the 59% yield described above was less than 10 mg. The major factor decreasing yield is still degradation of the chromophore in these reactions. The alcohol was activated in 63% yield as pentafluorophenyl carbonate **62**. I was unable to couple this to rapamycin however. The degradation of the chromophore led to a very small amount of product formation. Additional optimization of the reaction conditions should enable the synthesis of rapamycin conjugate **63**.
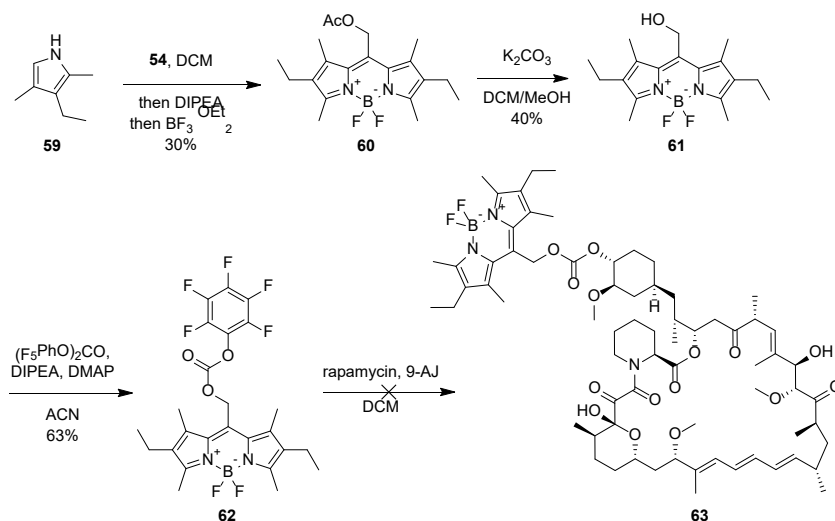
Scheme 1.12 - Attempted synthesis of a photocaged BODIPY-rapamycin conjugate.

I believe the electrophilicity of the boron is leading to the degradation observed in the above syntheses. All steps that exhibit degradation contain nucleophiles (DMAP, 9-AJ, basic methanol) that may be able to substitute onto the boron, with fluoride or the pyrrole nitrogen acting as a leaving group. The ability of BF$_3$ to act as an electrophile was demonstrated with the substitution of pyrroles to form the BODIPY chromophores **55** and **60**, so analogous reactions with other nucleophiles are plausible. The loss of boron coordination by the pyrrole nitrogen would lead to overall loss of fluorescence which is consistent with the degradation observed. If this is the case, the BODIPY caging group with a methylated boron described by the Winter group may limit this degradation somewhat, as the boron would be less electrophilic when methylated.[66]

1.3 CALI of Rapamycin Dimerization

1.3.1 Introduction to CALI of Proteins

Chromophore assisted light inactivation of proteins (CALI) is a method that allows for the spatially and temporally controlled degradation of proteins.[75] The precise inactivation of proteins

allows for a more thorough investigation of protein function. Most proteins have altered function either at different points in an organism's development or in response to external stimuli. The ability to temporarily deactivate proteins has allowed researchers to more thoroughly interrogate protein functions. CALI has been used to control synaptic function,[76] cellular adhesion,[77] enzyme function,[78] mitochondrial function,[79] and cell structure.[80]
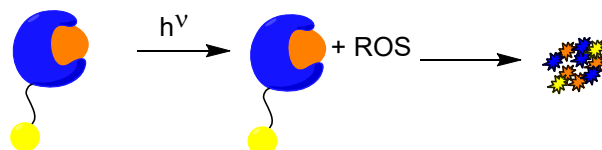
Figure 1.13 - The general principle of chromophore assisted light inactivation of proteins where the blue structure is a protein, the orange is its substrate, and the yellow circle is an ROS generator.

In principle, a reactive oxygen species (ROS) generating chromophore is conjugated to a protein so that subsequent irradiation generates ROS in close proximity to the target protein (**Figure 1.13**). The high level of ROS around the target then either modifies it such that is inactive or is degraded by the proteasome.[81] ROS generation generally follows one of two pathways. The Type 1 pathway is the oxidation of a nearby molecule (not oxygen) generating a negatively charged ROS generating chromophore that eventually reduces oxygen, generating the superoxide anion.[82] Type II involves the direct formation of $^1O_2$ from the ground state $^3O_2$.[82] The ROS generated are capable of modifying proteins in many ways, such as backbone cleavage/crosslinking or amino acid oxidation.[81,83] Sulfur containing residues are easily oxidized by peroxides and superoxide to sulfoxides and sulfones, while aryl residues are particularly prone to singlet oxygen oxidation via heteroatomic Diels-Alder reactions.[84] However, due to the short irradiations, localization to the protein target, and short half-lives of ROS ($^1O_2$ - 100 ns in cells,[85] superoxide - 9 ns in water,[86] hydroxyl radical - 1 ns in cells[87]), the ROS generated should generally not be exist long enough to have a significant impact on other cellular components. Singlet oxygen, the longest lived ROS described above, only diffuses 45 nm in cells.[85]
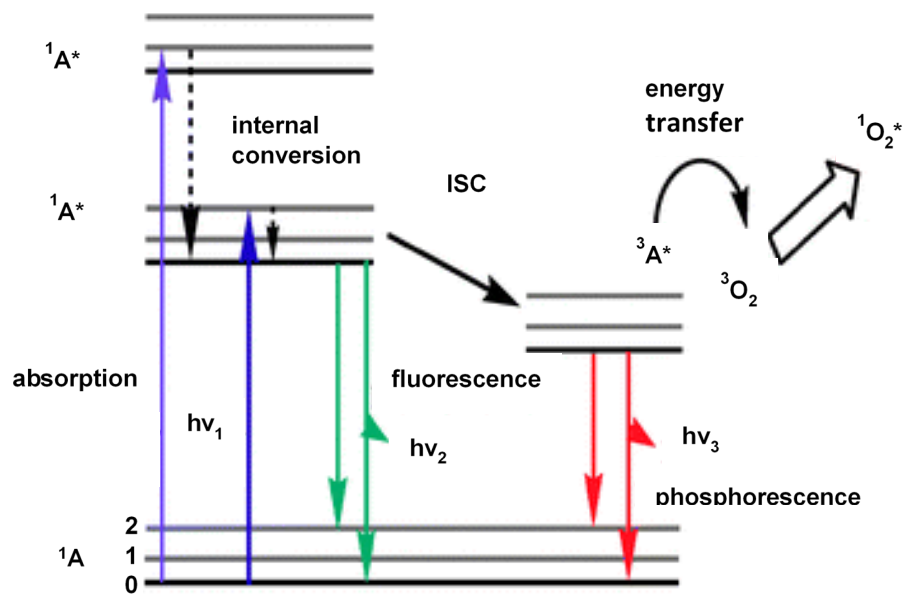
Figure 1.14 - Jablonski diagram showing transitions relevant to singlet oxygen production.[85] In the diagram, A is the ROS generating compound and asterisks indicate excited states. Adapted with permission from Ethirajan *et al*. The Role of Porphyrin Chemistry in Tumor Imaging and Photodynamic Therapy. Chemical Society Reviews 2011, 40 (1), 340–362. Copyright 2011 Royal Society of Chemistry.

The ROS generating chromophores used in CALI vary widely, but their method of ROS generation can be described with a Jablonski diagram (**Figure 1.14**). The process for generating ROS for all chromophores begins with the absorbance of a photon which causes the chromophore to go from its singlet ground state, ^1A, to its singlet excited state, $^1A^*$. The $^1A^*$ compound will release its energy in one of four ways. First, it can release its energy thermally through bond rotations or vibrations. This is unlikely for highly conjugated molecules since they are quite rigid. The second possibility, fluorescence, is the emission of light to return to the ^1A ground state. However, given the right conditions, an electron of the $^1A^*$ compound can undergo a forbidden spin transition known as intersystem crossing (ISC) to yield the triplet excited state ^3A of the compound. In the third possibility, the ^3A compound phosphoresces by releasing its energy as light and returning to the ^1A ground state. In the fourth possibility, the presence of a second compound, sometimes called a quencher, that has an excited state at a similar energy level as the ^3A state allows the electronic energy to be transferred to the quencher. With ROS generators that undergo Type II ROS generation, that quencher is oxygen, which is excited from its triplet ground state to its singlet excited state.

CALI was first reported by D. G. Jay in 1988 using the chromophore malachite green, more commonly used as a fluorophore.[78] Jay used a streptavidin-malachite green conjugate to inactivate biotinylated alkaline phosphatase *in vitro*. He then used a malachite green labelled antibody to inactivate acetylcholinesterase on cell surfaces. In research following Jay's initial publication, antibodies were injected into cells to degrade intracellular targets, thus highlighting the limitations of this approach.[88]

Genetic approaches were developed to avoid the perturbance caused by injections. In 2002, the Jacobson lab demonstrated that EGFP was a viable ROS generator for use in CALI as a fusion protein.[89] Though it has poor quantum yield for ROS generation, it was sufficient to degrade proteins it was fused to with 5 minute irradiations. In 2005, Sergey Lukyanov's lab published a mutant of a GFP homolog that they named KillerRed. KillerRed exhibited far superior quantum yield for ROS generation, primarily due to increased accessibility to the fluorescent chromophore via a water channel. However, KillerRed required dimerization for activity which led to abnormal cellular localization of some proteins. This led the Nagai lab to evolve a monomeric mutant of KillerRed known as SuperNova.[90] One genetic approach distinct from the GFP variants was developed by Roger Tsien's lab. He utilized a small protein that binds flavin mononucleotides which are capable of generating ROS.[91] He named this tag a mini Singlet Oxygen Generator, or miniSOG. A potential problem of the miniSOG method is the prevalence of the chromophore in cells. The flavin mononucleotide is plentiful in cells, leading to the potential for degradation of off target proteins.

In 2003, the first exogenous, cell-permeable CALI agent was published, also by the Tsien lab. ReAsH and FlAsH were used to selectively degrade proteins labelled with a tetracysteine motif, however, the cytotoxicity and tendency of these arsenic based reagents to bind to other cysteine rich proteins proved troublesome.[77] In 2009, a SNAP tag was used to conjugate fluorescein to tubulin in cells, giving a much more selective exogenous labelling method.[92] Two years later, a Halotag was used to couple eosin to Aurora B and stop cell division, introducing a reagent with greater cell permeability than the SNAPtag reagent CALI reagent and a more potent ROS tag.[93] More recently, the Kodadek lab has published a peptoid based CALI method.[94] Peptoids are similar to peptides, but the side chains are attached to the nitrogen of the backbone. The Kodadek lab found a peptoid agonist of the proteasome and attached a ROS generator to it to selectively inactivate the proteasome.

In **2.1**, activation of dimerization through the release of caging groups from rapamycin was discussed. While it is useful to be able to control the start point of chemical dimerization, it could also prove useful to control the end point of dimerization as well. The genetic approaches

discussed above may not prove feasible for controlling rapamycin dimerization. The addition of another protein into a complex already containing two fusion proteins may inhibit ternary complex formation. SNAP or Halotags may not work for the same reason. Conjugating a ROS-generating chromophore directly to rapamycin would minimize the perturbance to the system, while avoiding further protein modification. Additionally, the close proximity to FRB and FKBP may allow superior degradation of the ternary complex.

1.3.2 Eosin and Ru(II) Bipyridine Rapamycin

Several chromophores were examined as potential ROS generators to conjugate to rapamycin. An attempt to conjugate eosin to rapamycin was made, but a pure starting material could not be obtained commercially. Eosin is a fluorescein analog in which the xanthene dye has undergone four brominations (**64** in **Figure 1.15** is an amidated version). It is an effective ROS generator, with a singlet oxygen quantum yield ranging from 0.32-0.57 depending on purity and solvent.[95] The synthesis of the eosin-rapamycin conjugate was abandoned primarily because the eosin purchased always contained a mixture of compounds with 0-4 bromine atoms present. After attempting to convert eosin to an amide, a mixture of the brominated products were obtained (**Figure 1.15**). In addition to the impure starting material, the eosin chomophore proved difficult to purify, and low yields were attained for even the impure product. The difficulty in obtaining a pure stock is likely a result of its prevalence in cytoplasmic staining.[96] A high purity sample would not be needed for staining, so a difficult separation of the varying bromination products is impractical. Due to these difficulties, conjugation of rapamycin to a different chromophore was attempted.
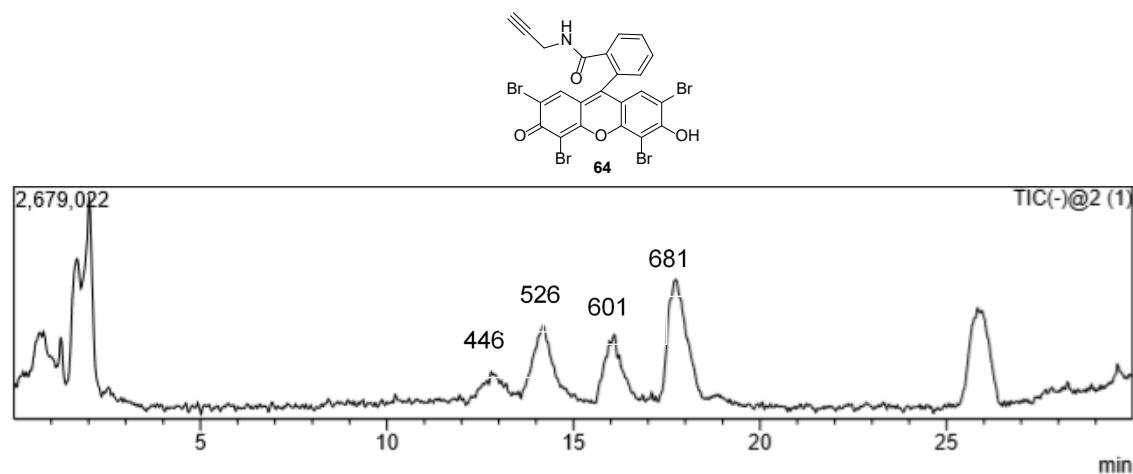
Figure 1.15 - LC/MS chromatogram with masses labelled for peaks representing non-brominated to tribrominated eosin analogs of **64**.

Ruthenium(II) coordinated by molecules of bipyridine and its derivatives have been developed for use primarily in photodynamic therapies,[97] but have also seen use in CALI functions.[94,98,99] Ru(II) bipyridine complexes are efficient ROS generators with a singlet oxygen quantum yield of 0.57, and thus have the potential to be potent CALI chromophores.[100] Additionally, as a halide salt, the Ru(II)-rapamycin conjugate would have far greater aqueous solubility than many other potential ROS generators, and despite their ionic nature many Ru(II) pyridinyl complexes are still taken into cells.[101,102]
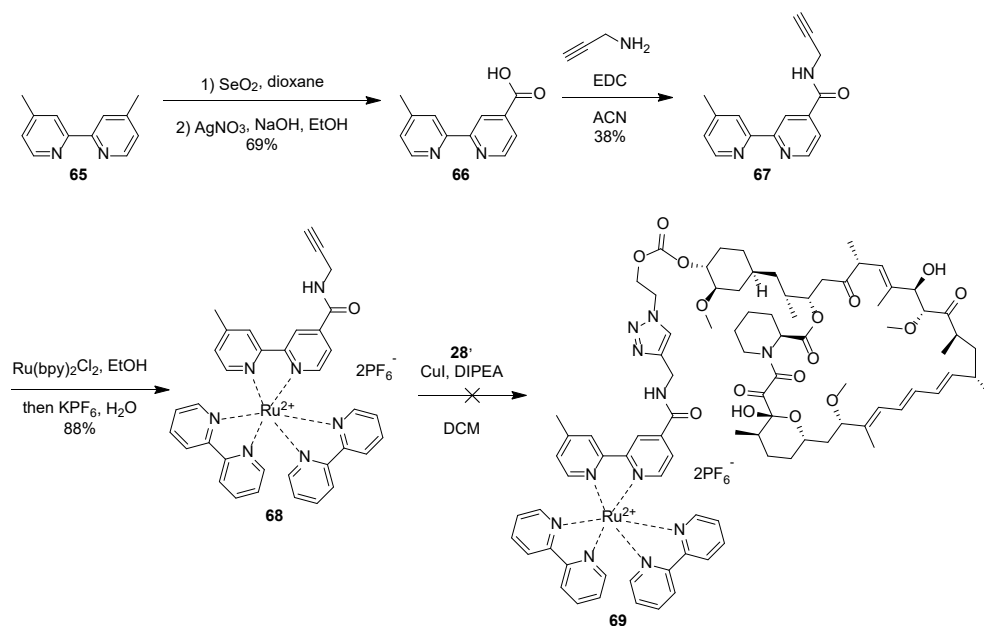
Scheme 1.13 - The attempted synthesis of a Ru(II)-based ROS generating rapamycin analog **69**.

A route was developed to conjugate rapamycin to a Ru(II) bipyridine complex as shown in **Scheme 1.13**. A bipyridine aldehyde was generated via selenium oxide oxidation of one methyl group of **65**. Silver nitrate oxidation was subsequently used to convert the aldehyde to an acid forming **66**.[103] Attempts at purification of the aldehyde or acid by column chromatography gave yields of 10% or lower. This led to the procedure shown, where the selenium oxidation product is further oxidized crude, generating a mixture of **65**, **66**, and the diacid. Compound **65** can be extracted from the crude solid through trituration with acetone. Then, the monoacid **66** is able to be extracted via Soxhlet extraction with acetone giving a 69% yield of the monoacid **66**. Carboxylic acid **66** was then coupled to propargyl amine to form **67** in 38% yield, giving an alkyne handle to click onto an azidomodified rapamycin.[104] The Ru(II) complex **68** was then formed through a simple coordination and converted to a hexafluorophosphate salt through the addition of excess KPF_6 in 88% yield.[104] As a hexafluorophosphate salt, the complex was quite nonpolar allowing column purification. However, in attempts to perform a click reaction in order to generate the ruthenium rapamycin conjugate **69**, it is theorized that the complex underwent a salt exchange with the CuI forming PF_6Cu and the ruthenium complex was coordinated by iodide because of its lack of mobility during TLC. In the synthesis of **68**, the ruthenium complex is soluble in water as a halide salt, but addition of excess KPF_6 formed the PF_6^- salt which was no longer soluble in

37

water, but was soluble in organic solvents. This indicates that the PF_6^- counterion is essential for the reduced polarity of the ruthenium complex. Thus, the substantial increase in polarity suggests that the PF_6^- counterion is no longer present. An attempt to reform the PF_6^- salt by dissolving it in water and adding excess KPF_6 was unsuccessful. If a salt exchange was happening under these conditions, it could be avoided if a strain promoted click reaction were used, as a copper salt would be unnecessary, or if $CuPF_6$ were used instead of copper iodide. Testing of the propargyl clicked rapamycin **29** in **Scheme 1.4** while working on this synthesis indicated that the Ru(II) clicked rapamycin **69** would be a poor dimerizer if it were synthesized.
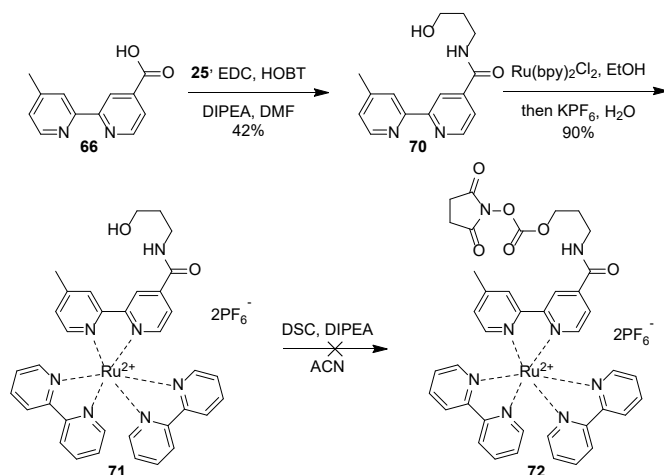
Scheme 1.14 - The proposed alternate synthesis towards a Ru(II)-based ROS generating rapamycin analog.

Based on the poor potential of the clicked Ru(II) rapamycin conjugate to act as a dimerizer, the synthetic scheme was altered to avoid the triazole resulting from a click reaction (**Scheme 1.14**). In the altered route, rather than coupling propargyl amine to **66**, 3-aminopropanol is used to create the amide **69**.[104] This avoids an ester that would potentially be cleaved by esterases, and instead allows for a carbonate coupling. The bipyridine alcohol was coordinated to Ru(II) to give the hexafluorophosphate salt **71**.[104] As with the synthesis of the Ru(II) rapamycin conjugate **69**, salt exchange issues prevented isolation of the activated carbonate that would be coupled to rapamycin. Attempts to couple rapamycin to the alcohol prior to Ru(II) complexation were also

ineffective. The activated carbonate of **70** could not be isolated, likely due to the instability of an activated carbonate in the presence of a pyridine moiety.

1.3.3 BODIPY Rapamycin

The third ROS generator attempted was a BODIPY chromophore. As shown in **Section 1.2.5** some versions of the BODIPY chromophore are a fluorophore or, if properly designed, a caging group. The fluorophore version would likely be possible to use as an ROS generator in CALI experiments, but in the same way that halogenation of fluorescein with bromine to generate eosin increases ROS generation, the halogenation of the BODIPY fluorophore makes it much more prone to generate ROS.[69] The iodinated BODIPY chromophore has a singlet oxygen quantum yield of 0.05-0.17 depending on the exact chromophore and solvent conditions. This is not as efficient as eosin or the Ru(II) bipyridine complexes, but is still an efficient ROS generator. This can be attributed to the heavy atom effect. The addition of heavy atoms to highly conjugated chromophores increases the likelihood of intersystem crossing taking place.[105,106] In the case of a BODIPY chromophore, once this electronically forbidden transition takes place, the molecule is likely to transfer its excited state energy to oxygen to generate singlet oxygen.
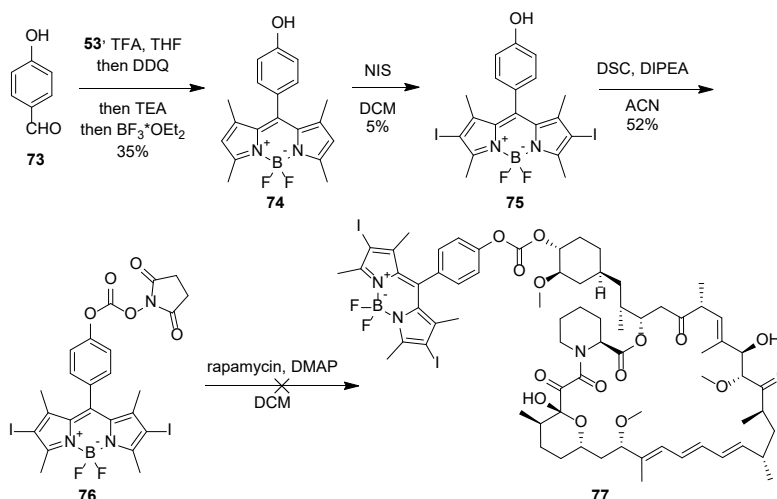
Scheme 1.15 - An attempted synthesis of a BODIPY based ROS generating rapamycin analog.

The first attempt to conjugate rapamycin to an iodinated BODIPY followed the route shown in **Scheme 1.15**. The BODIPY chromophore was generated as the phenol **74** from **72**.[107] The pyrrole C-H groups were subsequently iodinated via electrophilic aromatic substitution with the electrophilic iodine of *N*-iodosuccinimide (NIS) to yield **75**.[107] Poor conversion to **75** was observed with only a 5% yield, and the phenolic proton seemed to be quite acidic, complicating column purification. Activation of the phenol as the NHS carbonate **76** was achieved in 52% yield on a 10 mg scale, however attempts to scale up showed lower product conversion. Additionally, couplings to rapamycin showed no product formation by TLC or LCMS. This was likely because the phenol-BODIPY chromophore is a good leaving group, with the phenoxide charge generated upon release from the carbonate stabilized across the BODIPY chromophore. The instability of the carbonate led to high water sensitivity and the inability to purify via column chromatography.
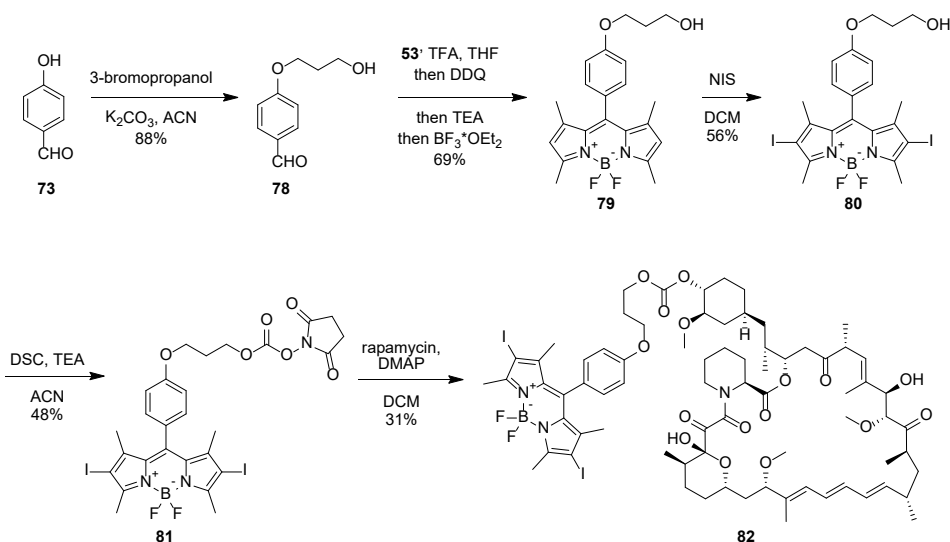
Scheme 1.16 - The synthesis of an ROS generating BODIPY rapamycin conjugate (**82**) with a propyl linker.

Realizing this problem, a modified BODIPY was synthesized (**Scheme 1.16**). Attempts to convert the phenolic BODIPY **75** directly to **80** were unsuccessful as the BODIPY chromophore was not stable to the basic reaction conditions. Thus, a propyl linker was attached to the benzaldehyde **73** prior to the BODIPY formation via S$_N$2 substitution yielding **78**.[108] Compound **78** was then converted to the BODIPY chromophore **79** in 69% yield, and the chromophore was iodinated with NIS to give **80** in 56% yield, a 51% improvement over the iodination to form **75**.[107]

This is explained by the easier chromatographic separation of **80** than **75** due to replacement of the phenol with an ether. The iodinated BODIPY **80** was then converted to the NHS carbonate **81** in 48% yield and was subsequently conjugated to rapamycin to give **82** in 31% yield.
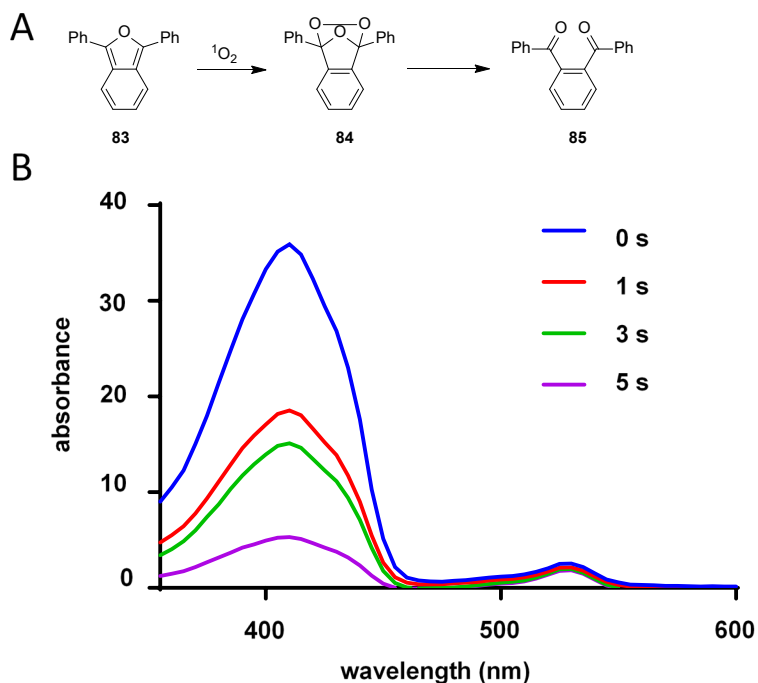
Figure 1.16 - A) Mechanism of diphenylisobenzofuran reaction with singlet oxygen. B) Loss of absorbance in a solution of **83** (250 µM) and **82** (25 µM) after irradiation with 530 nm light in ACN. The decrease in absorbance at 415 indicates production of singlet oxygen while absorbance at 530 nm indicates stability of the BODIPY chromophore.

To confirm the ROS generation of the compound, diphenylisobenzofuran (**83**) was used. Compound **83** contains a 2-benzofuran that is commonly used to detect singlet oxygen production, though it is capable of reaction with other ROS such as hydrogen peroxide and superoxide.[109,110] The furan is able to undergo a heteroatomic Diels-Alder reaction with singlet oxygen, generating endoperoxide **84** that collapses to diketone **85**, as shown in **Figure 1.16A**.[111] The diketone **85** loses the benzofuran conjugation of **83**, leading to a loss of absorption at 410 nm. A solution of **82** and **83** was generated and was irradiated with a 530 nm LED at an intensity of 300 mW/cm^2 for varying lengths of time. The loss of absorption at 410 nm in **Figure 1.16B**

indicates the formation of singlet oxygen, while minimal loss of the absorbance at 530 nm indicates the stability of the BODIPY chromophore to the singlet oxygen.
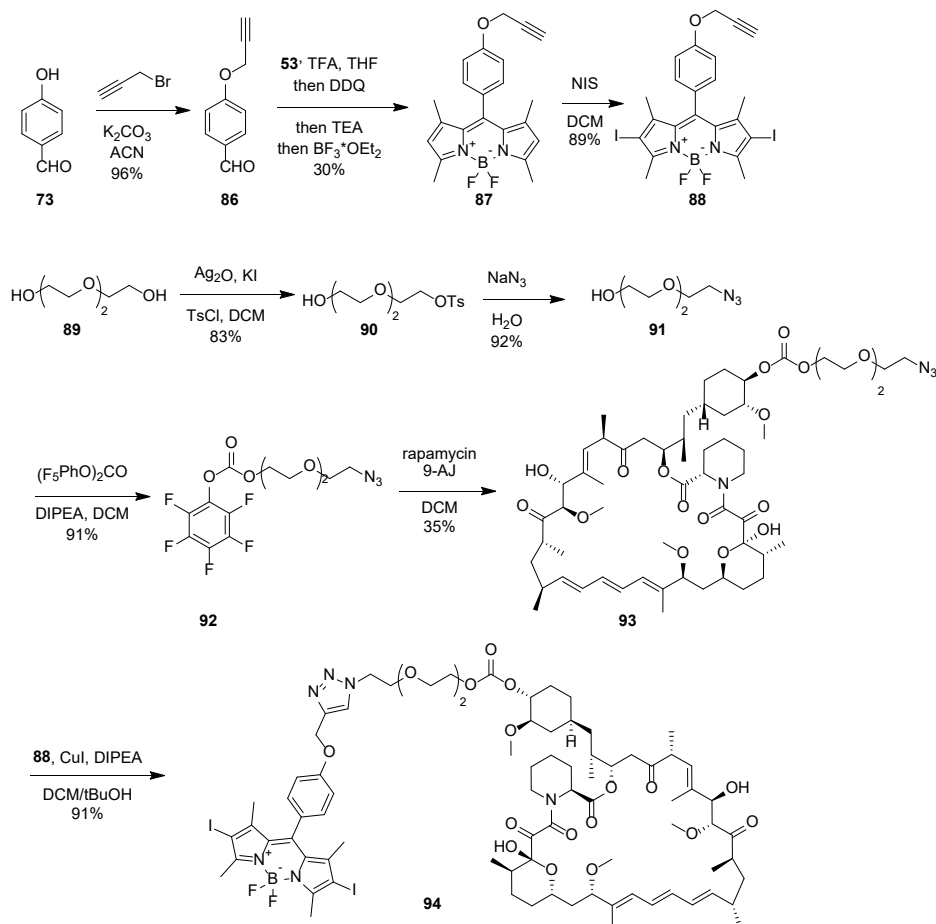
Scheme 1.17 - The synthesis a ROS generating BODIPY rapamycin conjugate (**94**) with a triethylene glycol linker.

Preliminary testing of the propyl linked BODIPY-rapamycin conjugate **82** revealed that it was a poor dimerizer relative to rapamycin (data not shown), so a second analog was made with a triethylene glycol linker (**Scheme 1.17**). The convergent synthesis began with the formation of the propargylated BODIPY chromophore **88.** The propargyl phenolic ether **86** was formed through an S_N2 reaction between propargyl bromide and **73**.[112] This was converted to the BODIPY chromophore **87** and iodinated using the same conditions shown in **Scheme 1.15** and **Scheme 1.16** to give the BODIPY **88**.[107] The other half of the convergent synthesis began with a

monotosylation of **89** with limiting tosyl chloride to give **90** in 83% yield.[113] Though silver oxide is a poor base, catalytic iodide is able to abstract a silver ion to create the much more basic AgOK salt which is able to effectively deprotonate triethylene glycol. The tosylate is exchanged for an azide through a standard S_N2 reaction yielding **91** in 92% yield.[113] The azidotriethylene glycol **91** was activated as the pentafluorophenylcarbonate **92**, which was coupled to rapamycin to give the azide-modified rapamycin **93** in 35% yield. The rapamycin-azide conjugate **93** and the BODIPY-alkyne **88** were clicked together to give the BODIPY-rapamycin conjugate **94** in 92% yield. The click reaction was run in the DCM/CuI/DIPEA system shown in **Scheme 1.4**, but *tert*-butanol was added as a cosolvent because literature reports state that nonpolar solvents can lead to formation of nonreactive copper-alkyne aggregates.[58] Attempts to synthesize the molecule through exclusively a carbonate linkage (no click reaction) were unsuccessful. The low conversion of the activated carbonate to product and propensity of the triethylene glycol-BODIPY motif to streak on silica gel prevented the isolation of the corresponding pure rapamycin analog.
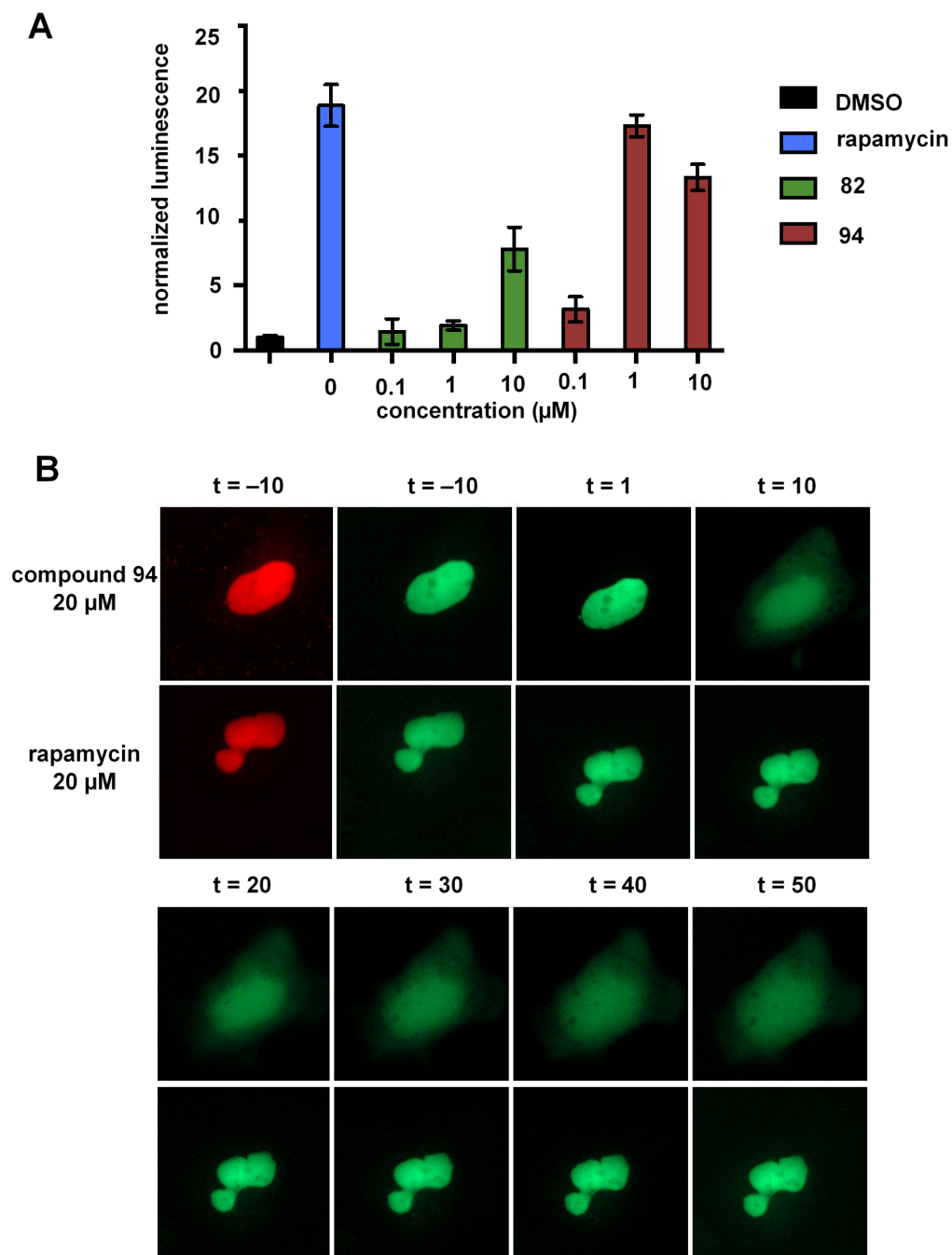
Figure 1.17 - Experiments performed by Taylor Courtney. A) Split luciferase assay in HEK293T cells. Part of luciferase is expressed as a fusion protein with FKBP and part is expressed as a fusion protein with FRB, addition of dimerizer produces active luciferase B) Nuclear translocation assay in Hela cells expressing GFP-FKBP and nuclear localized mCherry-NLS$_3$-FRB. Irradiation with a 530 nm LED was performed at t = 0 and all times are in minutes.

Taylor Courtney compared the abilities of the two BODIPY rapamycin conjugates **82** and **94** to form a ternary complex with FKBP and FRB in a split luciferase assay (**Figure 1.17A**). In this assay, one portion of luciferase is expressed as a fusion protein with FKBP, and the other portion is expressed as a fusion protein with FRB. In the absence of rapamycin (DMSO control), there is very little active luciferase, but with the addition of rapamycin, the two luciferase units are brought into close proximity and form an active luciferase enzyme. The split luciferase assay revealed that the triethylene glycol-linked conjugate **94** was a superior dimerizer to the propyl-linked conjugate **82**, and was comparable to rapamycin at 1 μM. However, based on previous testing by Taylor, it should be noted that rapamycin exhibits higher activity at 100 nM. At concentrations of 1 μM and higher, it is likely that the system is saturated with rapamycin so that the ternary complex doesn't form as frequently, but rather separate dimers of FKBP-rapamycin and FRB-rapamycin.

Attempts to irradiate with 530 nm light to inactivate the split luciferase proteins did not show reduced luminescence output in the assay, so other assays were performed to determine if this was an assay specific result or if there were problems with the compounds' ROS generation. Testing of **82** was stopped due to its lower binding affinity. To further interrogate the ability of **94** to be an effective CALI agent, Taylor performed a nuclear translocation assay (**Figure 1.17B**). Hela cells expressing GFP-FKBP and an excess of nuclear localized mCherry-NLS$_3$-FRB were incubated with 20 μM of rapamycin or BODIPY conjugate **94** for three hours, the media was changed and cells were incubated for one hour to remove excess **94.** This was repeated and after addition of fresh media to the cells for a third time, they were irradiated for 1 minute with the microscope's mCherry filter (43HE, ex. 550/25, em. 605/70). A substantial loss of GFP fluorescence was observed, as well as diffusion into the cytosol. The diffusion into the cytosol indicates a loss of functionality of the remaining FKBP and FRB fusions. A similar assay was performed, but with the use of a membrane localized reporter (data not shown), and **94** was able to similarly disrupt the dimerization. Additionally, quantification of fluorescence in the membrane localization assay showed a 60% loss of GFP fluorescence.

These assays demonstrate that the rapamycin analog **94** is capable of being used as a CALI reagent, but could be further optimized. It is still unclear why the reagent was unable to be used to degrade the proteins involved in the split luciferase assay. It's possible the proteins were oxidized but still functional. Additionally, the rapamycin conjugate **94** is a significantly worse dimerizer than native rapamycin. The washing out of excess **94** could be omitted with lower concentrations of a higher affinity BODIPY rapamycin analog. A high affinity analog may also reduce potential off-target protein degradation in cells.

1.4 Photoswitching Rapamycin

1.4.1 Photoswitching Chromophores

A class of compounds undiscussed to this point is photoswitching chromophores.[114–116] These compounds are able to undergo changes between two distinct structures upon irradiation with different wavelengths of light. Many chromophores have been reported in literature, but only three will be focused on in this document. These three photoswitching motifs are azobenzenes, arylazopyrazoles, and spiropyrans.
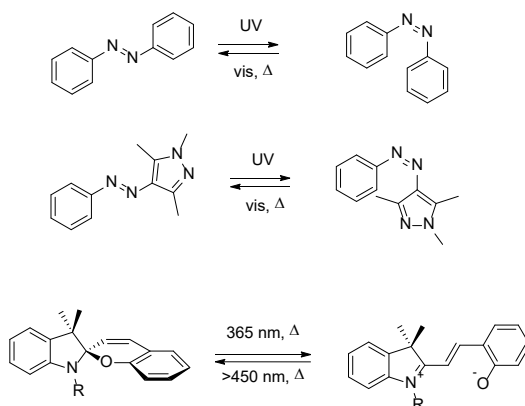
Figure 1.18 - The photoswitching properties of azobenzene, an arylazopyrazole, and a spiropyran are shown.

Azobenzenes are perhaps the best studied and most commonly used of the three chromophores.[117] Azobenzenes undergo a *cis*-to-*trans* isomerizations of the azo bond upon irradiation with either UV or visible light (**Figure 1.18**). The large change in end-to-end distance upon isomerization and reliable switching through multiple cycles with decades of evidence to supporting those properties utility in widespread applications has led many researchers to use it when developing photoswitches in various contexts.[118–120] Irradiation with UV light will cause a π → π* electronic excitation causing *trans*-azobenzenes to convert to *cis*-isomers. Irradiation with

visible light causes a n → π* electronic transition causing *cis*-isomers to switch to *trans*-isomers (**Figure 1.19**). The *cis*-isomer is also generally higher energy than the *trans*-isomer, which drives a thermal isomerization to *trans* in the dark. In addition to light and thermal driven isomerization, azobenzenes are also sensitive to acid catalyzed isomerization.[121] In this instance, protonation of an azo nitrogen reduces double bond character such that isomerization to the thermally favored *trans*-isomer is more readily achieved.
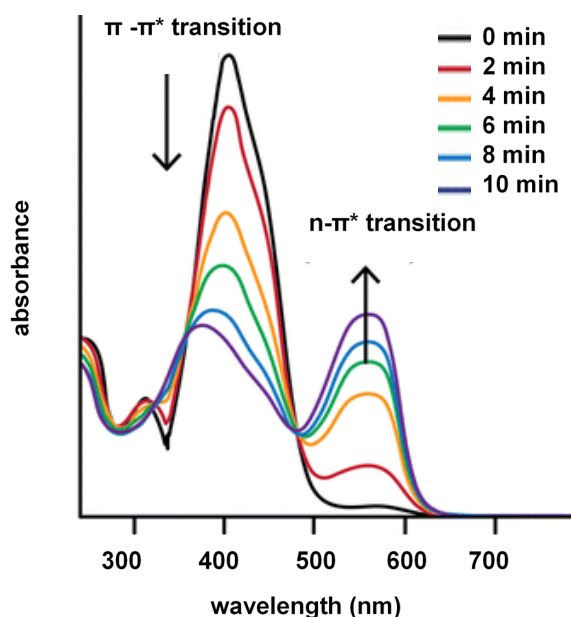
Figure 1.19 - A) A standard UV-vis spectrum of an azobenzene upon irradiation. Wavelengths of the transitions vary based on the electronics the system.[122] Adapted with permission from Park *et al*. Reversible Change of Wettability in Poly(ε-Caprolactone/Azobenzene) Honeycomb-Patterned Films by UV and Visible Light Illumination. Polym. Bull. 2017, 74 (10), 4235–4249. Copyright 2017 Springer Nature.

The second photoswitch shown in **Figure 1.18** is an arylazopyrazole motif, first published as a photoswitch in 2014 by the Fuchter group.[123] While structurally very similar to azobenzene, it contains a pyrazole on one side of the azo and an aryl group on the other side. Like an unsubstituted azobenzene, the best photostationary states are achieved with UV and visible light. Arylazopyrazoles usually have better photostationary states than azobenzene when being converted to the *trans*-isomer. The Ravoo group has rationalized that this is due to a forced twisting of the *cis*-isomer leading to a greater intensity of its n → π* absorbance allowing high

47

yielding conversions to the *trans*-isomer with red light.[124] Additionally, the π → π* of the *trans*-isomer is more than 10 times more intense than the *cis*-isomer at 365 leading to high yields of the *cis*-isomer. Arylazopyrazoles have a longer half-life for the *cis*-isomer than azobenzenes in the dark, often days or longer compared to hours for a common azobenzene.[125] The pyrrole methyl groups perpendicular to the phenyl in the *cis*-isomer lead to an increased energy barrier for transition to the *trans*-isomer.

The third and final motif shown in **Figure 1.18** is a spiropyran. The spiropyran undergoes isomerization to the charged merocyanine form upon irradiation with UV light, and the merocyanine converts back to the spiropyran upon irradiation with long wavelength visible light or thermally in the dark. Although this motif does not undergo as significant a structural change as azobenzenes, a significant property distinct from azobenzene photoswitches is the greater than 10 D change in dipole moment generated by switching between the charged merocyanine and uncharged spiropyran.[126] A second, less commonly utilized feature is the conversion between a planar and non-planar molecule, though it has been used for reversible intercalation of DNA.[127] When a spiropyran is irradiated with UV light, the C-O bond undergoes heterolytic cleavage to generate the merocyanine. The irradiation of the merocyanine with long wavelength light induces conversion back to the spiropyran via electronic excitation of the phenoxide in the pi system.

It should be noted that spiropyran isomerization is highly variable based on the environment it is in. The thermal equilibrium does not generally favor 100% spiropyran, but rather a majority spiropyran mixture in most cases.[128] That equilibrium will change based on the solvent, with more polar solvents favoring a greater merocyanine content. Additionally, the half-life of merocyanines are solvent dependent as well, with more polar solvents increasing the stability of the merocyanine.[128] Spiropyran isomerizations are also pH dependent. In most cases, a low pH will hinder conversion of the merocyanine to the spiropyran since this leads to protonation of the phenoxide which prevents its nucleophilic attack required to form the spiropyran.[129]

1.4.2 Photoswitches in Optical Control of Protein Function

Photoswitches have been used to control protein function through various strategies. One method was published by Schultz *et al.* utilizing an azobenzene containing unnatural amino acid.[130] The amino acid was used to modulate the affinity of a transcriptional regulator for its corresponding promoter enabling reversible transcriptional control with light. This was simply modifying the overall structure of the protein reversibly with an attached photoswitch. A second method pioneered by Trauner *et al.* had a potassium channel inhibitor tethered to the channel

with an azobenzene containing linker.[131] It was designed such that the linker allowed the inhibitor access to the channel as the *trans*-isomer, but as the *cis*-isomer the linker was too short for the inhibitor to reach the channel, thus allowing normal function. Another approach advocated by Trauner is the use of azologs to reversibly control inhibitor activity. Azologization is based on the premise that one isomer of azobenzene resembles various other structural motifs in biologically active molecules, but upon irradiation loses that structural similarity.[132] In the cited paper, the benzyl phenyl ether of fomocaine is azologized to allow for reversible control of the synaptic activity. A final approach used in reversible control of protein function is the introduction of an azobenzene crosslinker between two engineered cysteine residues. By introducing a photoswitchable linker between two cysteine residues of a protein, isomerization of the azobenzene photoswitch will allow for reversible control of protein conformation. Woolley first demonstrated this in peptides[133] and later in proteins.[134]

Photoswitches have been widely studied in biological contexts because of their potential for controlling both the activation and inactivation of biologically active molecules. The ability to define with precision the location and duration of activity of a molecule is the ideal way to study a biomolecule's function, leading to the abundance of research into incorporating photoswitches into biological systems.

1.4.3 Arylazopyrazole Rapamycin

Previously we have discussed both light-activated (**1.2**) and deactivated (**1.3**) rapamycin analogs, but an ideal rapamycin analog would be able to switch reversibly between an activated and deactivated state. This would allow a highly controlled window of activation of protein dimerization thus far unavailable. To achieve this, we considered both arylazopyrazole and spiropyran based photoswitches.
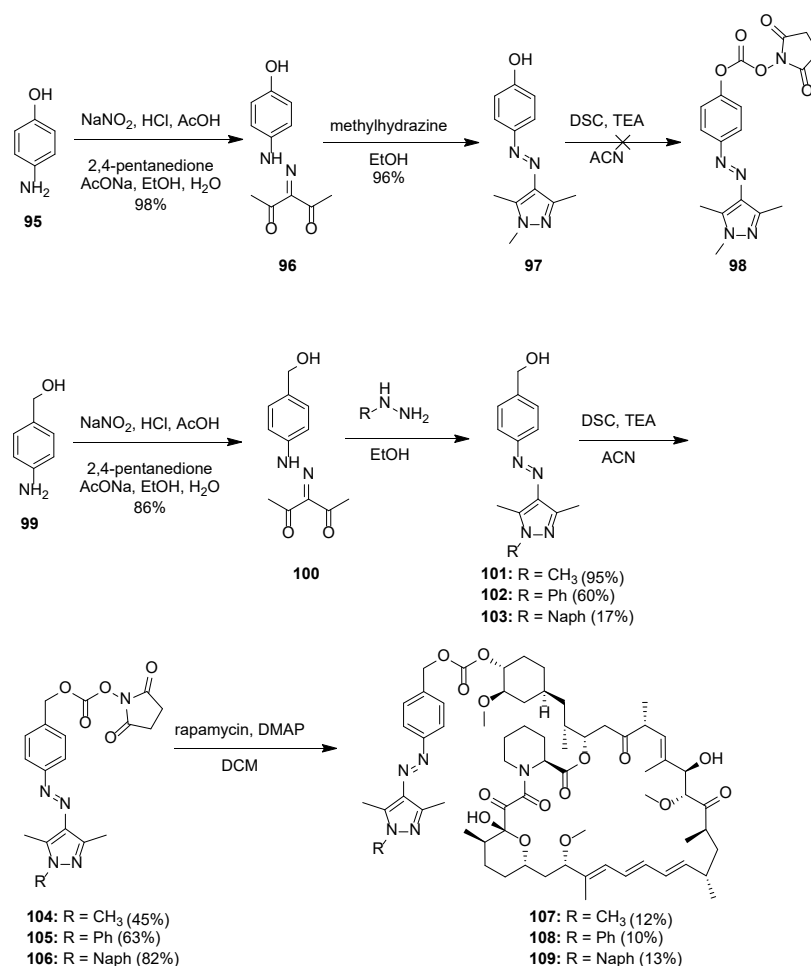
Scheme 1.18 - The syntheses of three arylazopyrazole substituted rapamycin analogs **107**-**109**.

First, we examined the use of arylazopyrazole photoswitches. To keep the photoswitching group as close to rapamycin as possible an attempt to couple rapamycin to the arylazopyrazole through a phenol was attempted (**Scheme 1.18**). The aniline **95** was converted to a diazonium salt and subsequently attacked by the enolate of 2,4-pentanedione to yield **96** in 98% yield.[125] The dione **96** is insoluble in the final reaction solvent allowing for a simple filtration to yield the pure product. The two ketones of **96** then form an imine and enamine with methylhydrazine to yield **97** in 96% yield, being driven forward by the thermodynamic favorability of aromatization and conjugation with the phenyl ring opposite the azo bond.[125] As seen earlier in **Scheme 1.15** with an attempted BODIPY rapamycin conjugation, the conversion of the phenol to an activated carbonate could not be achieved due to the ability of the phenol to function as a leaving group.

This was also the case with **98**, as the phenol of the arylazopyrazole makes the carbonate quite hydrolytically labile.

To circumvent this, a methylene was added via the benzyl alcohol starting material **99**. This was used to generate the dione **100** through the same conditions used to generate **96**. The hydrazine aromatization step is an easy way to incorporate structural diversity into the arylazopyrazole. The use of different hydrazines allows for differently substituted pyrazoles to attach to rapamycin. To test the effect of the steric bulk on the arylazopyrazole, methyl, phenyl, and naphthyl hydrazines were used to form arylazopyrazoles **101-103** respectively. The naphthyl and aryl aromatization reactions never fully progressed leading to the observed lower yields for **102** and **103**. Butyl and ethyl substituted pyrazoles were attempted with the corresponding hydrazines, but curiously no reaction was observed with these reagents. The arylazopyrazole alcohols **101**-**103** were converted to the corresponding NHS carbonates **104**-**106** in yields ranging from 45-82%, and the NHS carbonates were subsequently converted to rapamycin analogs **107**-**109** in 10-13% yields. These yields were lower than most other rapamycin couplings, but this was due to the pyrazole functionality preventing clean separations by column chromatography. The use of pentafluorophenyl carbonates resulted in poorer yields when attempted.
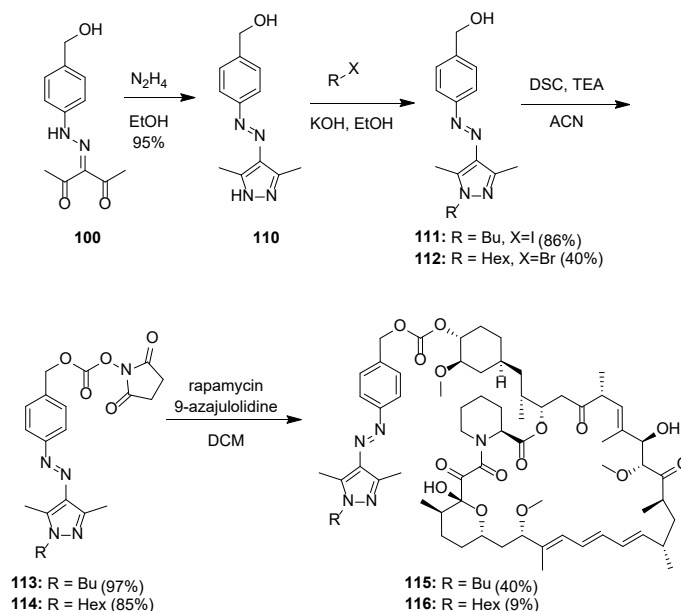
Scheme 1.19 - Syntheses of two rapamycin AAP conjugates **115** and **116**.

To investigate the effects of varying alkyl substituent length on the pyrazole, butyl, and hexyl analogs were synthesized (**Scheme 1.19**). Hydrazine was used to aromatize dione **100** in this case, generating the N-H pyrazole **110**.[124] Compound **110** was reacted with butyl iodide and hexyl bromide in the presence of KOH to yield the corresponding arylazopyrazoles **111** and **112**.[135] Some yield was lost to disubstitution products in these reactions since KOH was able to deprotonate the benzyl alcohol, but attempts to avoid this through the use of milder K_2CO_3 did not yield any product formation. Both butyl and hexyl AAPs were activated in greater than 80% yield as NHS carbonates **113** and **114**, then coupled to rapamycin to yield the butyl and hexyl AAP rapamycin analogs, **115** and **116** respectively.
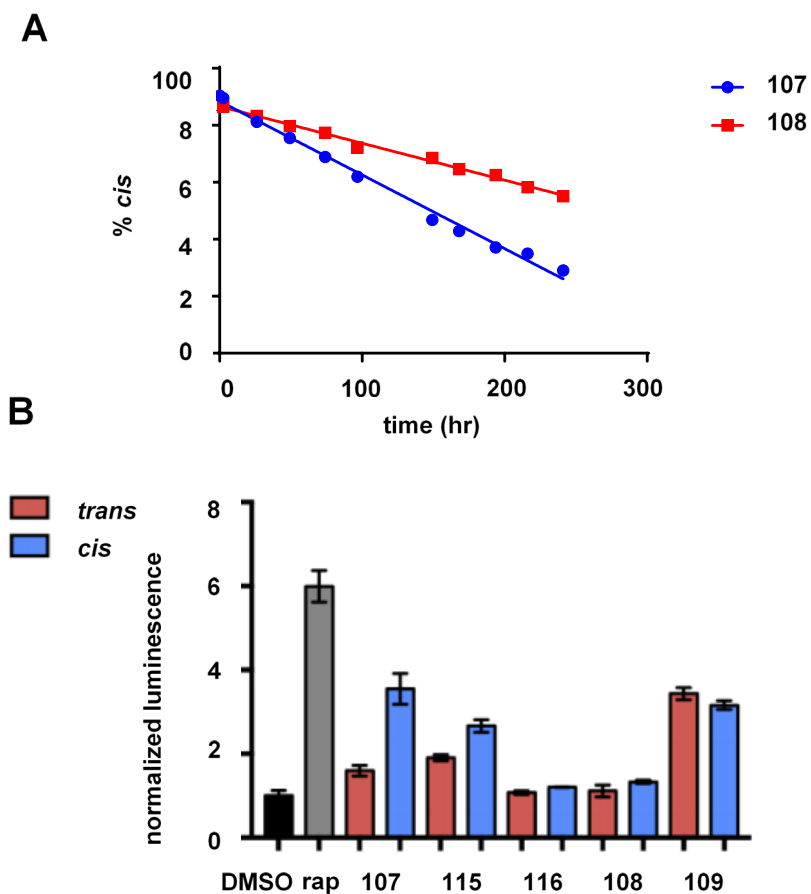
Figure 1.20 - A) Thermal stability of methyl (**107**) and phenyl (**108**) rapamycin analogs were examined by the relative integrations of *cis* and *trans* aryl proton signals in NMR in a deuterated DMSO/water system. B) Experiment run by Taylor Courtney. Relative activities of preformed *cis* and *trans* isomers of various AAP rapamycin analogs in a split luciferase assay in HEK293T cells.

The thermal stability of the methyl and phenyl analogs' *cis*-isomers (**107** and **108** respectively) were monitored by NMR in a deuterated DMSO/water system at 250 μM after a 30 minute irradiation on the Deiters lab UV transilluminator (**Figure 1.20A**). The half-lives were calculated from the plotting of the concentration of the *cis*-isomer, which is linear since the isomerization is zero-order. I did not obtain enough material of the naphthyl analog **109** to analyze the thermal stability and photoswitching; and a re-synthesis is necessary. The *cis*-isomers of the methyl and phenyl analogs were quite long lived with the methyl analog **107** showing a $t_{1/2}$ of 7.2 days and the phenyl analog **108** showing a $t_{1/2}$ of 13.9 days. The longer half-life of **108** could potentially be explained by a π interaction between the two phenyls in the *cis*-isomer. Additionally, the photostationary state of **107** was 91% *cis* with 365 nm irradiation and 95% *trans* with 530 nm irradiation. Phenyl analog **108** demonstrated a photostationary state of 87% *cis* with 365 nm light, and 94% *trans* with 530 nm light. As the N-phenyl electrons are not in conjugation with the arylazopyrazole core, they do not affect its switching wavelengths significantly as evidenced by the similarity in photostationary states of **107** and **108**.

Taylor Courtney tested the analogs in a split luciferase assay that revealed that the analog that showed the greatest selectivity for one isomer over the other was the methyl analog **107** (**Figure 1.20B**). It would make sense if bulkier R groups showed a greater difference in binding due to the larger change in overall structure upon isomerization, but this was not seen. A potential reason for this would be a hydrophobic effect allowing the larger R groups to increase binding favorability relative to the smaller groups. This could be easily tested by introducing a more polar group into the R group such as a carboxylic acid or amine.

With relatively poor selectivity demonstrated among these analogs, two options could be pursued to increase selectivity of one isomer over the other. Since variability is easily introduced to the pyrazole through different hydrazines or alkyl halides, more compounds could be screened to find a better analog using the current FKBP/FRB system. Alternatively, the days-long half-lives of the *cis*-isomers may allow for evolution of a *cis*-isomer specific FKBP/FRB system.

Beyond the selectivity concerns, it will also be essential to demonstrate reversibility of the binding in cells. Up to this point, only pre-irradiated arylazopyrazole-rapamycin conjugates have been used. If the ternary complex cannot be broken with light irradiation, there is substantially less incentive to use the system.

1.4.4 Spiropyran Rapamycin

In addition to the arylazopyrazole based photoswitches, it was thought that spiropyrans could prove an effective photoswitch to conjugate to rapamycin. The introduction of a charged merocyanine onto rapamycin may cause a substantial electrostatic repulsion more significant than that of sterics. Spiropyrans have been shown to modulate conformation and activity of proteins, so the incorporation of a spiropyran near the ternary complex could potentially disrupt it.[136,137]
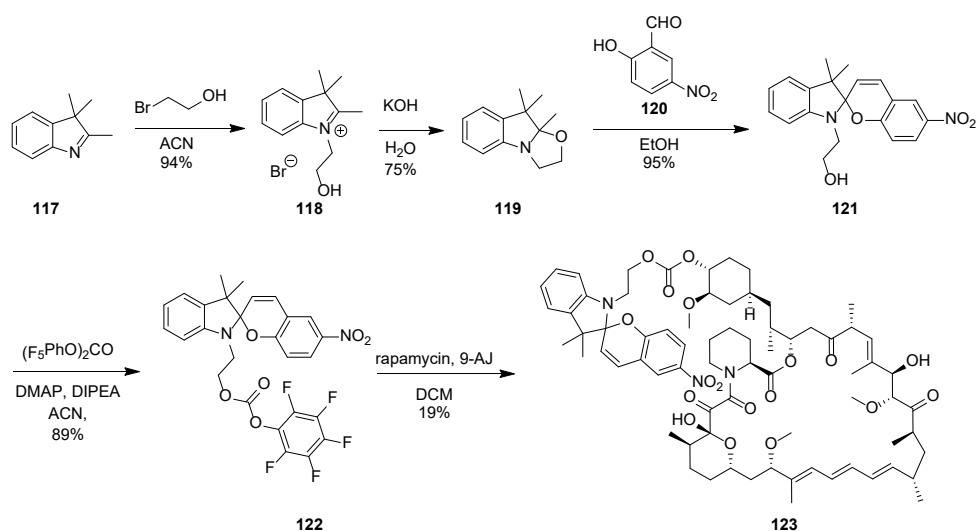
Scheme 1.20 - The synthesis of the spiropyran conjugated rapamycin analog **123**.

To synthesize a spiropyran conjugated rapamycin analog, the spiropyran was first synthesized from indolenine **117** (**Scheme 1.20**). The first step was a S_N2 substitution onto bromoethanol to give **118**, followed by cyclization to give **119**. The tricyclic indole then underwent a tandem substitution, condensation reaction with **120** to yield the spiropyran alcohol **121**. The alcohol was converted to the activated carbonate **122** and coupled to rapamycin to give **123** in 19% yield. Some product in the final rapamycin coupling was likely lost due to merocyanine formation in purification. Photoswitching was confirmed for rapamycin conjugate **123** in DMSO by NMR (data not shown).

Taylor Courtney tested the spiropyran conjugate **123** in a split luciferase assay and found that it showed very poor selectivity for one form over the other (**Figure 1.21**). Generally, the merocyanine was favored, but only by about 2-fold at 100 nM. Additionally, the binding seemed to be poor relative to rapamycin which is unsurprising due to the size of the spiropyran attached.
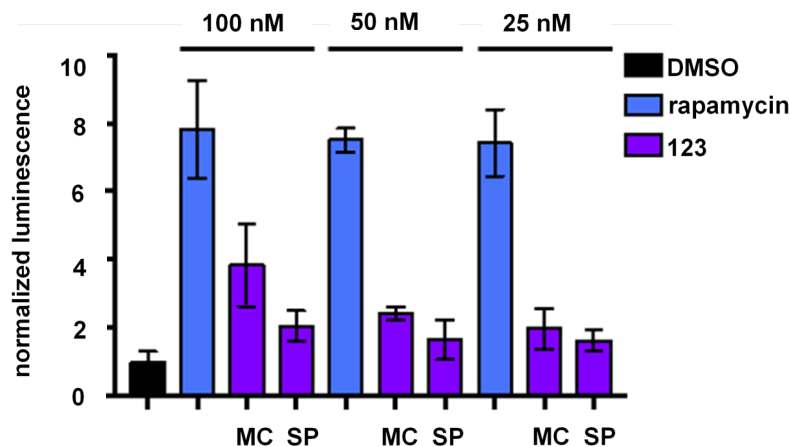
Figure 1.21 - Experiment performed by Taylor Courtney. Split luciferase assay in HEK293T cells at various concentration. MC is merocyanine which was generated with 447.5 nm light. SP is spiropyran which was generated with 365 nm light. The two forms of the photoswitch are shown in **Figure 1.18**.

There are two potential methods to optimize the system to improve preference for one form over the other. One method would be to mutate residues on the FKBP-FRB interface where the spiropyran is attached to rapamycin to try to make it more or less polar to better favor either the merocyanine or spiropyran form. This could be done in complement to the second method of improving the system; adding groups to one of the phenyl groups to try and increase activity of one form over the other.

1.5 Conclusions and Outlook

Several photocaged rapamycin analogs were examined in this chapter. An ANBP caged rapamycin was shown to effectively limit rapamycin activity until irradiated with visible light. The dimeric form of the ANBP photocage appears to be attainable with optimization. Several BIST caged compounds were examined, but release of the compounds after photolysis could not be achieved. A BODIPY caged rapamycin was also unable to be synthesized, but with optimization

of reaction conditions should be possible. BODIPY groups would likely be ideal photocages due to the low dimerization ability of the BODIPY conjugated rapamycin analogs examined in **1.3.3**.

The synthesis of an eosin or Ru(II) conjugated rapamycin for CALI of ternary complex formation could not be achieved. The Ru(II) conjugated rapamycin analog could not be synthesized due to salt exchange occurring in the final rapamycin click reaction. Use of a strained alkyne could avoid this issue in the future. Two ROS generating BODIPY-rapamycin conjugates were synthesized with different linkers. The degradation of the ternary complex was shown, but there was variability in effectiveness between assays. Also, an ROS generator-rapamycin conjugate with higher binding affinity for FKBP and FRB would be an advantage as the better of the two analogs synthesized still had a substantially worse binding affinity than native rapamycin. This could be accomplished by experimenting with longer linkers.

Several photoswitching rapamycin analogs were synthesized and tested for differential dimerization abilities between the two states of the photoswitch. Several arylazopyrazole analogs were tested, but many showed poor selectivity for one isomer over the other with the methylated arylazopyrazole showing the best with 2-4 fold higher binding affinity in the *cis*-isomer than in the *trans*-isomer. Differently substituted pyrazoles to identify a better analog would be easy to synthesize with the groundwork laid out here, but an alternative would be evolving a FKBP/FRB system that prefers one isomer over the other. A spiropyran conjugated rapamycin was also synthesized, but use in dimerization assays demonstrated only a 2-fold increase in binding for the merocyanine form over the spiropyran. Attempting to optimize this system would likely be time-consuming, and the diversity is synthetically easier to introduce with the arylazopyrazole.

1.6 Experimental

LED Light Sources

405 nm: LEDENGIN LZ1-10UA00-00U8 (purchased from Mouser Electronics)

415 nm: LUMILEDS LHUV-0415-0650 (purchased from Mouser Electronics)

447.5 nm: LUMILEDS LXML-PR02-A900 (purchased from Mouser Electronics)

530 nm: LUMILEDS LXML-PM01-0100 (purchased from Mouser Electronics)

General Procedures

All chemicals obtained from commercial sources were used without further purification unless stated otherwise. All reactions were performed in flame dried glassware under nitrogen

atmosphere and stirred magnetically unless otherwise indicated. For compound drying, the solution was passed over a pad of sodium sulfate on cotton in a funnel and the filtrate was collected. The solid was then washed with 2-3 times the solvent dried. For reactions run in a microwave reactor, a CEM Discover System (Model No. 908005) was used with a closed vessel. ^{1}H NMR spectra were obtained from a Bruker Avance III 400 MHz or Bruker Avance III 500 MHz with chemical shifts reported relative to either residual CHCl$_3$ (7.26 ppm), DMSO (2.50 ppm), or CH$_3$OD (3.30 ppm). Mass spectrometry was performed by University of Pittsburgh facilities.

Compounds **16**,[47] **26**,[57] **32**,[59] **52**,[65] **55**,[65] **66**,[103] **67**,[104] **68**,[104] **74**,[107] **75**,[107] **78**,[108] **86**,[112] **90**,[113] **91**,[113] **96**,[125] **97**,[125] **117**,[126] **118**,[126] **119**,[126] and **121**[126] were synthesized according to literature syntheses without any modifications and obtained yields matched reported ones.

1-(4'-(Dimethylamino)-4-nitro-[1,1'-biphenyl]-3-yl)ethan-1-ol (17). A solution of benzyl alcohol **16** (53 mg, 0.22 mmol, 1 eq), potassium carbonate (75 mg, 0.54 mmol, 2.5 eq), TBAB (65 mg, 0.22mmol, 1 eq), the phenylboronic acid (42 mg, 0.25 mmol, 1.1 eq), and palladium acetate (6 mg, 0.026 mmol, 0.1 eq) were suspended in ethanol (1.3 mL) and water (0.7 mL). The reaction mixture was heated in a microwave reactor in temperature mode to 90 °C for 15 minutes with stirring and cooling via the air flow feature of the instrument. The reaction mixture was diluted with brine (3 mL) and DCM (10 mL), and the DCM was collected. The organic layer was dried over sodium sulfate (approximately 500 mg), concentrated in vacuo, and the residue was purified via flash chromatography on silica gel (20% ethyl acetate in hexanes) to yield **17** as an orange solid (48 mg, 76% yield). ^{1}H NMR (500 MHz, CDCl$_3$) δ 8.00 (d, 2 H, J = 5.5 Hz), 7.57 (m, 3 H), 6.81 (d, 2 H, J = 7.5 Hz), 5.44 (q, 1 H, J = 4 HZ), 3.03 (s, 6 H), 1.62 (d, 3 H, J = 4 Hz); ^{13}C NMR (500 MHz, CDCl3) δ 150.9, 146.8 145.2, 141.9, 140.9, 133.6, 128.1, 126.0, 124.9, 112.6, 66.0, 40.3, 24.2; HRMS (ESI[+]) calcd for C$_{16}$H$_{19}$O$_3$N$_2$ (M+H)[+] 287.1390, found 287.1406.

1-(4'-(Dimethylamino)-4-nitro-[1,1'-biphenyl]-3-yl)ethyl (perfluorophenyl) carbonate (18). A solution of biphenyl **17** (25 mg, 0.09 mmol, 1 eq) and bis(pentafluorophenyl) carbonate (31 mg, 0.12 mmol, 1.3 eq) in dry acetonitrile (1 mL) under Ar was prepared. Triethylamine (0.05 mL, 0.36 mmol, 4 eq) was added and the reaction mixture was stirred at room temperature for 2 hours. The reaction mixture was concentrated in vacuo and the residue was purified via flash chromatography (gradient 25% ethyl acetate in hexanes → 50% ethyl acetate in hexanes) to yield **18** as a red solid (35 mg, 91% yield). ^{1}H NMR (500 MHz, CDCl$_3$) δ 8.12 (d, 1 H, J = 9 Hz), 7.90 (s, 1 H), 7.66 (d, 1 H, J = 8.5 Hz), 7.59 (d, 2 H, J = 9 Hz), 6.84 (d, 2 H, J = 8.5 Hz), 6.56 (q, 1 H, J = 6.5 Hz), 3.07 (s, 6 H), 1.85 (d, 3 H, J = 6.5 Hz).

ANBP rapamycin (19). A solution of the NHS carbonate **18** (35 mg, 0.2 mmol, 2 eq), rapamycin (96 mg, 0.1 mmol, 1 eq) and DMAP (65 mg, 0.5 mmol, 5 eq) in dry acetonitrile (1 mL)

under an inert atmosphere (Ar) was prepared. The reaction mixture was stirred at room temperature under Ar for 24 hours, then concentrated in vacuo, and the residue was purified via flash chromatography (gradient 10% ethyl acetate in DCM → 25% ethyl acetate in DCM) to yield **19** as an orange solid (13 mg, 10% yield). ^{1}H NMR (500 MHz, CD$_3$OD) δ 8.06 (d, 1 H, J = 8.5 Hz), 7.84 (s, 1 H), 7.69 (d, 1 H, J = 8.5 Hz), 7.59 (d, 2 H, J = 9 Hz), 6.84 (d, 2 H, J = 9 Hz), 6.24 (d, 1 H, J = 7 Hz), 6.24 (m, 2 H), 6.19 (q, 1 H, J = 6.5 Hz), 6.07 (d, 1 H, J = 11 Hz), 5.48 (m, 1 H), 5.22 (m, 1 H), 5.04 (m, 2 H), 4.4 (m, 1 H), 4.12 (m, 1 H), 3.95 (d, 1 H, J = 5 Hz), 3.66 (d, 1 H, J = 11.5 Hz), 3.52 (m, 1 H), 3.39 (d, 1 H, 8 Hz), 3.34 (s, 2 H), 3.24 (s, 3 H), 3.07 (s, 6 H), 2.83 (m, 1 H), 2.62 (m, 1 H), 2.46 (dd, 1 H, J = 8, 2.5 Hz), 2.21 (m, 3 H), 1.98 (m, 2 H), 1.85 (d, 2 H, J = 8 Hz), 1.80 (d, 2 H, J = 2.5 Hz), 1.71 (s, 3 H), 1.6 (m, 4 H), 1.42 (m, 4 H), 1.29 (b, 1 H), 1.13 (m, 1 H), 0.98 (d, 3 H, J = 7 Hz), 0.94 (d, 2 H, J = 6.5 Hz), 0.85 (m, 2 H), 0.83 (m, 4 H), 0.74 (q, 1 H, J = 7 Hz); ^{13}C NMR (500 MHz, CDCl$_3$) δ 208.6, 167.8, 151.3, 137.7, 132.7, 130.9, 127.7, 127.6, 127.0, 125.1, 112.4, 99.3, 83.4, 80.9, 78.1, 77.9, 77.6, 76.2, 74.1, 71.8, 67.2, 57.0, 56.5, 56.3, 54.9, 40.1, 39.9, 35.8, 31.3, 29.3, 26.4, 24.8, 24.6, 22.3, 20.8, 20.7, 20.4, 14.7, 14.5, 13.2, 12.9, 10.5, 9.9; HRMS (ESI$^+$) calcd for C$_{68}$H$_{96}$O$_{17}$N$_3$ (M+H)$^+$ 1226.6734, found 1226.6721.

4'-(Dimethylamino)-4-nitro-[1,1'-biphenyl]-3-carbaldehyde (20). A solution of benzaldehyde **12** (50 mg, 0.22 mmol, 1 eq), boronic acid **16** (43 mg, 0.26 mmol, 1.2 eq), Pd(PPh$_3$)$_3$ (5 mg, cat.), and Cs$_2$CO$_3$ (114 mg, 0.59 mmol, 2.7 eq) in water (1 mL) and ethanol (1.5 mL) was stirred at room temperature for 45 minutes. The reaction was diluted with water (2 mL) and extracted with DCM (2 x 5 mL), the organic layers were dried over approximately sodium sulfate (approximately 250 mg), concentrated in vacuo, and purified via flash chromatography on silica gel (gradient 0% ethyl acetate in hexanes → 10% ethyl acetate in hexanes) to yield **20** as a red solid (52 mg, 88% yield). ^{1}H NMR (500 MHz, CDCl$_3$) δ 10.47 (s, 1 H), 8.11 (d, 1 H, J = 10 Hz), 8.01 (s, 1 H), 7.81 (d, 1 H, J = 8 Hz), 7.55 (d, 2 H, J = 10 Hz), 6.74 (m, 2 H), 3.00 (s, 6 H); ^{13}C NMR (500 MHz, CDCl$_3$) δ 189.1, 151.3, 147.8, 146.9, 132.5, 129.4, 128.8, 128.2, 126.0, 125.5, 112.5, 40.2.

1-(4'-(Dimethylamino)-4-nitro-[1,1'-biphenyl]-3-yl)but-3-yn-1-ol (21). Activated Zn powder (100 mg, 1.53 mmol, 2.1 eq) suspended in DMF (1.5 mL) was cooled to 0 °C. Propargyl bromide (80 wt% in toluene, 0.11 mL, 0.88 mmol, 1.5 eq) was added and stirred for one hour. A solution of benzaldehyde **20** (163 mg, 0.62 mmol, 1 eq) in DMF (1 mL) was added dropwise and stirred for 30 minutes. The reaction was diluted with DCM (10 mL) and washed with 1 N HCl (2 x 10 mL), the organic layer was dried over sodium sulfate (approximately 500 mg), concentrated in vacuo, and purified via flash chromatography on silica gel (gradient hexanes → 0% ethyl acetate in DCM → 15% ethyl acetate in DCM) to yield **21** as a red solid (126 mg, 68% yield). ^{1}H NMR

(500 MHz, CDCl$_3$) δ 8.09 (d, 2 H, 10 Hz), 7.63 (m, 3 H), 6.82 (d, 2 H, J = 10 Hz), 5.62 (m, 1 H, J = 4 Hz), 3.06 (s, 6 H), 2.99 (m, 1 H), 2.78 (m, 1 H), 2.75 (m, 1 H), 2.15 (t, 1 H, J = 4 Hz); ^{13}C NMR (500 MHz, CDCl$_3$) δ 146.8, 145.0, 138.6, 128.2, 125.7, 125.4, 125.0, 112.5, 80.1, 71.7, 67.8, 40.3, 28.5.

1-(4'-(Dimethylamino)-4-nitro-[1,1'-biphenyl]-3-yl)but-3-yn-1-yl (perfluorophenyl) carbonate (22). Alcohol **21** (60 mg, 0.22 mmol, 1 eq), bis(pentafluorophenyl) carbonate (102 mg, 0.26 mmol, 1.2 eq), and DMAP (5 mg, cat.) were dissolved in acetonitrile (3 mL). DIPEA (0.075 mL, 0.44 mmol, 2 eq) was added and the reaction was stirred at room temperature for 1 hour. The solution was concentrated in vacuo and purified via flash chromatography on silica gel (gradient 0% ethyl acetate in hexanes → 20% ethyl acetate in hexanes) to yield **22** as a red solid (103 mg, 97% yield). The product was used without further characterization.

Alkynyl ANBP rapamycin (23). bis(pentafluorophenyl) carbonate **22** (103 mg, 0.213 mmol, 3 eq), rapamycin (65 mg, 0.071 mmol, 1 eq), and 9-azajulolidine (62 mg, 0.355 mmol, 5 eq) were dissolved in DCM (3 mL) and was stirred overnight at room temperature. The solution was concentrated in vacuo and purified via flash chromatography on silica gel (gradient 0% ethyl acetate in DCM → 20% ethyl acetate in DCM) to yield **23** as a red solid (36 mg, 40% yield). ^{1}H NMR (500 MHz, CDCl$_3$) δ 8.03 (t, 1 H, J = 5 Hz), 7.86 (s, 1 H), 7.55 (d, 1 H, J = 5 Hz), 7.48 (m, 2 H), 6.73 (m, 2 H), 6.40 (q, 1 H, J = 2.5 Hz), 6.30 (m, 2 H), 6.07 (dd, 1 H, J = 5, 2.5 Hz), 5.85 (m, 1 H), 5.45 (m, 1 H), 5.32 (m, 2 H), 5.09 (t, 1 H), 4.75 (d, 1 H, J = 5 Hz), 4.41 (m, 1 H), 4.05 (m, 1 H), 3.79 (m, 1 H), 3.61 (m, 3 H), 3.31 (m, 6 H), 3.09 (m, 4 H), 2.96 (d, 6 H, 5 Hz), 2.89 (m, 1 H), 2.69 (m, 1 H), 2.50 (dd, 1 H, J = 4, 2.5 Hz), 2.37 (m, 2 H), 2.03 (m, 4 H), 1.91 (m, 1 H), 1.72 (m, 3 H), 1.45 (m, 4 H), 1.28 (m, 4 H), 1.09 (d, 2 H, J = 7 Hz), 1.01 (d, 2 H, J = 7.5 Hz), 0.98 (m, 4 H), 0.87 (m, 4 H), 0.76 (q, 1 H, J = 7.5 Hz); ^{13}C NMR (500 MHz, CDCl$_3$) δ 169.2, 153.7, 151.0, 144.9, 144.8, 135.6, 135.3, 133.7, 103.2, 128.2, 126.4, 125.8, 125.7, 124.9, 124.7, 112.5, 112.4, 98.5, 80.9, 80.7, 78.8, 72.6, 72.5, 71.5, 67.2, 59.4, 59.3, 57.6, 57.3, 55.9, 51.3, 46.6, 44.2, 41.4, 40.7, 40.3, 40.2, 38.2, 35.9, 35.1, 34.7, 33.7, 32.8, 31.6, 31.3, 29.7, 29.5, 29.1, 27.3, 27.0, 25.9, 25.3, 22.7, 21.5, 17.9, 17.4, 15.5, 13.4, 13.1, 12.6, 12.1, 9.8, 9.1; HRMS (ESI$^+$) calcd for C$_{70}$H$_{96}$O$_{17}$N$_3$ (M+H)$^+$ 1250.6734, found 1250.6701.

3-Azidopropyl (2,5-dioxopyrrolidin-1-yl) carbonate (27). A solution of 3-azidopropan-1-ol **26** (65 mg, 0.64 mmol, 1 eq) in dry acetonitrile (5 mL) under nitrogen was prepared. DSC (296 mg, mmol, eq) and triethylamine (0.1 ml, 0.72 mmol, 1.1 eq) were added and the reaction mixture was stirred overnight at 60 °C. The reaction mixture was diluted with ethyl acetate (10 mL) and washed with water (4 x 5 mL) and brine (2 x 5 mL). The organic layer was dried over sodium sulfate (approximately 500 mg), concentrated in vacuo, and the residue was purified via

flash chromatography on silica gel (5% methanol in DCM) to yield **27** as a colorless oil (150 mg, 96% yield). ^{1}H NMR (500 MHz, CDCl$_3$) δ 4.42 (t, 2 H, J = 6.5 Hz), 3.47 (t, 2 H, J = 6.5 Hz), 2.84 (s, 4 H), 1.99 (pent, 2 H, J = 6.5 Hz).

Propylazido rapamycin (28). A solution of NHS carbonate **27** (191 mg, 0.79 mmol, 5 eq), DMAP (59 mg, 0.48 mmol, 2 eq), and rapamycin (135 mg, 0.15 mmol, 1 eq) in dry DCM (2 mL) was stirred at room temperature for 4 hours. The reaction mixture was then diluted with ethyl acetate (10 mL) and washed with pH 3 HCl (2 x 7 mL), water (2 x 7 mL), and brine (7 mL). The organic layer was dried over sodium sulfate (approximately 500 mg), concentrated in vacuo, and the residue was purified via flash chromatography on silica gel (gradient 15% ethyl acetate in DCM → 25% ethyl acetate in DCM) to yield **28** as a white solid (47 mg, 31% yield). ^{1}H NMR (500 MHz, CD$_3$OD) δ 6.45 (dd, 1 H, J = 11, 9.5 Hz), 6.27 (dd, 1 H, J = 11, 10 Hz), 6.10 (m, 2 H), 5.45 (m, 1 H), 5.24 (d, 1 H, J = 13 Hz), 5.06 (m, 1 H), 4.43 (m, 1 H), 4.19 (m, 3 H), 3.98 (d, 1 H, J = 6.5 Hz), 3.68 (m, 1 H), 3.47 (t, 2 H, J = 6.5 Hz), 3.19 (m, 2 H), 3.13 (s, 3 H), 2.80 (dd, 1 H, J = 11, 3 Hz), 2.62 (m, 1 H), 2.49 (dd, 1 H, J = 11, 7 Hz), 2.33 (m, 1 H), 2.12 (m, 1 H), 2.05 (m, 2 H), 1.92 (m, 2 H), 1.75 (s, 3 H), 1.70 (m, 2 H), 1.65 (s, 3 H), 1.44 (m, 4 H), 1.31 (m, 2 H), 1.15 (m, 1 H), 1.11 (m, 2 H), 1.04 (m, 4 H), 0.98 (m, 4 H), 0.88 (m, 4 H), 0.79 (q, 1 H, J = 7 Hz). HRMS (ESI$^+$) calcd for C$_{55}$H$_{83}$O$_{15}$N$_4$ (M+H)$^+$ 1039.5849, found 1039.5825.

Propargyl alcohol clicked rapamycin (29). A suspension of azido rapamycin **28** (10 mg, 0.01 mmol, 1 eq), copper sulfate (2.1 mg, 0.01 mmol, 1 eq), sodium ascorbate (2.4 mg, 0.01 mmol, 1 eq), in *tert*-butanol (0.75 mL) was created. Water (0.75 mL) was added, followed by propargyl alcohol (16 mg, 0.30 mmol, 30 eq), and the reaction mixture was stirred overnight. The reaction mixture was diluted with ethyl acetate (5 mL) and washed with water (4 x 4 mL). The organic layer was concentrated in vacuo and the residue was purified via flash chromatography on silica gel (5% methanol in DCM) to yield a white solid (9 mg, 85% yield). ^{1}H NMR (500 MHz, CD$_3$OD) δ 7.88 (s, 1 H), 6.38 (dd, 1 H, J = 11, 9 Hz), 6.23 (dd, 1 H, J = 11, 8.5 Hz), 6.15 (dd, 1 H, J = 9, 8.5 Hz), 6.06 (d, 1 H, J = 10 Hz), 5.45 (m, 1 H), 5.19 (d, 1 H, J = 7 Hz), 5.06 (m, 1 H), 4.63 (s, 2 H), 4.43 (m, 3 H), 4.19 (m, 4 H), 3.98 (d, 1 H, J = 6.5 Hz), 3.68 (m, 1 H), 3.47 (t, 2 H, J = 7 Hz), 3.19 (q, 2 H, J = 7 Hz), 3.13 (s, 3 H), 2.80 (m, 1 H), 2.62 (m, 1 H), 2.47 (dd, 1 H, J = 7, 3.5 Hz), 2.34 (m, 3 H), 2.12 (m, 2 H), 2.07 (m, 2 H), 1.88 (d, 1 H), 1.75 (s, 3 H), 1.70 (m, 4 H), 1.65 (s, 3 H), 1.62 (m, 2 H) 1.44 (m, 4 H), 1.31 (t, 2 H, J = 7 Hz), 1.15 (m, 1 H), 1.11 (m, 2 H), 1.04 (m, 4 H), 0.98 (m, 4 H), 0.88 (m, 4 H); ^{13}C NMR (500 MHz, CD$_3$OD) δ 169.0, 154.2, 143.7, 139.8, 134.6, 127.7, 99.2, 84.3, 83.9, 83.4, 82.1, 80.9, 80.7, 76.2, 74.2, 65.7, 63.2, 59.3, 57.0, 56.4, 54.9, 54.0, 51.3, 45.6, 44.9, 44.0, 41.2 40.7, 40.0, 35.5, 35.1, 34.6, 34.5, 31.3, 30.7, 29.2, 27.5, 27.0,

26.3, 24.9, 23.5, 22.3, 20.3, 17.6 14.8, 14.5, 14.2, 13.0, 12.9, 12.4, 9.6; HRMS (ESI$^+$) calcd for $C_{58}H_{89}O_{16}N_4$ (M+H)$^+$ 1097.6268, found 1097.6268.

Clicked BIST rapamycin dimer (31). A solution of the dialkyne **30** (3 mg, 0.005 mmol, 1 eq), copper iodide (12 mg, 0.063 mmol, 12 eq), and azido rapamycin **28** (11 mg, 0.011 mmol, 2.1 eq) in dry DCM (0.4 mL) under nitrogen was prepared. DIPEA (0.05 mL, 0.5 mmol, 100 eq) was added and the reaction mixture was stirred for 15 hours. The reaction mixture was concentrated in vacuo and the residue was purified via flash chromatography on silica gel (55% ethyl acetate in DCM) to yield **31** as a red solid (9 mg, 69% yield). ^{1}H NMR (500 MHz, CD$_3$OD) δ 8.03 (d, 2 H, J = 8.5 Hz), 7.70 (s, 2 H), 7.53 (d, 2 H, J = 8.5 Hz), 7.31 (d, 2 H, J = 11 Hz), 7.13 (s, 2 H), 6.95 (d, 2 H, J = 11 Hz) 6.38 (m, 4 H), 6.18 (dd, 2 H, J = 9, 4 Hz), 5.97 (d, 2 H, J = 9 Hz), 5.53 (dd, 2 H, J = 9, 4 Hz), 5.41 (d, 2 H, J = 6 Hz), 5.29 (m, 2 H), 5.15 (m, 1 H), 4.51 (m, 6 H), 4.13 (m, 6 H), 3.88 (t, 2 H, J = 7 Hz), 3.68 (m, 1 H), 3.52 (m, 4 H), 3.42 (s, 6 H), 3.32 (s, 4 H), 2.95 (d, 2 H, J = 4.5 Hz), 2.73 (m, 2 H), 2.33 (m, 8 H), 2.07 (m, 4 H), 1.88 (m, 8 H), 1.75 (s, 6 H), 1.70 (m, 8 H), 1.65 (s, 3 H), 1.62 (m, 4 H) 1.46 (m, 8 H), 1.31 (t, 4 H, J = 7 Hz), 1.21 (m, 2 H), 1.13 (m, 4 H), 1.07 (m, 8 H), 0.96 (m, 4 H), 0.88 (m, 4 H); HRMS (ESI$^+$) calcd for $C_{142}H_{196}O_{40}N_{10}S$ (M+H)+ 2711.3033, found 2711.3040.

(2-Nitro-5-vinylphenyl)methanol (33). A solution of benzyl alcohol **32** (450 mg, 2 mmol, 1 eq) and tetrakis palladium triphenylphosphine (47 mg, 0.3 mmol, 0.15 eq) in 19 mL dimethoxyethane was prepared. A solution of potassium carbonate (267 mg, 2 mmol, 1 eq) in water (5.5 mL) was added to the reaction mixture. Vinylboronic anhydride pyridine complex (243 mg, 1 mmol, 0.5 eq) was added and the reaction mixture was stirred at 110 °C for 22 hours. The reaction mixture was concentrated in vacuo and the residue was purified via flash chromatography on silica gel (gradient 0% ethyl acetate in hexanes → 30% ethyl acetate in hexanes) to yield **33** as an orange solid (346 mg, 97% yield). ^{1}H NMR (500 MHz, CDCl$_3$) δ 8.10 (d, 1 H, J = 8 Hz), 7.74 (s, 1 H), 7.47 (d, 1 H, J = 6.5 Hz), 6.77 (dd, 1 H, J = 17.5, 11 Hz), 5.95 (d, 1 H, J = 17.5 Hz), 5.51 (d, 1 H, J = 11 Hz), 4.99 (d, 2 H, J = 6.5 Hz), 2.55 (t, 1 H, J = 6.5 Hz). ^{13}C NMR (500 MHz, CDCl$_3$) δ 146.5, 143.4, 143.0, 137.4, 134.9, 127.6, 125.8, 118.8, 62.7; HRMS (ESI$^+$) calcd for $C_9H_8O_3N$ (M+H)$^+$ 178.0504, found 178.0495.

***tert*-Butyldimethyl((2-nitro-5-vinylbenzyl)oxy)silane (34).** A solution of styrene **33** (365 mg, 2 mmol, 1 eq), TBSCl (338 mg, 2.2 mmol, 1.1 eq), and imidazole (152 mg, 2.2 mmol, 1.1 eq) in dry acetonitrile (10 mL) under nitrogen was stirred at room temperature for 1.5 hours. The reaction mixture was diluted with ethyl acetate (5 mL), filtered, the filtrate was concentrated in vacuo, and the residue was purified via flash chromatography on silica gel (5% ethyl acetate in hexanes) to yield **34** as an orange solid (545 mg, 93% yield). ^{1}H NMR (500 MHz, CDCl$_3$) δ 8.10

(d, 1 H, J = 8 Hz), 7.96 (s, 1 H), 7.40 (d, 1 H, J = 8.5 Hz), 6.79 (dd, 1 H, J = 17.5, 11 Hz), 5.93 (d, 1 H, J = 17.5 Hz), 5.48 (d, 1 H, J = 11 Hz), 5.12 (s, 2 H), 0.99 (s, 9 H), 0.16 (s, 6 H); ^{13}C NMR (500 MHz, CDCl$_3$) δ 145.3, 143.7, 143.0, 138.9, 135.5, 127.9, 125.2, 118.1, 62.2, 34.7, 31.6, 22.6, 14.1; HRMS (ESI$^+$) calcd for C$_{15}$H$_{24}$O$_3$NSi (M+H)$^+$ 294.1520, found 294.1537.

2,5-Bis((*E*)-3-(((*tert*-butyldimethylsilyl)oxy)methyl)-4-nitrostyryl)thiophene   (35). A solution of styrene **34** (78 mg, 0.27 mmol, 3 eq), 2,5-dibromothiophene (10 μL, 0.09 mmol, 1 eq), LiCl (12 mg, 0.3 mmol, 3.3 eq), NaHCO$_3$ (25 mg, 0.3 mmol, 3.3 eq), TBACl (40 mg, 0.15 mmol, 1.67 eq) in dry DMF (2 mL) under argon was prepared. TPGS-750-M (0.2 mL) and Pd(OAc)$_2$ (5 mg, 0.02 mmol, 0.25 eq) were added. The reaction mixture was heated for 110 °C for 1 hour. The reaction mixture was diluted with ethyl acetate (10 mL), washed with water (4 x 4 mL) and brine (4 mL), dried over sodium sulfate (approximately 500 mg), and concentrated in vacuo. The residue was purified via flash chromatography on silica gel (5% ethyl acetate in hexanes) to yield **35** as a red solid (40 mg, 66% yield). ^{1}H NMR (500 MHz, CDCl$_3$) δ 8.12 (d, 2 H, J = 8 Hz), 7.98 (s, 2 H), 7.46 (d, 2 H, J = 8 Hz), 7.01 (d, 2 H, J = 17.5 Hz), 5.38 (d, 4 H), 5.13 (s, 2 H), 5.10 (d, 2 H, J = 17.5 Hz), 0.99 (s, 18 H), 0.16 (s, 12 H); ^{13}C NMR (500 MHz, CDCl$_3$) δ 144.9, 142.4, 142.3, 139.3, 135.5, 129.1, 127.1, 125,7, 125.6, 125.5, 125.3, 124.9, 124.8, 118.2, 62.3, 62.2, 26.0, 25.9, 18.5, -5.3, -5.4; HRMS (ESI$^+$) calcd for C$_{34}$H$_{47}$N$_2$O$_6$Si$_2$S (M+H)$^+$ 667.2693, found 667.2680.

2-Nitro-5-vinylbenzyl acetate (37). A solution of benzyl alcohol **32** (100 mg, 0.56 mmol, 1 eq) and DMAP (14 mg, 0.11 mmol, 0.2 eq) in dry DCM (2 mL) under nitrogen was prepared. DIPEA (0.15 mL, 0.86 mmol, 1.5 eq) was added and the solution was cooled to 0 °C. Acetic anhydride (0.06 mL, 0.67 mmol, 1.2 eq) was added and the reaction mixture was stirred in the dark overnight. The reaction mixture was diluted with ethyl acetate (10 mL), washed with 0.1 N HCl (2 x 10 mL), saturated sodium bicarbonate (2 x 10 mL), water (10 mL) and brine (10 mL). The organic layer were concentrated in vacuo to yield **37** as a pale yellow solid (112 mg, 91% yield). ^{1}H NMR (500 MHz, CDCl$_3$) δ 8.10 (d, 1 H, J = 8.5 Hz), 7.55 (s, 1 H), 7.50 (d, 1 H, J = 8.5 Hz), 6.77 (dd, 1 H, J = 17.5, 11 Hz), 5.92 (d, 1 H, 17.5 Hz), 5.51 (d, 1 H, J = 11 Hz), 5.32 (s, 2 H), 2.18 (s, 3 H); ^{13}C NMR (500 MHz, CDCl$_3$) δ 170.3, 145.2, 143.0, 134.9, 132.6, 126.9, 125.7, 118.8, 63.1, 20.8; HRMS (ESI$^+$) calcd for C$_{11}$H$_{12}$O$_4$N (M+H)$^+$ 222.0761, found 222.0763.

(((1*E*,1'*E*)-Thiophene-2,5-diylbis(ethene-2,1-diyl))bis(6-nitro-3,1-phenylene))bis(methylene) diacetate (38). A solution of benzyl ester **37** (50 mg, 0.23 mmol, 3 eq), 2,5-dibromothiophene (8.5 μL, 0.075 mmol, 1 eq), LiCl (10 mg, 0.25 mmol, 3.3 eq), NaHCO$_3$ (30 mg, 0.25 mmol, 3.3 eq), TBACl (34 mg, 0.13 mmol, 1.67 eq) in dry DMF (1.7 mL) under argon was prepared. TPGS-750-M (0.2 mL) and Pd(OAc)$_2$ (5 mg, 0.002 mmol, 0.25 eq) were added. The reaction mixture was heated for 110 °C for 1 hour. The reaction mixture was diluted with ethyl

acetate (10 mL), washed with water (4 x 4 mL) and brine (4 mL), dried over sodium sulfate (approximately 500 mg), and concentrated in vacuo. The residue was purified via flash chromatography on silica gel (10% ethyl acetate in hexanes) to yield **38** as a red solid (23 mg, 39% yield). ^{1}H NMR (500 MHz, CDCl$_3$) δ 8.14 (d, 2 H, J = 8.5 Hz), 7.60 (s, 2 H), 7.56 (d, 2 H, J = 8.5 Hz), 7.34 (d, 2 H, J = 16 Hz), 7.12 (s, 2 H), 6.95 (d, 2 H, J = 16 Hz), 5.55 (s, 4 H), 2.21 (s, 6 H).

(((1*E*,1'*E*)-Thiophene-2,5-diylbis(ethene-2,1-diyl))bis(6-nitro-3,1-phenylene))dimethanol (36). A solution of diacetyl ester **38** (23 mg, 0.05 mmol, 1 eq) in methanol (1 mL) was prepared. Potassium carbonate (15 mg, 0.1 mmol, 2 eq) was added and the reaction mixture was stirred for 4.5 hours. The reaction mixture was filtered, the filtrate was concentrated in vacuo, and the residue was purified via flash chromatography on silica gel (20% ethyl acetate in DCM) to yield **36** as a red solid (20 mg, 51% yield). ^{1}H NMR (500 MHz, DMSO-d$_6$) δ 8.12 (d, 2 H, J = 8.5 Hz), 8.04 (s, 2 H), 7.78 (d, 2 H, J = 10.5 Hz), 7.75 (d, 2 H, J = 16 Hz), 7.41 (s, 2 H), 7.16 (d, 2 H, J = 16.5 Hz), 5.63 (t, 2 H, J = 5.5 Hz), 4.90 (d, 4 H, J = 5.5 Hz); ^{13}C NMR (500 MHz, DMSO-d$_6$) 179.8, 160.2, 159.4, 158.2, 143.3, 141.4, 127.5, 126.8, 125.1, 64.9; HRMS (ESI$^+$) calcd for C$_{23}$H$_{19}$O$_8$N$_2$S (M+H)$^+$ 483.0857, found 483.0845.

2-Nitro-5-vinylbenzyl (perfluorophenyl) carbonate (40). A solution of benzyl alcohol **33** (100 mg, 0.56 mmol, 1 eq) and bis(pentafluorophenyl) carbonate (215 mg, 0.56 mmol, 1 eq) in dry acetonitrile (4 mL) was prepared. DIPEA (0.41 mL, 2.35 mmol, 4 eq) was added and the solution was stirred in the dark overnight. The reaction mixture was concentrated in vacuo and the residue was purified via flash chromatography on silica gel (10% ethyl acetate in hexanes) to yield **40** as a pale yellow oil (192 mg, 89% yield). ^{1}H NMR (500 MHz, CD$_3$OD) δ 8.20 (d, 1 H, J = 11 Hz), 7.67 (s, 1 H), 7.56 (d, 1 H, J = 10.5 Hz), 6.80 (dd, 1 H, J = 22, 14 Hz), 5.99 (d, 1 H, J = 22 Hz), 5.96 (s, 2 H), 5.56 (d, 1 H, J = 14 Hz).

Styrene rapamycin (41). A solution of 9-azajulolidine (76 mg, 0.44mmol, 4 eq), rapamycin (100 mg, 0.11 mmol, 1 eq) in dry DCM (4 mL) was prepared. Pentafluorophenyl carbonate **40** (85 mg, 0.22 mmol, 2 eq) was added to the solution, the reaction mixture was stirred overnight, the mixture was concentrated in vacuo, and the residue was purified via flash chromatography on silica gel (gradient 10% ethyl acetate in DCM → 30% ethyl acetate in DCM) to yield **41** as a pale yellow solid (48 mg, 40% yield). ^{1}H NMR (500 MHz, CD$_3$OD) δ 8.15 (d, 1 H, J = 8.5 Hz), 7.72 (s, 1 H), 7.67 (d, 1 H, J = 8.5 Hz), 6.85 (dd, 1 H, J = 11, 5 Hz), 6.48 (m, 1 H), 6.30 (d, 1 H, J = 11 Hz), 6.19 (d, 1 H, J = 10 Hz), 6.10 (d, 1 H, J = 8 Hz), 6.05 (d, 1 H, J = 11 Hz), 5.55 (m, 3 H), 5.36 (d, 1 H, J = 5 Hz), 5.11 (m, 2 H), 4.54 (m, 1 H), 4.13 (m, 3 H), 4.01 (d, 1 H, J = 8 Hz), 3.72 (m, 1 H), 3.61 (d, 1 H, J = 4 Hz), 3.41 (s, 3 H), 3.29 (m, 4 H), 3.16 (s, 3 H), 2.88 (d, 1 H, J = 10 Hz),

2.69 (m, 1 H), 2.50 (m, 1 H), 2.33 (m, 2 H), 2.11 (m, 2 H), 1.90 (m, 1 H), 1.8 (m, 3 H), 1.68 (m, 2 H), 1.50 (m, 4 H), 1.11 (d, 1 H, J = 7 Hz), 1.05 (m, 4 H), 0.98 (m, 8 H); ^{13}C NMR (500 MHz, CDCl$_3$) δ 139.4, 134.8, 127.7, 127.0, 126.4, 126.1, 125.3, 117.8, 99.3, 83.4, 80.9, 80.8, 76.2, 74.2, 65.7, 57.0, 56.4, 54.9, 51.3, 45.9, 44.1, 40.2, 40.1, 35.8, 35.1, 34.3, 31.3, 30.8, 29.3, 26.4, 24.8, 22.3, 20.7, 14.8, 14.5, 14.2, 13.0, 12.9, 12.4, 9.6; HRMS (ESI$^+$) calcd for C$_{61}$H$_{86}$O$_{17}$N$_2$Na (M+H)$^+$ 1141.5807, found 1141.5809.

BIST rapamycin dimer (42). A solution of styrene rapamycin **41** (40 mg, 0.035 mmol, 3 eq), sodium bicarbonate (3.4 mg, 0.04 mmol, 3.3 eq), TBACl (6 mg, 0.02 mmol, 1.67 eq), LiCl (2.2 mg, 0.04 mmol, 3.3 eq), 2-5 dibromothiophene (1.36 µL, 0.012 mmol, 1 eq) in dry DMF (0.5 mL) under nitrogen was prepared. Palladium acetate (1 mg, 0.004 mmol, 0.35 eq) was added and the solution was heated to 110 °C in the dark for 1.5 hours. The reaction mixture was diluted with ethyl acetate (5 mL), washed with water (4 x 2 mL), and brine (5 mL). The organic layer was dried over sodium sulfate (approximately 500 mg), concentrated in vacuo, and the residue was purified via flash chromatography on silica gel (25% ethyl acetate in DCM → 50% ethyl acetate in DCM) to yield **42** as a red solid (11 mg, 39% yield). ^{1}H NMR (500 MHz, CD$_3$OD) δ 8.11 (d, 2 H, J = 8.5 Hz), 7.82 (m, 4 H), 7.68 (d, 2 H, J = 16 Hz), 7.32 (s, 2 H), 7.09 (d, 1 H, J = 16 Hz), 6.41 (m, 2 H), 6.19 (m, 1 H), 6.08 (d, 1 H, J = 10 Hz), 5.72 (s, 1 H), 5.47 (m, 3 H), 5.26 (d, 1 H, J = 3 Hz), 5.05 (d, 1 H, J = 6 Hz), 4.98 (m, 2 H), 4.46 (m, 1 H), 4.03 (m, 3 H), 3.92 (s, 1 H), 3.61 (d, 1 H, J = 7 Hz), 3.48 (m, 2 H), 3.16 (m, 4 H), 3.01 (s, 3 H), 2.69 (m, 1 H), 2.37 (m, 2 H), 2.24 (m, 1 H), 2.11 (m, 3 H), 1.92 (m, 1 H), 1.76 (m, 3 H), 1.59 (m, 2 H), 1.43 (m, 4 H), 1.04 (t, 2 H, J = 7 Hz), 0.99 (m, 4 H), 0.92 (m, 4 H), 0.83 (m, 4 H); HRMS (ESI$^+$) calcd for C$_{13}$H$_{16}$O$_3$N$_5$ (M+H)$^+$ 2336.0854, found 2336.0811.

Benzyl (2-nitro-5-vinylbenzyl) carbonate (43). A solution of pentafluorophenyl carbonate **40** (173 mg, 0.49mmol, 1 eq) in DCM (3 mL) was prepared. Benzyl alcohol (264 mg, 2.44 mmol, 5 eq) and DMAP (169 mg, 1.46 mmol, 3 eq) were added and the solution was stirred at room temperature for 4 hours. The reaction mixture was concentrated in vacuo and the residue was purified via flash chromatography on silica gel (gradient 0% ethyl acetate in hexanes → 10% ethyl acetate in hexanes) to yield **43** as a yellow oil (140 mg, 97% yield). ^{1}H NMR (300 MHz, CDCl$_3$) δ 8.12 (d, 1 H, J = 8.7 Hz), 7.54 (s, 1 H), 7.49 (d, 1 H, J = 8.7 Hz), 7.38 (m, 5 H), 6.70 (dd, 1 H, J = 17.7, 11.1 Hz), 5.92 (d, 1 H, J = 17.7), 5.63 (s, 2 H), 5.47 (d, 1 H, J = 11.1 Hz) , 5.21 (s, 2 H), 4.75 (s, 1 H); ^{13}C NMR (400 MHz, CDCl$_3$) δ 154.7, 145.8, 143.3, 135.0, 134.8, 132.5, 128.8, 126.1, 125.9, 119.0, 70.2, 66.3; HRMS (ESI$^+$) calcd for C$_{17}$H$_{15}$O$_5$NNa (M+Na)$^+$ 336.0842, found 336.0833.

Dibenzyl((((1*E*,1'*E*)-thiophene-2,5-diylbis(ethene-2,1-diyl))bis(6-nitro-3,1-phenylene))bis(methylene)) bis(carbonate) (44). A solution of carbonate **43** (100 mg, 0.32 mmol, 3 eq), sodium bicarbonate (36 mg, 0.35 mmol, 3.3 eq), TBACl (93 mg, 0.18 mmol, 1.67 eq), LiCl (18 mg, 0.35 mmol, 3.3 eq), 2-5 dibromothiophene (15 µL, 0.1 mmol, 1 eq) in dry DMF (1.5 mL) under nitrogen was prepared. Palladium acetate (7.5 mg, 0.025 mmol, 0.25 eq) was added and the solution was heated to 110 °C in the dark overnight. The reaction mixture was diluted with ethyl acetate (10 mL), washed with water (3 x 5 mL), the organic layer was collected, and dried over sodium sulfate (approximately 500 mg). The solution was concentrated in vacuo and the residue was purified via flash chromatography on silica gel (gradient 0% ethyl acetate in hexanes → 40% ethyl acetate in hexanes) to yield **44** as an orange oil (43 mg, 43% yield). ^{1}H NMR (300 MHz, CDCl$_3$) δ 8.17 (d, 2 H, J = 8.7 Hz), 7.66 (s, 2 H), 7.54 (d, 2 H, J = 8.7), 7.37 (m, 12 H), 7.09 (s, 2 H), 6.92 (d, 2 H, J = 16.2), 5.66 (s, 4 H), 5.25 (s, 4 H); ^{13}C NMR (500 MHz, CDCl$_3$) δ 154.7, 142.7, 142.3, 134.9, 132.9, 129.4, 128.8, 128.7, 128.5, 126.5, 126.2, 126.1, 125.9, 125.7, 70.2, 66.3; HRMS (ESI$^+$) calcd for C$_{38}$H$_{31}$O$_{10}$N$_2$S (M+H)$^+$ 707.1694, found 707.1632.

1-(2-Nitro-5-((*E*)-2-(5-((*E*)-4-nitrostyryl)thiophen-2-yl)vinyl)phenyl)ethyl (perfluorophenyl) carbonate (46). A solution of BIST alcohol **45** (30 mg, 0.7 mmol, 1 eq), bis(pentafluorophenyl) carbonate (42 mg, 1.1 mmol, 1.5 eq), and DMAP (2 mg, cat.) in dry acetonitrile (2 mL) was created. DIPEA (0.04 mL, 2.1 mmol, 3 eq) was added, the reaction mixture was stirred overnight in the dark, then concentrated in vacuo. The residue was purified via flash chromatography on silica gel (gradient 0% ethyl acetate in hexanes → 20% ethyl acetate in hexanes) to yield **46** as an orange solid (30 mg, 67% yield). ^{1}H NMR (500 MHz, CDCl$_3$) δ 8.24 (d, 2 H, J = 8.5 Hz), 8.12 (d, 1 H, J = 8.5), 7.79 (s, 1 H), 7.62 (m, 3 H), 7.40 (dd, 2 H, J = 16, 11 Hz), 7.16 (q, 2 H, J = 6 Hz), 7.00 (d, 2 H, J = 16 Hz), 6.52 (q, 1 H, J = 6 Hz), 1.86 (d, 3 H, J= 6.5 Hz).

Asymmetric BIST rapamycin (47). A solution of carbonate **46** (30 mg, 0.05 mmol, 2 eq), rapamycin (22 mg, 0.02 mmol, 1 eq), and 9-AJ (21 mg, 0.12 mmol, 5 eq) in DCM (2 mL) was stirred overnight at room temperature. The reaction mixture was concentrated in vacuo and the residue was purified via flash chromatography on silica gel (gradient 0% ethyl acetate in DCM → 40% ethyl acetate in DCM) to yield **47** as an orange solid (3.8 mg, 21% yield). ^{1}H NMR (500 MHz, CD$_3$OD) δ 8.14 (d, 2 H, J = 8.5 Hz), 7.93 (d, 1 H, J = 8.5 Hz), 7.65 (m, 4 H), 7.50 (m, 2 H), 7.12 (s, 2 H), 6.99 (m, 2 H), 6.43 (t, 1 H, J = 10 Hz), 6.15 (m, 3 H), 6.00 (d, 1 H, J = 10 Hz), 5.15 (m, 1 H), 4.97 (m, 2 H), 4.37 (m, 1 H), 4.09 (t, 1 H, J = 6.5 Hz), 4.01 (m, 1 H), 3.88 (d, 1 H, J = 7 Hz), 3.59 (d, 1 H, J = 10 Hz), 3.44 (d, 1 H, J = 6.5 Hz), 3.37 (s, 1 H), 3.17 (d, 3 H, J = 7 Hz), 3.04 (s, 3 H), 2.72 (m, 1 H), 2. 52 (m, 1 H), 2.38 (m, 1 H), 2.20 (m, 2 H), 20.5 (m, 1 H), 1.95 (m, 2 H), 1.82

(m, 1 H), 1.72 (s, 2 H), 1.633 (m, 2 H), 1.55 (m, 4 H), 1.33 (m, 2 H), 1.12 (m, 2 H), 0.98 (m, 4 H), 0.90 (m, 8 H); HRMS (ESI$^+$) calcd for $C_{74}H_{99}O_{19}N_4S$ (M+H)$^+$ 1379.6624, found 1379.6606.

4,4'-difluoro-8-acetoxymethyl-1,3,5,7-tetramethyl-4-bora-3a,4a-diaza-*s*-indacene (57). BODIPY alcohol **56** (30 mg, 0.11 mmol, 1 eq), bis(pentafluorophenyl) carbonate (63 mg, 0.16 mmol, 1.5 eq), and DMAP (26 mg, 0.21 mmol, 2 eq) were dissolved in dry acetonitrile (1 mL) and stirred for 30 minutes in the dark. The reaction mixture was diluted with ethyl acetate (10 mL) and washed with water (2 x 5mL). The organic layer was dried over sodium sulfate (approximately 500 mg) and concentrated in vacuo. The residue was purified via flash chromatography on silica gel (gradient 20% ethyl acetate in hexanes → 35% ethyl acetate in hexanes) to yield **57** as a purple solid (7 mg, 15% yield). ^{1}H NMR (500 MHz, CDCl$_3$) δ 6.02 (s, 2 H), 5.46 (s, 2 H), 2.44 (s, 6 H), 2.32 (s, 6 H).

4,4'-Difluoro-8-hydroxymethyl-1,3,5,7-tetramethyl-4-bora-3a,4a-diaza-*s*-indacene (60). Pyrrole **59** (129 mg, 1.05 mmol, 2 eq) was dissolved in DCM (1.5 mL) and cooled to 0 °C. Acetoxyacetyl chloride (0.07 mL, 0.65 mmol, 1.2 eq) was added dropwise and the solution was stirred for 30 minutes, then the solution was warmed to room temperature and stirred for 2 hours in the dark. DIPEA (0.37 mL, 2.1 mmol, 4 eq) was added dropwise, followed by boron trifluoride diethyletherate (0.27 mL, 2.1 mmol, 4 eq) 15 minutes later. The reaction mixture was stirred for 30 minutes, then concentrated in vacuo. The residue was purified via flash chromatography on silica gel (gradient 0% ethyl acetate in hexanes → 30% ethyl acetate in hexanes) to yield **60** as a purple crystalline solid (81 mg, 30% yield). Characterization was confirmed with reference.[138]

2,6-Diethyl-4,4'-difluoro-8-acetoxymethyl-1,3,5,7-tetramethyl-4-bora-3a,4a-diaza-*s*-indacene (61). BODIPY ester **61** (29 mg, 0.078 mmol, 1 eq) and potassium carbonate (34 mg, 0.23 mmol, 3 eq) were suspended in a solution of DCM (0.5 mL) and methanol (0.5 mL) and stirred at room temperature for 3 hours in the dark. The suspension was filtered, the filtrate was concentrated in vacuo, and the residue was purified via flash chromatography on silica gel (gradient 0% ethyl acetate in hexanes → 20% ethyl acetate in hexanes) to yield **60** as a purple crystalline solid (9.6 mg, 40% yield). Characterization was confirmed with reference.[73]

2,6-Diethyl-4,4'-difluoro-8-hydroxymethyl-1,3,5,7-tetramethyl-4-bora-3a,4a-diaza-*s*-indacene (62). BODIPY alcohol **61** (9.6 mg, 0.029 mmol, 1 eq), DMAP (1 mg, cat.), and bis(pentafluorophenyl) carbonate (17 mg, 0.043 mmol, 1.5 eq) were dissolved in DCM (1 mL). DIPEA (0.01 mL, 0.043 mmol, 1.5 eq) was added and the reaction mixture was stirred for 45 minutes in the dark. The reaction mixture was concentrated in vacuo and purified via flash chromatography on silica gel (gradient 0% ethyl acetate in hexanes → 20% ethyl acetate in

hexanes) to yield **62** as a purple oil (10 mg, 63% yield) and was used without further characterization.

N-(3-Hydroxypropyl)-4'-methyl-[2,2'-bipyridine]-4-carboxamide (70). A solution of bipyridine **66** (50 mg, 0.23 mmol, 1 eq), EDC (45 mg, 0.23 mmol, 1 eq), and HOBT (35 mg, 0.25 mmol, 1.1 eq) were dissolved in DMF (1 mL) at 0 °C. Aminopropanol (28 mg, 0.37 mmol, 1.6 eq) was added dropwise and the reaction mixture was stirred overnight at room temperature. The reaction mixture was concentrated in vacuo and purified via flash chromatography on silica gel (gradient 0 methanol in DCM → 10% methanol in DCM) to yield **70** as a white solid (26 mg, 42% yield). ^{1}H NMR (500 MHz, CD$_3$OD) δ 8.70 (d, 1 H, J = 4.8 Hz), 8.52 (s, 1 H), 8.28 (d, 1 H, J = 5.1), 7.78 (d, 1 H, J = 5.1 Hz), 7.50 (b, 1 H), 7.20 (d, 1 H, J = 5.1 Hz), 3.74 (t, 2 H, J = 6 Hz), 3.66 (q, 2 H, J = 6 Hz), 2.47 (s, 3 H), 1.84 (p, 2 H, J = 6 Hz), 1.24 (t, 1 H, J = 6 Hz); ^{13}C NMR (500 MHz, DMSO-d$_6$) δ 165.2, 156.5, 155.1, 150.3, 149.6, 148.6, 143.4, 125.8, 121.9, 121.8, 118.5, 59.0, 37.2, 32.7, 21.5; HRMS (ESI$^+$) calcd for C$_{15}$H$_{18}$O$_2$N$_3$ (M+H)$^+$ 272.1394, found 272.1394.

Propyl alcohol Ru(II) tris-bypridinyl 2PF$_6^-$ (71). A solution of bipyridine **70** (4 mg, 0.014 mmol, 1 eq) and Ru(bpy)$_2$Cl$_2$ (7 mg, 0.014 mmol, 1 eq) in ethanol (1 mL) stirred under reflux for 5 hours. The reaction mixture was concentrated in vacuo and redissolved in water (2 mL). Potassium hexafluorophosphate (20 mg, excess) was added and the mixture was swirled for 30 minutes. The red solid was filtered and purified via flash chromatography on silica gel (gradient 0% methanol in DCM → 10% methanol in DCM) to yield **71** as a red solid (10 mg, 90% yield). ^{1}H NMR (500 MHz, CD$_3$OD) δ 8.98 (s, 1 H), 8.66 (d, 4 H, J = 5 Hz), 8.61 (s, 1 H), 8.13 (t, 4 H, J = 5 Hz), 7.94 (d, 1 H, J = 4 Hz), 7.84 (d, 1 H, J = 4 Hz), 7.79 (d, 4 H, J = 5 Hz), 7.74 (d, 1 H, J = 4 Hz), 7.63 (d, 1 H, J = 4 Hz), 7.48 (t, 4 H, J = 5 Hz), 7.36 (d, 1 H, J = 4 Hz), 3.66 (t, 2 H, J = 6 Hz), 3.51 (t, 2 H, J = 5 Hz), 2.59 (s, 3 H), 1.85 (p, 2 H, J = 5 Hz); ^{13}C NMR (500 MHz, DMSO-d$_6$) δ 157.7, 157.0, 156.9, 156.8, 156.1, 152.3, 151.8, 151.6, 150.4, 142.6, 138.5, 129.4, 128.3, 125.9, 125.6, 124.9, 121.9, 58.9, 46.3, 37.4, 32.6, 21.2; HRMS (ESI$^+$) calcd for C$_{35}$H$_{33}$O$_2$N$_7$Ru (M+)$^{2+}$ 342.5864, found 342.5872.

4,4-Difluoro-2,6-diiodo-1,3,5,7-tetramethyl-8-(4-(oxy-2,5-dioxopyrrolidin-1-yl carbonate)phenyl)- 4-bora-3a,4a-diaza-s-indacene (76). A solution of BODIPY phenol **75** (4 mg, 0.006 mmol 1 eq) and DSC (5 mg, 0.024 mmol, 4 eq) in acetonitrile (1 mL) was stirred overnight at room temperature in the dark. The reaction mixture was concentrated in vacuo and purified via flash chromatography on silica gel (DCM) to yield **76** as purple solid (3.6 mg, 52% yield). The product was used without further characterization.

4,4-Difluoro-1,3,5,7-tetramethyl-8-(4-(propanoloxyphenyl)- 4-bora-3a,4a-diaza-s-indacene (79). A solution of benzaldehyde **78** (57 mg, 0.32 mmol, 1 eq) in dry THF (10 mL) under

nitrogen was prepared. TFA (2 drops) and 2,4-dimethylpyrrole (112 mg, 1.2 mmol, 3.6 eq) were added and the reaction mixture was stirred overnight in the dark. DDQ (75 mg, 0.33 mmol, 1 eq) in dry THF (12 mL) under nitrogen was added and the reaction mixture was stirred for 4 hours. Triethylamine (2 mL, 27 mmol, 8.5 eq) was added and the reaction was cooled to 0 °C. Boron trifluoride diethyletherate (2 mL, 12.3 mmol, 3.9 eq) was added and the reaction mixture was stirred overnight. The mixture was filtered through celite, the celite was rinsed with DCM (approximately 20 mL), and the combined organic components was concentrated in vacuo. The residue was purified via flash chromatography on silica gel twice (gradient 0% ethyl acetate in DCM → 20% ethyl acetate in DCM) to yield **79** as a brown solid (87 mg, 69% yield). ^{1}H NMR (500 MHz, CDCl$_3$) δ 7.16 (d, 2 H, J = 8.5 Hz), 7.00 (d, 2 H, J = 8.5 Hz), 5.97 (s, 2 H), 4.17 (t, 2 H, J = 6 Hz), 3.90 (t, 2 H, J = 6 Hz), 2.55 (s, 6 H), 2.09 (pent, 2 H, J = 6 Hz), 1.43 (s, 6 H).

4,4-Difluoro-2,6-diiodo-1,3,5,7-tetramethyl-8-(4-propanoloxyphenyl)- 4-bora-3a,4a-diaza-*s*-indacene (80). A solution of the BODIPY **79** (566 mg, 1.42 mmol, 1 eq) and *N*-iodosuccinimide (637 mg, 2.84 mmol, 2 eq) in dry DCM (4 mL) was prepared. The reaction mixture was stirred for 10 hours in the dark, concentrated in vacuo, and the residue was purified via flash chromatography on silica gel (gradient 0% ethyl acetate in DCM → 20% ethyl acetate in DCM) to yield **80** as a purple solid (516 mg, 56% yield). ^{1}H NMR (300 MHz, CDCl$_3$) δ 7.12 (d, 2 H, J = 8.7 Hz), 7.02 (d, 2 H, J = 8.7 Hz), 4.19 (t, 2 H, J = 6 Hz), 3.92 (t, 2 H, J = 6 Hz), 2.63 (s, 6 H) 2.11 (pent, 2 H, J = 6 Hz) 1.44 (s, 6 H), ^{13}C NMR (400 MHz, CDCl$_3$) δ 177.0, 159.8, 156., 145.3, 141.5, 131.7, 129.1, 126.9, 115.4, 85.5, 65.7, 60.2, 32.0, 29.6, 17.2, 16.0, 14.2; HRMS (ESI$^+$) calcd for C$_{22}$H$_{24}$O$_2$N$_2$BF$_2$I$_2$ (M+H)$^+$ 650.9983, found 650.9914.

4,4-Difluoro-2,6-diiodo-1,3,5,7-tetramethyl-8-(4-(propanoxy-2,5-dioxopyrrolidin-1-yl carbonate)oxyphenyl)- 4-bora-3a,4a-diaza-*s*-indacene (81). A solution of the BODIPY **80** (60 mg, 0.09 mmol, 1 eq), and DSC (29 mg, 0.11 mmol, 1.2 eq) in dry acetonitrile (2 mL) was prepared. TEA (0.1 mL, 0.72 mmol, 8 eq) was added and the reaction mixture was stirred for 2.5 hours in the dark. The mixture was concentrated in vacuo, and the residue was purified via flash chromatography on silica gel (5% ethyl acetate in DCM) to yield **81** as a purple solid (35 mg, 48% yield). ^{1}H NMR (500 MHz, CDCl$_3$) δ 7.12 (d, 2 H, J = 8.5 Hz), 7.02 (d, 2 H, J = 8.5 Hz), 4.57 (t, 2 H, J = 6.5 Hz), 4.14 (t, 2 H, J = 6.5 Hz), 2.84 (s, 4 H), 2.63 (s, 6 H), 2.11 (pent, 2 H, J = 6.5 Hz), 1.43 (s, 6 H).

BODIPY propyl rapamycin (82). A solution of NHS carbonate **81** (36 mg, 0.045 mmol, 1.33 eq), rapamycin (30 mg, 0.033 mmol, 1 eq), and DMAP (10 mg, 0.82 mmol, 1.8 eq) in DCM (1 mL) was stirred at room temperature for 20 hours in the dark. The reaction mixture was concentrated in vacuo and purified via flash chromatography on silica gel (gradient 0% ethyl

acetate in DCM → 35% ethyl acetate in DCM) to yield **82** as a purple solid (16 mg, 31% yield). ^{1}H NMR (500 MHz, CD$_3$OD) δ 7.24 (d, 2 H, J = 8.5 Hz), 7.15 (d, 2 H, J = 8.5 Hz), 6.48 (dd, 1 H, J = 14.5, 10 Hz), 6.35 (m, 1 H), 6.19 (dd, 1 H, J = 14.5, 11 Hz), 6.10 (d, 1 H, J = 10 Hz), 5.49 (m, 2 H), 5.23 (d, 1 H, J = 6.5 Hz), 5.09 (m, 2 H), 4.46 (m, 1 H), 4.37 (t, 2 H, 6.5 Hz), 4.28 (p, 2 H, J = 6.5 Hz), 4.00 (d, 1 H, J = 4 Hz), 3.69 (d, 1 H, J = 7 Hz), 3.52 (m, 1 H), 3.40 (s, 3 H), 3.27 (s, 3 H), 3.16 (m, 3 H), 2.72 (d, 1 H, J = 6.5 Hz), 2.60 (s, 6 H), 2.49 (dd, 1 H, J = 12, 7.5 Hz), 2.28 (m, 1 H), 2.22 (m, 4 H), 2.05 (m, 2 H), 1.91 (m, 1 H), 1.82 (s, 3 H), 1.72 (m, 3 H), 1.57 (m, 2 H), 1.52 (s, 6 H), 1.49 (m, 4 H), 1.25 (t, 1 H, J = 6.5 Hz), 1.20 (d, 2 H, J = 6.5 Hz), 1.01 (d, 2 H, J = 7 Hz), 0.99 (d, 2 H, J = 6.5 Hz), 0.86 (m, 5 H).

4,4-Difluoro-1,3,5,7-tetramethyl-8-(4-(propargyloxyphenyl)-   4-bora-3a,4a-diaza-*s*-indacene (87). A solution of benzaldehyde **86** (333 mg, 2.1 mmol, 1 eq) in dry THF (45 mL) under nitrogen was prepared. TFA (2 drops) and 2,4-dimethylpyrrole (0.8 mL, 7.8 mmol, 3.7 eq) were added and the reaction mixture was stirred overnight. DDQ (500 mg, 2.1 mmol, 1 eq) in dry THF (20 mL) under nitrogen was added and the reaction mixture was stirred for 4 hours in the dark. Triethylamine (12 mL, 86 mmol, 40 eq) was added and the reaction was cooled to 0 °C. Boron trifluoride diethyletherate (12 mL, 97 mmol, 45 eq) was added and the reaction mixture was stirred overnight. The mixture was filtered through celite, the celite was washed with DCM, and the solvents were concentrated in vacuo. The residue was purified via flash chromatography on silica gel two times (DCM) to yield **87** as a dark solid (242 mg, 30% yield). ^{1}H NMR (500 MHz, CDCl$_3$) δ 7.19 (d, 2 H, J = 8.5 Hz), 7.08 (d, 2 H, J = 8.5 Hz), 5.97 (s, 2 H), 4.75 (s, 2 H), 2.56 (s, 6 H), 2.54 (s, 1 H), 1.42 (s, 6 H); ^{13}C NMR (500 MHz, CDCl$_3$) δ 158.2, 155.4, 143.1, 141.5, 131.8, 129.3, 128.1, 121.2, 115.7, 56.1, 14.5; HRMS (ESI[+]) calcd for C$_{22}$H$_2$ON$_2$BF$_2$ (M+H)[+] 379.1788, found 379.1797.

4,4-Difluoro-2,6-diiodo-1,3,5,7-tetramethyl-8-(4-propargyloxyphenyl)- 4-bora-3a,4a-diaza-*s*-indacene   (88). A solution of BODIPY **87** (200 mg, 0.53 mmol, 1 eq) and *N*-iodosuccinimide (637 mg, 1.07 mmol, 2 eq) in dry DCM (5 mL) was prepared. The reaction mixture was stirred for 10 hours in the dark, concentrated in vacuo, and the residue was purified via flash chromatography on silica gel (50% DCM in hexanes) to yield **88** as a purple solid (296 mg, 89% yield). ^{1}H NMR (500 MHz, CDCl$_3$) δ 7.16 (d, 2 H, J = 8.5 Hz), 7.11 (d, 2 H, J = 8.5 Hz), 4.77 (s, 2 H), 2.64 (s, 6 H), 2.57 (s, 1 H), 1.44 (s, 6 H); ^{13}C NMR (500 MHz, CDCl$_3$) δ 158.5, 156.7, 145.3, 141.2, 131.7, 129.2, 127.7, 116.0, 56.1, 17.1, 16.0; HRMS (ESI[+]) calcd for C$_{22}$H$_{20}$ON$_2$BF$_2$I$_2$ (M+H)[+] 630.9721, found 630.9724.

2-(2-(2-Azidoethoxy)ethoxy)ethyl (perfluorophenyl) carbonate (92). A solution of triethylene glycol azide **91** (50 mg, 0.29 mmol, 1 eq) and bis(pentafluorophenyl) carbonate (134

mg, 0.37 mmol, 1.3 eq) in DCM (3 mL) was prepared. DIPEA (0.16 mL, 0.86 mmol, 3 eq) was added and the reaction mixture was stirred for 1 hour. The reaction mixture was concentrated in vacuo and the residue was purified via flash chromatography on silica gel (gradient 10% ethyl acetate in hexanes → 20% ethyl acetate in hexanes) to yield **92** as a colorless oil (106 mg, 91% yield). ^{1}H NMR (500 MHz, CDCl$_3$) δ 4.47 (p, 2 H, J = 4.5 Hz), 3.80 (p, 2 H, J = 4.8 Hz), 3.67 (m, 6 H), 3.37 (t, 2 H, J = 5.1 Hz).

Triethylene glycol azido rapamycin (93). A solution of pentafluorophenyl carbonate **92** (96 mg, 0.3 mmol, 2 eq), rapamycin (128 mg, 0.14 mmol, 1 eq) and DMAP (75 mg, 0.6 mmol, 4 eq) in dry DCM (2 mL) was stirred overnight at room temperature. The reaction mixture was concentrated in vacuo and purified via flash chromatography on silica gel (gradient 30% ethyl acetate in DCM → 50% ethyl acetate in DCM) to yield **93** as a white solid (47 mg, 30% yield). ^{1}H NMR (500 MHz, CD$_3$OD) δ 6.36 (dd, 1 H, J = 14.5, 10 Hz), 6.19 (dd, 1 H, J = 14.5, 9 Hz), 6.10 (d, 1 H, J = 10 Hz), 6.02 (d, 1 H, J = 9 Hz), 5.39 (dd, 1 H, J = 16.5, 11 Hz), 5.17 (d, 1 H, J = 8 Hz), 5.00 (m, 2 H), 4.39 (m, 1 H), 4.16 (t, 4 H, J = 6.5 Hz), 4.05 (m, 1 H), 3.90 (d, 1 H, J = 7 Hz), 3.69 (m, 1 H), 3.65 (p, 4 H, J = 6.5 Hz), 3.49 (p, 4 H, J = 6.5 Hz), 3.40 (m, 1 H), 3.39 (s, 2 H), 3.25 (s, 3 H), 3.19 (m, 2 H), 3.05 (m, 3 H), 2.9 (m, 1 H), 2.72 (m, 2 H), 2.55 (m, 1 H), 2.39 (dd, 1 H, J = 16.5, 11 Hz), 2.22 (t, 1 H, J = 6 Hz), 2.16 (m, 1 H), 2.06 (m, 2 H), 2.01 (m, 2 H), 1.81 (d, 2 H, J = 6.5 Hz), 1.75 (s, 3 H), 1.63 (m, 5 H), 1.52 (d, 2 H, J = 7 Hz), 1.32 (q, 2 H, J = 6.5 Hz), 1.21 (m, 2 H), 1.10 (m, 2 H), 0.98 (d, 2 H, J = 6.5 Hz), 0.95 (d, 2 H, J = 7 Hz), 0.90 (d, 2 H, J = 6.5 Hz), 0.81 (d, 2 H, J = 6.5 Hz), 0.77 (d, 2 H, J = 7 Hz); ^{13}C NMR (500 MHz, CDCl$_3$) δ 219.4, 208.2, 169.2, 166.8, 154.8, 140.2 136.1, 135.6, 133.7, 130.2, 129.6, 126.6, 126.4, 98.8, 98.5, 84.8, 84.4, 80.8, 80.3, 77.4, 77.2, 77.0, 76.7, 75.5, 72.5, 69.1, 67.2, 66.8, 61.8, 59.4, 57.5, 55.9, 51.3, 50.7, 46.6, 44.2, 41.5, 40.7, 40.2, 38.8, 38.2, 35.7, 35.1, 33.8, 33.2, 32.88, 31.3, 29.7, 27.3, 27.0, 25.3, 21.5, 20.7, 16.2, 16.0, 15.9, 13.8, 13.1, 10.3, 10.2; HRMS (ESI$^+$) calcd for C$_{58}$H$_{91}$O$_{17}$N$_4$ (M+H)$^+$ 1115.6374, found 1115.6362.

Triethylene glycol BODIPY rapamycin (94). A solution of BODIPY alkyne **88** (10 mg, 0.015 mmol, 2 eq), CuI (6 mg, 0.30 mmol, 4 eq), and azido rapamycin **93** (7 mg, 0.07 mmol, 1 eq) in dry DCM (1.75 mL) in the dark was prepared. DIPEA (0.05 mL, 0.29 mmol, 4 eq) was added and the solution was stirred at room temperature for 2 hours. The reaction mixture was concentrated in vacuo and the residue was purified via flash chromatography on silica gel (gradient 30% ethyl acetate in DCM → 50% ethyl acetate in DCM) to yield **94** as a purple solid (10 mg, 91% yield). ^{1}H NMR (500 MHz, CD$_3$OD) δ 8.23 (s, 1 H), 7.31 (s, 4 H), 6.36 (dd, 1 H, J = 14.5, 10 Hz), 6.19 (dd, 1 H, J = 14.5 9 Hz), 6.10 (d, 1 H, J = 10 Hz), 6.02 (d, 1 H, J = 9 Hz), 5.51 (s, 2 H), 5.39 (m, 1 H), 5.17 (d, 1 H, J = 6.5 Hz), 4.98 (m, 2 H), 4.38 (m, 1 H), 4.16 (t, 4 H, J = 6.5

Hz), 4.05 (m, 1 H), 3.88 (d, 1 H, J = 3 Hz), 3.70 (m, 1 H), 3.65 (p, 4 H, J = 6.5 Hz), 3.48 (p, 4 H, J = 6.5 Hz), 3.40 (m, 1 H), 3.39 (s, 2 H), 3.22 (s, 3 H), 3.16 (m, 2 H), 3.05 (m, 3 H), 2.90 (m, 1 H), 2.72 (m, 2 H), 2.62 (s, 6 H), 2.55 (m, 1 H), 2.38 (dd, 1 H, J = 10, 8 Hz), 2.22 (t, 1 H, J = 6.5 Hz), 2.15 (d, 1 H, J = 7 Hz), 2.06 (m, 2 H), 2.00 (m, 2 H), 1.81 (d, 2 H, J = 5 Hz), 1.74 (s, 3 H), 1.63 (m, 5 H), 1.55 (d, 2 H, J = 6.5 Hz), 1.44 (s, 6 H), 1.30 (q, 2 H J = 5 Hz), 1.21 (m, 2 H), 1.11 (m, 2 H), 0.97 (d, 2 H, J = 6.5 Hz), 0.95 (d, 2 H, J = 7 Hz), 0.89 (d, 2 H, J = 5 Hz), 0.81 (d, 2 H, J = 6.5 Hz), 0.77 (d, 2 H, J = 7 Hz); ^{13}C NMR (500 MHz, CDCl$_3$) δ 219.4, 208.2, 169.2, 166.8, 159.4, 156.6, 154.8, 145.3, 141.4 136.1, 135.6, 133.7, 130.2, 129.8, 127.2, 126.4, 124.3, 115.8, 98.5, 85.6, 84.4, 80.8, 80.3, 77.4, 75.5, 70.5, 69.5, 69.0, 66.7, 62.1, 59.4, 57.5, 55.9, 51.3, 50.4, 46.6, 44.2, 41.5, 40.5, 38.8, 38.2, 35.7, 35.1, 33.8, 33.2, 32.88, 31.3, 29.7, 27.3, 25.3, 21.5, 20.7, 17.2, 16.0, 15.9, 13.8, 13.2, 10.2; HRMS (ESI$^+$) calcd for C$_{80}$H$_{110}$O$_{18}$N$_6$BF$_2$I$_2$ (M+H)$^+$ 1745.6022, found 1745.6071.

3-(2-(4-(Hydroxymethyl)phenyl)hydrazineylidene)pentane-2,4-dione (100). Benzyl alcohol **99** (1.25 g, 10.1 mmol, 1 eq) was dissolved in acetic acid (15 mL) and cooled to 0 °C. Concentrated HCl (2.3 mL) was added dropwise. Sodium nitrite (839 mg, 12.1 mmol, 1.2 eq) was dissolved in minimal H$_2$O and added dropwise to the reaction mixture. After 45 minutes, a solution of 2,4-pentanedione (1.35 mL, 13.4 mmol, 1.3 eq), sodium acetate (2.46 mg, 30.9 mmol, 3 eq), ethanol (10 mL) and H$_2$O (6 mL) was added in portions. After stirring overnight at room temperature, the yellow precipitate was collected. The solid was washed with hexanes, and dried under vacuum to yield **100** as a bright yellow solid (1.055 g, 44% yield). ^{1}H NMR (500 MHz, CDCl$_3$) δ 14.78 (b, 1 H), 7.43 (s, 4 H), 4.74 (s, 2 H), 2.63 (s, 3 H), 2.52 (s, 3 H). ^{13}C NMR (500 MHz, CDCl$_3$) δ 197.2, 140.9, 139.3, 128.0, 115.9, 63.3, 30.1, 25.1, 21.4; HRMS (M+H)$^+$ calcd for C$_{13}$H$_{17}$ON$_4$ (M+H)$^+$ 245.1397, found 245.1404.

(*E*)-(4-((1,3,5-Trimethyl-1*H*-pyrazol-4-yl)diazenyl)phenyl)methanol (101). A solution of diketone **100** (1.055 g, mmol, 1 eq) in ethanol (50 mL) was heated to reflux with stirring. Methylhydrazine (4.5 mL, excess) was added to the solution, and the reaction mixture was stirred for 2.5 hours. The reaction mixture was then concentrated in vacuo to yield **101** as an orange solid (952 mg, 87% yield). ^{1}H NMR (400 MHz, CDCl$_3$) δ 7.78 (d, 2 H, J = 8 Hz), 7.45 (d, 2 H, J = 8 Hz), 4.76 (s, 2H), 3.78 (s, 3H), 2.58 (s, 3 H), 2.50 (s, 3 H); ^{13}C NMR (500 MHz, CDCl$_3$) δ 153.2, 142.5, 142.0, 138.7, 127.4, 122.0, 65.0, 35.9, 18.4, 13.8, 10.0; HRMS (ESI$^+$) calcd for C$_{13}$H$_{17}$ON$_4$ (M+H)$^+$ 245.1397, found 245.1404.

(*E*)-(4-((3,5-Dimethyl-1-phenyl-1*H*-pyrazol-4-yl)diazenyl)phenyl)methanol (102). A solution of diketone **100** (201 mg, 0.85 mmol, 1 eq) in ethanol (5 mL) was prepared. Phenylhydrazine (0.1 mL, 0.85 mmol, 1 eq) was added and the reaction mixture was stirred under

72

reflux for 2 hours. The reaction mixture was then concentrated in vacuo and the residue was purified via flash chromatography on silica gel (1% acetone in chloroform) to yield **102** as an orange solid (157 mg, 60 % yield). ^{1}H NMR (500 MHz, CDCl$_3$) δ 7.71 (d, 2 H, J = 8 Hz), 7.51 (m, 7 H), 4.74 (s, 3H), 2.65 (s, 3 H), 2.59 (s, 3 H); ^{13}C NMR (500 MHz, CDCl$_3$) δ 153.1, 143.9, 142.4, 139.2, 138.9, 136.2, 129.3, 128.2, 127.5, 124.9, 122.1, 64.9, 14.0, 11.4; HRMS (ESI$^+$) calcd for C$_{18}$H$_{19}$ON$_4$ (M+H)$^+$ 307.1553, found 307.1554.

(*E*)-(4-((3,5-Dimethyl-1-(naphthalen-1-yl)-1*H*-pyrazol-4-yl)diazenyl)phenyl)methanol (103). A solution of diketone **100** (200 mg, 0.85 mmol, 1 eq) and napthylhydrazine (170 mg, 1.07 mmol, 1.25 eq) in ethanol (10 mL) was stirred at room temperature overnight. The reaction mixture was concentrated in vacuo and purified via flash chromatography on silica gel (1% acetone in chloroform) to yield **103** as an orange solid (50 mg, 17% yield). ^{1}H NMR (500 MHz, CDCl$_3$) δ 8.03 (d, 1 H, J = 9 Hz), 7.98 (d, 1 H, J = 9 Hz), 7.87 (d, 2 H, J = 8 Hz), 7.55 (m, 7 H), 4.77 (s, 2 H), 2.68 (s, 3 H), 2.45 (s, 3 H); ^{13}C NMR (500 MHz, CD$_3$OD) δ 152.8, 143.5, 141.1, 134.6, 130.0, 128.1, 127.5, 126.7, 125.5, 122.1, 114.3, 109.4, 78.1, 63.5, 25.1, 14.1, 12.5, 9.2; HRMS (ESI$^+$) calcd for C$_{22}$H$_{21}$ON$_4$ (M+H)$^+$ 357.1710, found 357.1728.

(*E*)-2,5-Dioxopyrrolidin-1-yl (4-((1,3,5-trimethyl-1*H*-pyrazol-4-yl)diazenyl)benzyl) carbonate (104). A solution of benzyl alcohol **101** (75 mg, 0.31 mmol, 1 eq) and DSC (104 mg, 0.41 mmol, 1.3 eq) in dry acetonitrile (1.5 mL) under nitrogen was prepared. Triethylamine (0.07 mL, 0.95 mmol, 3 eq) was added and the reaction mixture was stirred for 4 hours. The mixture was concentrated in vacuo, and the residue was purified via flash chromatography on silica gel (gradient 15% ethyl acetate in DCM → 40% ethyl acetate in DCM) to yield **104** as an orange solid (53 mg, 45% yield). ^{1}H NMR (300 MHz, CDCl$_3$) δ 7.77 (d, 2 H, J = 6.9 Hz), 7.45 (d, 2 H, J = 8.7 Hz), 5.27 (s, 2H), 3.75 (2, 3H), 2.80 (s, 4H), 2.54 (s, 3 H), 2.46 (s, 3 H).

(*E*)-4-((3,5-Dimethyl-1-phenyl-1*H*-pyrazol-4-yl)diazenyl)benzyl (2,5-dioxopyrrolidin-1-yl) carbonate (105). A solution of benzyl alcohol **102** (61 mg, 0.20 mmol, 1 eq) and DSC (120 mg, 0.47 mmol, 2.4 eq) in dry acetonitrile (2 mL) was prepared. Triethylamine (0.2 mL, 2.72 mmol, 13 eq) was added and the reaction mixture was stirred at room temperature for 20 hours, then concentrated in vacuo. The residue was purified via flash chromatography on silica gel (1% acetone in chloroform) to yield **105** as an orange solid (56 mg, 63% yield). ^{1}H NMR (500 MHz, CDCl$_3$) δ 7.59 (d, 2 H, J = 8.5 Hz), 7.49 (d, 2 H, J = 8.5 Hz), 7.38 (m, 5 H), 5.18 (s, 2 H), 2.83 (s, 3 H), 2.65 (s, 3 H), 2.58 (s, 4 H).

(*E*)-4-((3,5-Dimethyl-1-(naphthalen-1-yl)-1*H*-pyrazol-4-yl)diazenyl)benzyl (2,5-dioxopyrrolidin-1-yl) carbonate (106). A solution of benzyl alcohol **103** (69 mg, 0.19 mmol, 1 eq) and DSC (74 mg, 0.29 mmol, 1.5 eq) in dry acetonitrile (3 mL). Triethylamine (0.08 mL, 0.6

mmol, 3 eq) was added and the reaction mixture was stirred overnight. The reaction mixture was concentrated in vacuo and the residue was purified via flash chromatography on silica gel (0% ethyl acetate in DCM → 5% ethyl acetate in DCM) to yield **106** as an orange solid (90 mg, 96% yield). ^{1}H NMR (500 MHz, CDCl$_3$) δ 8.00 (d, 1 H, J = 8.5 Hz), 7.95 (d, 1 H, J = 8.5 Hz), 7.85 (d, 2 H, J = 8 Hz), 7.50 (m, 7 H), 5.38 (s, 2 H), 2.66 (s, 4 H), 2.59 (s, 3 H), 2.42 (s, 3 H).

Methyl arylazopyrazole rapamycin (107). A solution of NHS carbonate **104** (53 mg, 0.14 mmol, 1.4 eq), rapamycin (94 mg, 0.10 mmol, 1 eq), and DMAP (48 mg, 0.39 mmol, 3.9 eq) in dry DCM (1 mL) under nitrogen was prepared. The reaction mixture was stirred at room temperature overnight, concentrated in vacuo, and the residue was purified via flash chromatography on silica gel (20% ethyl acetate in DCM → 40% ethyl acetate in DCM) to yield **107** as a yellow solid (16 mg, 12% yield). ^{1}H NMR (500 MHz, CD$_3$OD) δ 7.77 (d, 2 H, J = 8.5 Hz), 7.49 (d, 2 H, J = 8.5 Hz), 6.48 (dd, 1 H, J = 12, 10 Hz), 6.30 (dd, 1 H, J = 12, 9 Hz), 6.21 (d, 1 H, J = 9 Hz), 6.12 (d, 1 H J = 10 Hz), 5.47 (dd, 1 H, J = 11, 9.5 Hz), 5.22 (m, 3 H), 5.11 (m, 2 H), 4.51 (m, 1 H), 4.16 (m, 2 H), 4.01 (d, 1 H, J = 3 Hz), 3.78 (s, 3 H), 3.39 (s, 2 H), 3.26 (s, 3 H), 3.11 (s, 3 H), 2.81 (d, 1 H, J = 7 Hz), 2.67 (m, 4 H), 2.47 (s, 3 H), 2.31 (m, 2 H), 2.16 (m, 2 H), 1.91 (d, 1 H, J = 6.5 Hz), 1.82 (s, 2 H), 1.71 (s, 3 H), 1.64 (m, 2 H), 1.53 (m, 1 H), 1.48 (q, 2 H, J = 6.5 Hz), 1.33 (m, 1 H), 1.21 (m, 2 H), 1.09 (d, 2 H, J = 6.5 Hz), 1.01 (d, 2 H, J = 7 Hz), 0.98 (d, 2 H, J = 7 Hz), 0.90 (d, 2 H, J = 7 Hz), 0.83 (d, 2 H, J = 6.5 Hz); ^{13}C NMR (500 MHz, CD$_3$OD) δ 207.3, 198.4, 169.7, 167.8, 139.4, 136.9, 134.6, 132.7, 130.9, 129.1, 128.8, 127.7, 126.4, 121.4, 1202, 99.3, 85.9, 83.4, 80.9, 76.2, 74.1, 68.6, 67.2, 56.9, 54.9, 51.3, 45.9, 44.1, 40.4, 40.1, 40.0, 38.5, 35.8, 35.1, 34.7, 34.3, 33.7, 32.6, 31.3, 30.0, 29.3, 26.6, 26.5, 24.8, 24.7, 22.3, 20.7, 20.4, 19.6, 14.7, 14.5, 14.2, 13.0, 12.4, 9.6, 8.4; HRMS (ESI$^+$) calcd for C$_{65}$H$_{94}$O$_{15}$N$_5$ (M+H)$^+$ 1184.6741, found 1184.6750.

Phenyl arylazopyrazole rapamycin (108). A solution of NHS carbonate **105** (56 mg, 0.12 mmol, 3 eq), rapamycin (38 mg, 0.04 mmol, 1 eq), and DMAP (25 mg, 0.22 mmol, 5.5 eq) in dry DCM (1 mL) under nitrogen was prepared and stirred overnight. The reaction mixture was concentrated in vacuo, then the residue was purified via flash chromatography on silica gel (30% ethyl acetate in DCM) to yield **108** as an orange solid (5 mg, 10% yield). ^{1}H NMR (500 MHz, CD$_3$OD) δ 7.73 (d, 2 H, J = 8.5 Hz), 7.48 (m, 7 H), 6.40 (dd, 1 H, J = 12, 10 Hz), 6.22 (dd, 1 H, J = 12 Hz, 9 Hz), 6.14 (d, 1 H, J = 10 Hz), 6.06 (d, 1 H, J = 9 Hz), 5.39 (dd, 1 H, J = 14, 10 Hz), 5.17 (m, 3 H), 5.03 (m, 2 H), 4.41 (m, 1 H), 4.14 (m, 2 H), 4.11 (d, 1 H, J = 7 Hz), 4.02 (m, 1 H), 3.92 (d, 1 H, J = 3 Hz), 3.61 (d, 1 H, J = 6.5 Hz), 3.50 (d, 1 H, J = 6.5 Hz), 3.37 (s, 3 H), 3.29 (s, 3 H), 3.21 (s, 3 H), 3.05 (s, 3 H), 2.72 (d, 1 H, J = 6.5 Hz), 2.59 (s, 3 H), 2.48 (s, 3 H), 2.41 (dd, 1 H, J = 12, 6 Hz), 2.20 (m, 1 H), 2.09 (m, 2 H), 1.81 (d, 1 H, J = 7 Hz), 1.78 (s, 3 H), 1.64 (m, 4 H),

1.45 (m, 2 H), 1.29 (m, 3 H), 1.11 (m, 1 H), 0.98 (d, 2 H, J = 6.5 Hz), 0.91 (d, 2 H, J = 6 Hz), 0.85 (d, 2 H, J = 7 Hz), 0.81 (d, 2 H, J = 7 Hz), 0.77 (d, 2 H, J = 6.5 Hz); ^{13}C NMR (500 MHz, CD$_3$OD) δ 207.3, 198.4, 169.7, 167.8, 153.4, 144.4, 139.4, 138.7, 137.8, 137.6, 132.7, 130.9, 129.1, 128.9, 127.7, 125.1, 124.9, 121.6, 120.3, 99.3, 85.9, 83.4, 80.9, 80.5, 76.2, 74.1, 68.5, 57.0, 56.5, 54.9, 51.3, 45.9, 44.1, 40.4, 40.0, 38.5, 35.8, 35.1, 34.3, 33.7, 32.6, 31.3, 30.8, 30.0, 29.3, 26.4, 24.7, 22.3, 20.7, 20.4, 14.7, 14.6, 14.2, 13.0, 12.6, 12.4, 10.1, 9.8, 9.5; HRMS (ESI$^+$) calcd for C$_{70}$H$_{96}$O$_{15}$N$_5$ (M+H)$^+$ 1246.6897, found 1246.6929.

Naphthyl arylazopyrazole rapamycin (109). A solution of the NHS carbonate **106** (90 mg, 0.18 mmol, 3 eq), DMAP (40 mg, 0.33 mmol, 5.5 eq) and rapamycin (50 mg, 0.06 mmol, 1 eq) in dry DCM (3 mL) under nitrogen was prepared. The reaction was stirred at room temperature for 2 days, then concentrated in vacuo. The residue was purified via flash chromatography on silica gel (gradient 35% ethyl acetate in DCM → 50% ethyl acetate in DCM) to yield **109** as an orange solid (9 mg, 13% yield). ^{1}H NMR (500 MHz, CD$_3$OD) δ 8.17 (d, 1 H, J = 9 Hz), 8.11 (d, 1 H, J = 9 Hz), 7.86 (m, 2 H), 7.60 (m, 8 H), 7.38 (d, 1 H, J = 8.5 Hz), 6.48 (dd, 1 H, J = 14, 10 Hz), 6.32 (dd, 1 H, J = 14, 9 Hz), 6.10 (m, 2 H), 5.51 (m, 2 H), 5.38 (t, 1 H, J = 6 Hz), 5.26 (m, 3 H), 5.12 (m, 2 H), 4.62 (m, 1 H), 4.29 (m, 2 H), 4.05 (d, 1 H, J = 6.5 Hz), 3.73 (d, 1 H, J = 8 Hz), 3.58 (d, 1 H, J = 6.5 Hz), 3.49 (m, 5 H), 3.17 (s, 3 H), 3.05 (m, 1 H), 2.89 (s, 3 H), 2.89 (m, 1 H), 2.62 (s, 2 H), 2.45 (m, 1 H), 2.30 (m, 1 H), 2.17 (m, 1 H), 2.02 (m, 2 H), 1.91 (m, 1 H), 1.81 (m, 2 H), 1.77 (m, 1 H), 1.59 (m, 4 H), 1.48 (m, 1 H), 1.31 (m, 1 H), 1.17 (m, 2 H), 1.09 (m, 1 H), 0.98 (d, 2 H, 7 Hz), 0.92 (d, 2 H, 6.5 Hz), 0.81 (m, 6 H); ^{13}C NMR (500 MHz, CDCl$_3$) δ 208.2, 169.2, 166.8, 1154.8, 153.6, 144.2, 141.1, 140.2, 136.7, 136.1, 135.5, 1335.2, 134.3, 133.7, 130.3, 130.2, 129.9, 129.6, 129.1, 128.9, 128.2, 127.6, 128.9, 128.2, 127.6, 126.8, 126.7, 126.4, 125.3, 125.1, 122.9, 122.1, 120.6, 98.5, 84.8, 84.4, 80.9, 80.5, 69.1, 67.2, 59.4, 57.6, 55.9, 55.8, 53.4, 51.3, 46.6, 44.2, 41.5, 40.7, 40.2, 38.9, 38.3, 36.1, 35.8, 35.2, 34.7, 33.2, 32.8, 31.6, 31.3, 29.7, 29.1, 27.3, 27.1, 26.9, 25.3, 22.7, 21.5, 20.7, 20.6, 18.8, 16.4, 16.3, 16.1, 15.9, 15.8, 14.1, 14.0, 13.8, 13.1, 12.9, 11.4, 10.7, 10.3, 10.1; HRMS (ESI$^+$) calcd for C$_{74}$H$_{98}$O$_{15}$N$_5$ (M+H)$^+$ 1296.7054, found 1296.7084.

(*E*)-(4-((3,5-Dimethyl-1*H*-pyrazol-4-yl)diazenyl)phenyl)methanol (110). Dione **100** (500 mg, 2.1 mmol, 1 eq) and hydrazine (0.134 mL, 4.2 mmol, 2 eq) were dissolved in ethanol (10 mL) and stirred at room temperature for 1 hour. The reaction mixture was concentrated in vacuo to give **110** as an orange solid (502 mg, 95% yield). ^{1}H NMR (500 MHz, CD$_3$OD) δ 7.41 (d, 2 H, J = 8.5 Hz), 7.13 (d, 2 H, J = 8.5 Hz), 4.35 (s, 2 H), 3.29 (q, 1 H, J = 6.5 Hz), 2.26 (t, 1 H, J = 2.5 Hz), 2.20 (s, 6 H), 0.85 (t, 1 H, J = 6.5 Hz); ^{13}C NMR (500 MHz, CD$_3$OD) δ 152.8, 146.7,

143.1, 134.2, 130.8, 128.3, 127.1, 121.4, 115.1, 63.9; HRMS (ESI$^+$) calcd for $C_{12}H_{15}ON_4$ (M+H)$^+$ 231.1240, found 231.1237.

(**E**)-(4-((1-Butyl-3,5-dimethyl-1**H**-pyrazol-4-yl)diazenyl)phenyl)methanol (**111**). A suspension of arylazopyrazole **110** (100 mg, 0.44 mmol, 1 eq) and KOH (24 mg, 0.44 mmol, 1 eq) in acetonitrile (6 mL) was created. Butyl iodide (0.054 mL, 0.48 mmol, 1.1 eq) was added and heated under reflux overnight. The reaction mixture was concentrated in vacuo and the residue was purified via flash chromatography on silica gel (gradient 0% ethyl acetate in DCM → 30% ethyl acetate in DCM) to yield **111** as a yellow solid. ^{1}H NMR (500 MHz, CDCl$_3$) δ 7.79 (d, 2 H, J = 8.5 Hz), 7.47 (d, 2 H, J = 8.5 Hz), 4.78 (s, 2 H), 4.05 (t, 2 H, J = 7 Hz), 2.60 (s, 3 H), 2.52 (s, 3 H), 1.83 (p, 2 H, J = 7 Hz), 1.59 (s, 1 H), 1.41 (hex, 2 H, J = 7 Hz), 0.98 (t, 3 H, J = 7 Hz); ^{13}C NMR (500 MHz, CDCl$_3$) δ 153.3, 142.4, 141.9, 138.4, 135.0, 127.5, 121.9, 65.1, 48.9, 32.1, 19.9, 14.0, 13.7, 9.9; HRMS (ESI$^+$) calcd for $C_{16}H_{23}ON_4$ (M+H)$^+$ 287.1879, found 287.1866.

(**E**)-1-(4-((4-(Hydroxymethyl)phenyl)diazenyl)-3,5-dimethyl-1**H**-pyrazol-1-yl)hexan-1-one (**112**). A suspension of arylazopyrazole **110** (100 mg, 0.44 mmol, 1 eq) and KOH (24 mg, 0.44 mmol, 1 eq) in acetonitrile (8 mL) was created. Bromohexane (71 mg, 0.44 mmol, 1 eq) was added and the reaction mixture was heated to reflux overnight. The reaction mixture was concentrated in vacuo and the residue was purified via flash chromatography on silica gel (gradient 0% ethyl acetate in DCM → 20% ethyl acetate in DCM) to yield **111** as an orange oil (57 mg, 40%). ^{1}H NMR (500 MHz, CDCl$_3$) δ 7.80 (d, 2 H, J= 8.5 Hz), 7.48 (d, 2 H, J = 8.5 Hz), 4.78 (s, 2 H), 4.04 (t, 2 H, J = 6.5 Hz), 2.61 (s, 3 H), 2.53 (s, 3 H), 1.73 (p, 2 H, J = 6.5 Hz), 1.35 (m, 6 H), 0.92 (t, 3 H, J = 6.5 Hz); ^{13}C NMR (500 MHz, CD$_3$OD) δ 153.3, 142.4, 141.9, 138.4, 135.0, 127.5, 121.9, 65.1, 49.1, 31.4, 30.0, 26.4, 22.5, 14.0, 9.9; HRMS (ESI$^+$) calcd for $C_{68}H_{100}O_{15}N_5$ (M+H)$^+$ 1226.7225, found 1226.7210.

(**E**)-4-((1-Butyl-3,5-dimethyl-1**H**-pyrazol-4-yl)diazenyl)benzyl (2,5-dioxopyrrolidin-1-yl) carbonate (**113**). A solution of arylazopyrazole **111** (50 mg, 0.18 mmol, 1 eq), DSC (67 mg, 0.27 mmol, 1.5 eq), and DMAP (5 mg, cat.) in acetonitrile (3 mL) was prepared. DIPEA (0.09 mL, 0.54 mmol, 3 eq) was added and the reaction mixture was stirred at room temperature for 3 hours. The reaction mixture was concentrated in vacuo and purified via flash chromatography on silica gel (gradient 0% ethyl acetate in DCM → 25% ethyl acetate in DCM) to yield **113** as an orange oil (73 mg, 97% yield). ^{1}H NMR (500 MHz, CDCl$_3$) δ 7.79 (d, 2 H, J = 8.5 Hz), 7.59 (d, 2 H, J = 8.5 Hz), 5.20 (s, 2 H), 4.05 (t, 2 H, J = 6.5 Hz), 2.61 (s, 3 H), 2.52 (s, 3 H), 1.86 (p, 2 H, J = 6.5 Hz), 1.39 (p, 2 H, J = 6.5 Hz), 1.29 (m, 4 H), 1.02 (t, 3 H, J = 6.5 Hz).

(**E**)-2,5-Dioxopyrrolidin-1-yl (4-((1-hexanoyl-3,5-dimethyl-1**H**-pyrazol-4-yl)diazenyl)benzyl) carbonate (**114**). A solution of arylazopyrazole **112** (55 mg, 0.16 mmol, 1

eq), DSC (53 mg, 0.21 mmol, 1.3 eq), and DMAP (5 mg, cat.) in acetonitrile (3 mL) was created. DIPEA (0.1 mL, 0.32 mmol, 2 eq) was added and the reaction mixture was stirred for 1.5 hours. The reaction mixture was concentrated in vacuo and the residue was purified via flash chromatography on silica gel (gradient 0% ethyl acetate in DCM → 15% ethyl acetate in DCM) to yield **114** as an orange oil (64 mg, 85% yield). ^{1}H NMR (500 MHz, CDCl$_3$) δ 7.72 (d, 2 H, J = 8.5 Hz), 7.41 (d, 2 H, J = 8.5 Hz), 5.29 (s, 2 H), 3.95 (t, 2 H, J = 7 Hz), 2.78 (s, 4 H), 2.52 (s, 3 H), 2.43 (s, 3 H), 1.77 (m, 2 H), 1.26 (m, 6 H), 0.81 (m, 3 H).

Butyl arylazopyrazole rapamycin (115). A solution of arylazopyrazole **113** (73 mg, 0.17 mmol, 4 eq), rapamycin (39 mg, 0.04 mmol, 1 eq), and 9-azajulolidine (37 mg, 0.21 mmol, 5 eq) in DCM (3 mL) was stirred overnight at room temperature. The reaction mixture was concentrated in vacuo and the residue was purified via flash chromatography on silica gel (gradient 0% ethyl acetate in DCM → 30% ethyl acetate in DCM) to yield **115** as a yellow solid (21 mg, 40% yield). ^{1}H NMR (500 MHz, CD$_3$OD) δ 7.79 (d, 2 H, J = 8.5 Hz), 7.45 (d, 2 H, J = 8.5 Hz), 6.45 (dd, 1 H, J = 12, 10 Hz), 6.33 (dd, 1 H, J = 12, 9 Hz), 6.19 (d, 1 H, J = 9 Hz), 6.10 (d, 1 H, J = 10 Hz), 5.51 (m, 1 H), 5.26 (m, 2 H), 5.17 (m, 1 H), 4.63 (t, 1 H, J = 3 Hz), 4.51 (m, 3 H), 4.04 (m, 2 H), 4.00 (d, 1 H, J = 6.5 Hz), 3.71 (d, 1 H, J = 6.5 Hz), 3.59 (d, 1 H, J = 7.5 Hz), 3.48 (m, 2 H), 3.41 (s, 2 H), 3.29 (s, 3 H), 3.15 (s, 3 H), 2.98 (b, 1 H), 2.87 (d, 1 H, J = 7 Hz), 2.71 (d, 1 H, J = 3 Hz), 2.60 (s, 3 H), 2.49 (s, 3 H), 2.32 (m, 1 H), 2.08 (m, 2 H), 1.91 (t, 1 H, J = 6.5 Hz), 1.84 (m, 2 H), 1.73 (m, 2 H), 1.54 (m, 1 H), 1.47 (q, 2 H, J = 7 Hz), 1.40 (m, 2 H), 1.38 (s, 2 H), 1.11 (m, 2 H), 1.09 (d, 2 H, J = 7 Hz), 1.02 (m, 6 H), 0.97 (d, 2 H, J = 6.5 Hz), 0.89 (m, 5 H); ^{13}C NMR (500 MHz, CDCl$_3$) δ 208.2, 169.2, 166.8, 154.8, 153.7, 142.4, 140.2, 138.6, 136.2, 136.1, 135.1, 133.7, 130.2, 129.6, 129.0, 128.9, 128.8, 126.7, 126.4, 121.9, 121.8, 120.5, 98.5, 84.8, 84.4, 80.9, 80.4, 75.5, 69.1, 67.2, 59.4, 57.6, 55.9, 55.8, 53.4, 51.3, 48.9, 46.6, 44.2, 41.4, 40.7, 40.2, 38.9, 38.3, 35.8, 35.7, 35.2, 34.7, 34.5, 33.7, 33.2, 32.1, 32.0, 29.7, 29.0, 27.3, 27.1, 26.9, 25.2, 24.3, 22.7, 21.7, 21.6, 20.7, 20.6, 19.9 19.8, 16.4, 16.3, 16.1, 16.0, 15.9, 15.8, 14.1, 13.9, 13.8, 13.7, 13.6, 13.1, 11.4, 10.2, 10.0, 9.9; HRMS (ESI$^+$) calcd for C$_{68}$H$_{100}$O$_{15}$N$_5$ (M+H)$^+$ 1226.7210, found 1226.7225.

Hexyl arylazopyrazole rapamycin (116). A solution of arylazopyrazole **114** (110 mg, 0.21 mmol, 3 eq), rapamycin (64 mg, 0.07 mmol, 1 eq), and 9-azajulolidine (61 mg, 0.35 mmol, 5 eq) in DCM (3 mL) was stirred overnight at room temperature. The reaction mixture was concentrated in vacuo and the residue was purified via flash chromatography on silica gel (gradient 0% ethyl acetate in DCM → 25% ethyl acetate in DCM) to yield **116** as a yellow solid (8.3 mg, 9% yield). ^{1}H NMR (500 MHz, CD$_3$OD) δ 7.78 (d, 2 H, J = 8.5 Hz), 7.52 (d, 2 H, J = 8.5 Hz), 6.44 (dd, 1 H, J = 12, 10 Hz), 6.27 (dd, 1 H, J = 12, 9 Hz), 6.17 (d, 1 H, J = 10 Hz), 6.11 (d,

1 H, J = 9 Hz), 5.49 (m, 2 H), 5.22 (m, 2 H), 5.10 (m, 2 H), 4.52 (m, 1 H), 4.19 (d, 1 H, J = 3 Hz), 4.11 (t, 2 H, J = 6.5 Hz), 4.01 (d, 1 H, J = 7 Hz), 3.71 (d, 1 H, J = 6.5 Hz), 3.59 (t, 1 H, J = 7 Hz), 3.47 (m, 1 H), 3.42 (s, 3 H), 3.27 (s, 3 H), 3.15 (s, 3 H), 2.89 (d, 1 H, J = 7 Hz), 2.61 (s, 3 H), 2.51 (s, 3 H), 2.32 (m, 1 H), 2.29 (d, 1 H, J = 6.5 Hz), 2.19 (m, 1 H), 2.10 (m, 3 H), 1.97 (m, 1 H), 1.88 (s, 3 H), 1.78 (m, 2 H), 1.61 (m, 2 H), 1.50 (p, 2 H, J = 7 Hz), 1.44 (m, 6 H), 1.22 (m, 2 H), 1.10 (d, 2 H, J = 6.5 Hz), 1.01 (d, 2 H, J = 7 Hz), 0.99 (d, 2 H, J = 7 Hz), 0.91 (m, 4 H), 0.82 (d, 2 H, J = 6.5 Hz) ^{13}C NMR (500 MHz, CDCl$_3$) δ 208.2, 169.2, 166.8, 154.8, 153.7, 142.4, 140.2, 138.6, 136.2, 136.1, 135.5, 135.1, 133.7, 130.2, 129.6, 129.0, 128.9, 126.7, 126.4, 121.9, 120.5, 98.5, 84.8, 84.4, 80.9, 80.4, 75.5, 69.1, 67.1, 59.4, 57.6, 55.9, 55.8, 53.4, 51.3, 49.1, 46.6, 44.2, 41.4, 40.7, 40.2, 38.9, 38.2, 35.8, 35.2, 34.7, 34.5, 33.7, 33.2, 32.8, 31.6, 31.4, 31.3, 30.0, 29.9, 29.7, 29.6, 29.0, 27.3, 27.1, 26.9, 26.4, 26.2, 25.3, 22.7, 22.5, 21.5, 21.0, 20.7, 20.6, 18.8, 16.4, 16.2, 16.1, 15.9, 15.8, 14.1, 13.9, 13.8, 10.1, 11.4, 10.2, 10.1, 9.9; HRMS (ESI$^+$) calcd for C$_{74}$H$_{98}$O$_{15}$N$_5$ (M+H)$^+$ 1254.7523, found 1254.7505.

2-(3',3'-Dimethyl-6-nitrospiro[chromene-2,2'-indolin]-1'-yl)ethyl (perfluorophenyl) carbonate (122). A solution of spiropyran **121** (50 mg, 0.14 mmol, 1 eq), bis(pentafluorophenyl) carbonate (96 mg, 0.21 mmol, 1.5 eq), and DMAP (5 mg, cat.) in acetonitrile (2 mL) was prepared. DIPEA (0.09 mL, 0.42 mmol, 3 eq) was added and the mixture was stirred for 1 hour. The reaction mixture was concentrated in vacuo and purified via flash chromatography on silica gel (20% ethyl acetate in hexanes) to yield **122** as a red oil (71 mg, 90% yield). ^{1}H NMR (500 MHz, CDCl$_3$) δ 8.02 (s, 1 H), 8.01 (s, 1 H), 7.22 (t, 1 H, J = 6.8 Hz), 7.11 (d, 1 H, J = 7.2 Hz), 6.93 (m, 2 H), 6.76 (d, 1 H, J = 8.4 Hz), 6.63 (d, 1 H, J = 8.4 H), 5.92 (d, 1 H, J = 8 Hz), 4.47 (m, 2 H), 3.63 (m, 1 H), 3.48 (m, 1 H), 1.29 (s, 3 H), 1.18 (s, 3 H).

Spiropyran rapamycin (123). A solution of carbonate **122** (71 mg, 0.13 mmol, 2.1 eq), rapamycin (60 mg, 0.06 mmol, 1 eq), and 9-azajulolidine (56 mg, 0.30 mmol, 5 eq) in DCM (2 mL) was stirred at room temperature overnight. The reaction mixture was concentrated in vacuo and the residue was purified via flash chromatography on silica gel (gradient 0% ethyl acetate in DCM → 35% ethyl acetate in DCM) to give **123** as a beige solid (15 mg, 19% yield). ^{1}H NMR (500 MHz, CD$_3$OD) δ 8.12 (m, 1 H), 8.04 (m, 1 H), 7.16 (t, 1 H, J = 8 Hz), 7.09 (m, 2 H), 6.85 (t, 1 H, J = 8 Hz), 6.81 (d, 1 H, J = 6.5 Hz), 6.71 (d, 1 H, J = 7 Hz), 6.49 (m, 1 H), 6.29 (m, 1 H), 6.21 (t, 1 H, J = 10 Hz), 6.13 (d, 1 H, J = 9 Hz), 6.03 (d, 1 H, J = 8 Hz), 5.49 (m, 1 H), 5.28 (d, 1 H, J = 3 Hz), 5.13 (m, 1 H), 4.44 (m, 3 H), 4.20 (m, 2 H), 4.02 (t, 2 H, J = 6.5 Hz), 3.72 (d, 1 H, J = 7 Hz), 3.60 (m, 2 H), 3.49 (m, 3 H), 3.39 (s, 2 H), 3.27 (s, 3 H), 3.19 (s, 3 H), 2.89 (d, 1 H, J = 7 Hz), 2.68 (m, 1 H), 2.51 (m, 1 H), 2.33 (m, 1 H), 2.30 (d, 1 H, J = 6.5 Hz), 2.21 (m, 2 H), 2.08 (t, 2 H, J = 3 Hz), 1.92 (d, 2 H, J = 6.5 Hz), 1.82 (s, 3 H), 1.71 (s, 3 H), 1.68 (m, 2 H), 1.57 (m, 1 H), 1.50 (m, 2 H),

1.37 (m, 2 H), 1.20 (s, 3 H), 1.18 (m, 1 H), 1.11 (d, 2 H, J = 6.5 Hz), 1.07 (d, 2 H, J = 7 Hz), 1.01 (d, 2 H, J = 6.5 Hz), 0.90 (m, 4 H); ^{13}C NMR (500 MHz, CD$_3$OD) δ 213.0, 208.8, 198.5, 169.4, 167.8, 159.4, 154.9, 146.7, 141.2, 139.4, 137.8, 137.0, 132.7, 130.1, 128.1, 127.7, 127.4, 127.0, 125.4, 122.5, 121.7, 121.4, 121.3, 119.5, 118.9, 115.2, 106.7, 106.4, 106.3, 99.3, 83.4, 80.7, 76.2, 74.2, 67.2, 57.0, 56.5, 56.4, 54.9, 52.5, 52.4, 51.3, 47.6, 45.9, 44.1, 40.4, 40.1, 35.8, 33.8, 32.6, 31.3, 30.8, 30.0, 29.3, 26.5, 24.9, 24.6, 22.3, 20.7, 20.4, 18.8, 14.7, 14.6, 14.2, 13.1, 12.4, 9.6; HRMS (ESI$^+$) calcd for C$_{72}$H$_{98}$O$_{18}$N$_3$ (M+H)$^+$ 1293.6824, found 1293.6827.

2.0 Unnatural Amino Acid Syntheses

2.1 Introduction

2.1.1 Unnatural Amino Acid Mutagenesis

Proteins are essential for all cellular processes, playing key roles in signal transduction, cell division, metabolism, and enzymatic catalysis. Most proteins are comprised of combinations of the 20 canonical amino acids that are encoded by three base codons. DNA is transcribed to messenger RNA (mRNA) that is used as a template by the ribosome for protein synthesis in a process known as translation. For translation to produce a functioning, full length protein several components are required. Once the mRNA template has bound to the ribosome, aminoacylated transfer RNAs (tRNAs) carry amino acids to the ribosome. The codons of the mRNA are then matched to complementary tRNA anticodons. The matching of the tRNA anticodons puts the charged amino acid in position for amine substitution onto the preceding tRNA's ester-linked amino acid, generating the amide of the peptide backbone. Once one of three stop codon sequences (UAG, UGA, or UAA) enters the ribosome, the mRNA is idle until a release factor facilitates release of the mRNA strand since there are no tRNAs containing anticodons complimentary to the stop codons.

Once released into the cytoplasm, the protein is folded and can be modified to provide greater structural diversity than the canonical amino acids will allow. The functionality provided by the 20 natural amino acids is limited to carboxylic acids, amides, amines, thiols, thioethers, alcohols, alkyl, and aryl substituents. Post-translational modification of these functional groups can entail phosphorylation, acetylation, glycosylation, methylation, ubiquitinylation, among many others.[139] These post-translational modifications allow for the modulation of a protein's activity beyond what is possible with canonical amino acids. For example, phosphorylation is often used to regulate enzymatic activity and polyubiquitinylation can lead to degradation, though ubiquitin can serve more roles than simply marking a protein for degradation.[139,140] In addition to the canonical amino acids and their post translational modifications, two much less common amino acids have been discovered incorporated in prokaryotes and archae. The amino acid selenocysteine was found to be incorporated by the UGA codon,[141] and the amino acid pyrrolysine was found to be incorporated by the UAG codon.[142]

Protein biosynthesis has since been modified to allow researchers to incorporate unnatural amino acids (UAAs) into proteins. To ensure only the correct amino acids are charged onto the appropriate tRNAs, the aminoacyl tRNA synthetases that charge tRNAs are highly specific for the tRNA and the amino acid that they are conjugating. Misacylation of a tRNA would lead to the wrong amino acid being incorporated into the final protein which could render it inactive. Researchers have been able to incorporate UAAs by introducing tRNA synthetases from other organisms. These tRNA synthetases are often modified to confer specificity for the desired unnatural amino acid. Though the UAA will likely not be incorporated by natural synthetases due to their high specificity, the newly introduced, modified synthetase may incorporate natural amino acids in addition to the UAA. The tRNA that interacts with the introduced synthetase often contains an AUC anticodon complementary to the UAG amber stop codon. The amber stop codon is used since it the least prevalent stop codon, thus minimizing the extension of nontarget proteins with the incorporation of the UAA. Specificity for the amber tRNA is essential to prevent the charging of other tRNAs with the UAA. Once a tRNA is charged with its amino acid, it is incorporated by the ribosome based on matching of codons and anticodons, thus no further modification to the system is necessary.

The Schultz group first introduced unnatural amino acids into *E. coli* in 2001 with the incorporation of *O*-methyl tyrosine using a modified *M. jannaschii* tyrosyl-tRNA/synthetase pair.[143] Schultz *et al*. achieved this by evolving the tyrosyl-tRNA synthetase to charge exclusively *O*-methyl tyrosine onto a tRNA containing the UAG anticodon. Additionally, the tRNA had to be modified so that it was not recognized by any *E. coli* synthetases, ensuring that it would only be charged with the *O*-methyl tyrosine. The orthogonal tRNA/synthetase pair developed has been used to incorporate many amino acids into *E. coli* since the initial publication, but is not orthogonal in mammalian cells.[144] The amino acids incorporated with the *M. jannaschii* system include functionalities such as azides and alkynes for click chemistry, boronic acids, and benzophenone for photocrosslinking.[144]

The lack of orthogonality was addressed by the introduction of the pyrrolysyl tRNA synthetase (PylRS)/tRNA pair derived from the archaea *M. barkeri* which is orthogonal in bacterial, mammalian, and yeast cells.[145] The PylRS/tRNA natural function is to incorporate pyrrolysine, but is fairly promiscuous, potentially due to pyrrolysine's structural dissimiliarity from other amino acids not necessitating evolution of a highly specific synthetase.[146] The PylRS/tRNA system and mutants of it have been used to incorporate functionalities on UAAs such as azides, alkynes, photocaged lysine, small molecule caged lysine, and photocrosslinkers.[144]

An additional *E. coli* derived TyrRS/tRNA pair has been developed that is orthogonal in mammalian cells, but not in bacterial cells.[145] This synthetase system has been used to incorporate azides, photocrosslinkers, and halogenated tyrosine analogs, but has not been used frequently in the past decade due to the popularity of the PylRS/tRNA system.[147,148]
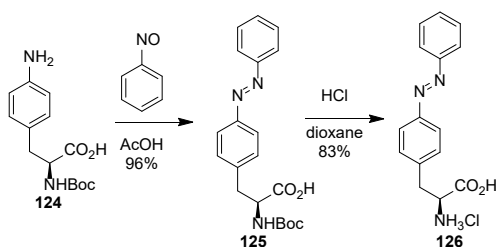
2.2 Photoswitching Amino Acids

2.2.1 Background

Photoswitchable groups have been used to modulate a variety of biological processes through the spatial and temporal activation and inactivation of various ion channels,[131,132] receptors,[149–151] and enzymes.[134,152,153] This generally requires the conjugation of a photoswitchable group to a protein or small molecule. However, the genetic encoding and thereby incorporation of a photoswitching group site-specifically into proteins would allow for more robust results to be obtained. As described in **1.4.2**, many methods of using photoswitches to modulate protein activity involve modification of the protein by introducing new nucleophilic residues or other genetic engineering. The incorporation of a photoswitch as an amino acid minimally modifies the protein, while still allowing the researcher to insert the photoswitch anywhere in the protein with high specificity. Additionally, unlike an azologization approach, the photoswitchable UAA could be used with any protein, an inhibitor compatible with azologization does not need to be found, and avoids any potential promiscuity that an azalog might exhibit.

The Schultz group has previously reported the synthesis and incorporation of the azobenzene-modified UAA **126** in *E. coli* in 2006, the first report of UAA mutagenesis to incorporate a photoswitching amino acid.[130] The amino acid had previously been incorporated into proteins via chemical acylation of tRNAs, but had not had a synthetase developed to incorporate it.[154–156] A tRNA synthetase/tRNA pair originating from *M. jannaschii* was evolved to be capable of incorporating the azobenzene amino acid in *E. coli*. The incorporated UAA **126** was used to reversibly control the binding affinity of the transcription factor CAP to its cofactor cAMP. UAA **126** was inserted into the binding interface of CAP and cAMP and it was demonstrated that when irradiating with 365 nm light, the *cis*-isomer was formed resulting in a 4-fold lower affinity for cAMP. Hoppmann *et al.* further developed azobenzene containing UAAs with the development of several photoswitching, crosslinking UAAs.[157] The attachment of an alkene,

ketone, or benzyl chloride onto the azobenzene incorporated allowed crosslinking of the UAA within the protein, so that when irradiated, the photoswitching has a larger overall impact on protein structure. John *et al.* also reported a series of azobenzene-containing UAAs with various aryl substitutions capable of being isomerized with visible light to generate both isomers.[158] However, none these photoswitches had photostationary states greater than 80% when generating either isomer. A tetrafluorinated azobenzene-containing UAA was later incorporated by our lab.[159] This UAA exhibited greater than 80% photostationary states when generating both isomers, a vast improvement over the previously published systems.

To provide an established photoswitching phenylalanine derivative for biological experiments the synthesis of the azobenzene based amino acid **126** was performed (**Scheme 2.1**). The two-step synthesis began with a Mills reaction wherein the nitroso functionality of nitrosobenzene is protonated to facilitate attack by the aniline of **124**, with a subsequent azo formation releasing water yielding **125** in 96% yield. A simple acidic deprotection of the Boc group yielded **126** in 83% yield. UAA **126** was then used in future biological experiments by Taylor Courtney as a control to compare UAA incorporation of synthesized UAAs to that of **126**.

Scheme 2.1 - The synthesis of azobenzene containing UAA **126**.[130]

2.2.2 Arylazopyrazole Amino Acid

Since the publication of the azobenzene-containing UAA **126**, superior photoswitches have been developed, such as *ortho*-fluorinated azobenzenes[160] and arylazopyrazoles.[123] These photoswitches exhibit superior photostationary states and maintain longer half-lives than azobenzene photoswitches.[123,160] Previously in our lab, a tetrafluorinated azobenzene UAA was synthesized and incorporated.[159] However, the synthesis of the fluorinated azobenzene UAA was lengthy, expensive, and produced a racemic product. However, it was used to effectively control

the activity of firefly luciferase, further demonstrating the utility of a photoswitching UAA. The fluorinated UAA exhibited photostationary states of 91% *cis* upon irradiation with 530 nm light and 84% *trans* upon irradiation with 405 nm light. Alkyl substituted arylazopyrazoles have been shown to have photostationary states of 88% *cis* with 365 nm irradiation and 92% *trans* with 520 nm light making them comparable to fluorinated azobenzenes in that respect.[125] Their synthesis is also generally higher yielding than those of *ortho*-fluorinated azobenzenes, making them a more accessible photoswitching motif.[124,135,160]

The synthesis of an arylazopyrazole containing UAA (**Scheme 2.2**) began with the diazotization of flurorenylmethoxycarbonyl (Fmoc) protected 4-aminophenylalanine (**127**). The diazonium salt is then substituted onto by the enolate of 2,4-pentanedione to yield **128** in 52% yield. This is substantially lower than the yields achieved with similar reactions performed in **1.4.3**. Though the Fmoc group is relatively acid stable, it does hydrolyze under these strongly acidic diazotization conditions. The reaction must be limited to 10 minutes to minimize loss of the Fmoc group despite the diazotization being incomplete. Loss of the Fmoc group at this stage makes purification substantially more challenging. The subsequent reaction utilizes methylhydrazine in two distinct conversions; deprotection of the Fmoc group and formation of the pyrazole from the dione functionality through imine and enamine formations. After concentration of the reaction mixture, suspension of the solid in 4 N HCl in dioxane yields the HCl salt of **129**.
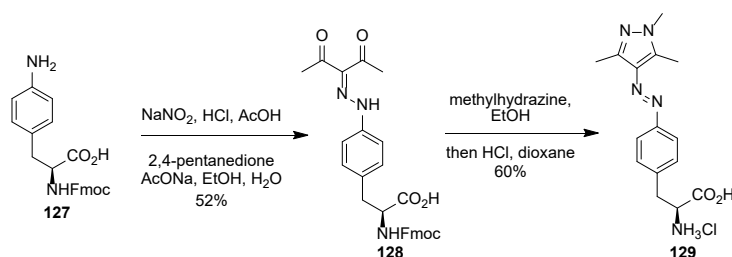
Scheme 2.2 - The synthesis of an arylazopyrazole containing UAA.

Once **129** was synthesized, Taylor Courtney tested it for incorporation of the UAA in mammalian cells. Several mutants of the PylRS/tRNA system were screened for expression of an mCherry-UAG-EGFP reporter construct. Using this reporter, all cells should express mCherry, but if the PylRS synthetase is unable to charge its tRNA, the tRNA will not be able to facilitate incorporation of **129** at the stop codon, so the mRNA will stop being translated after formation of

mCherry. However, if the tRNA is charged with **129**, the mRNA transcript continues to be translated after mCherry, and EGFP is expressed. A compatible synthetase/tRNA system was derived from the *M. barkeri* archaea PylRS (mutations L270F, L274M, N311G, C313G, Y349F),[161] but the synthetase was also able to charge the tRNA with other amino acids (likely phenylalanine due to its structural similarity), resulting in background expression of EGFP (**Figure 2.1A**). The synthetase used in mammalian expression was identified by testing for incorporation using a sfgfp-Y-151TAG-His$_{6x}$ construct in *E. coli*. Purification on nickel resin of the cell lysate should retain only the full-length proteins that incorporated the at the UAA TAG codon. UAA **126** was also tested to allow for a comparison of incorporation efficiency with this synthetase. It can be seen in **Figure 2.1B** that there is incorporation of an amino acid other than **129** since Coomassie staining revealed cells not treated with **129** produced some full-length protein, though at a much lower efficiency.
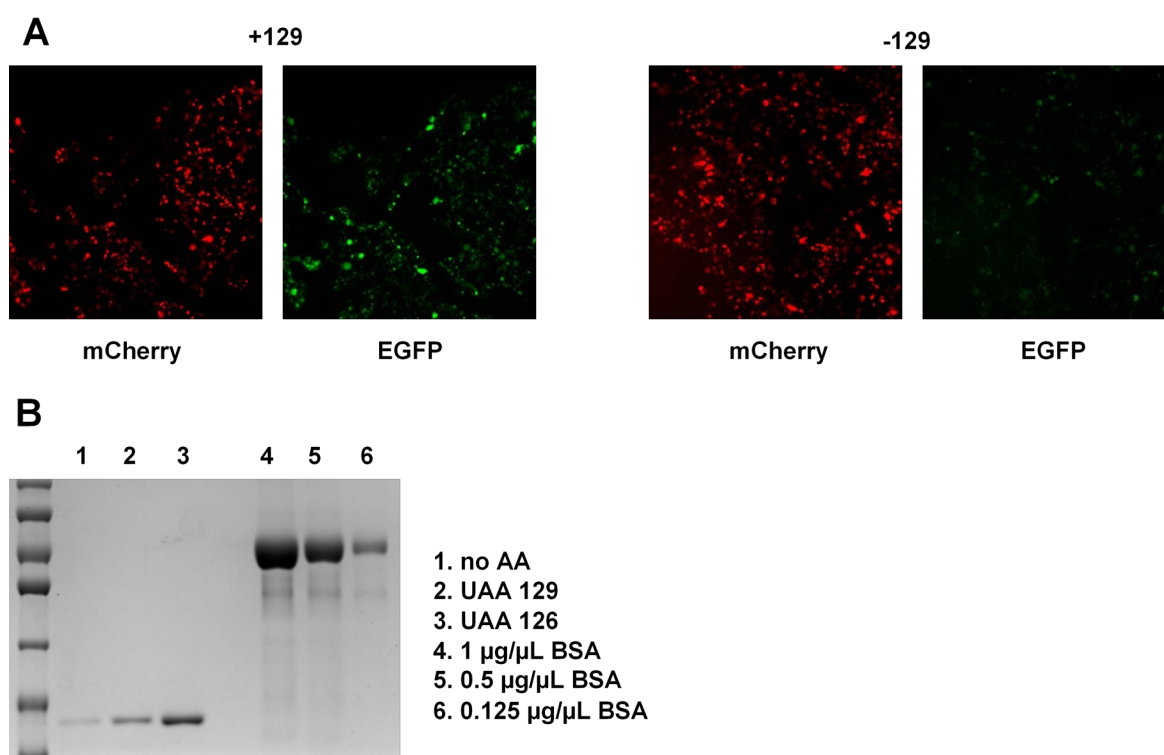

Figure 2.1 - Experiments performed by Taylor Courtney A)Expression of an mCherry-UAG-EGFP construct in HEK293T cells using a mutated PylRS/tRNA system to incorporate **129**, and B) Coomassie staining of nickel purified lysed *E. coli* expressing sfgfp-TAG-His$_{6x}$.

This system could be improved with optimization of the tRNA synthetase used for incorporation. Methods have been developed for the directed evolution of synthetases to incorporate UAAS of interest.[162,163] This would be an effective method to cut down background activity. Furthermore, use of the amino acid to probe a biological function would be advantageous. A demonstration of its ability to reversibly control either protein binding affinity or enzyme activity could provide a platform for further use by other researchers.

2.2.3 Phenazopyridine Amino Acid

A third, phenazopyridine-containing photoswitchable UAA was synthesized in addition to the azobenzene and arylazopyrazole containing amino acids. Phenazopyridines have been shown to have the ability to coordinate biologically-relevant metals such as iron,[164] zinc,[165] manganese,[166] and cobalt.[167] In fact, phenazopyridine is a drug used to treat urinary tract infections, but when taken chronically or in large quantities has caused cyanosis due to its ability to coordinate iron, further demonstrating its coordinating efficacy.[168] The incorporation of the phenazopyridine motif into a UAA would potentially allow for reversible metal binding of an amino acid. In one potential function, if the amino acid were incorporated in a hydrophobic binding interface, it may be able to reversibly draw a metal cation into the region, disrupting a protein-protein interaction. The amino acid could also be incorporated into a portion of a protein that binds a structurally or enzymatically necessary metal. Isomerization of the UAA could disrupt the stabilizing/catalytic effect of the metal, causing a significant loss of protein structure or activity.

To synthesize a phenazopyridine containing UAA, I planned to follow a route similar to Schultz's synthesis of **126**, coupling an arylnitroso to **124** in a Mills reaction followed by HCl deprotection (**Scheme 2.3**). I initially attempted direct oxidation of **130** to the corresponding nitroso with oxone, however, these reactions suffered from consistently low yields (< 10%). One patent had reported this method,[169] but most literature reports utilized a sulfilimine intermediate prior to oxidation to the nitroso.[170,171] Taking this into account, **130** was first converted to a sulfilimine with *N*-chlorosuccinimide (NCS) and dimethyl sulfide, and then oxidized with *m*-chloroperoxybenzoic acid (mCPBA). Attempts to purify via column chromatography resulted in low yields, but NMR of the oxidation reaction's crude material suggested the presence of the nitroso. Thus, a Mills reaction was conducted on the crude nitroso (14-fold excess based on theoretical yield from starting aminopyridine) with limiting **124** yielding **131** in 3% yield over 3 steps from **130**. However, from the more expensive **124**, the yield was 42%. After isolation of **131**, a simple HCl deprotection yielded the HCl salt **132**.
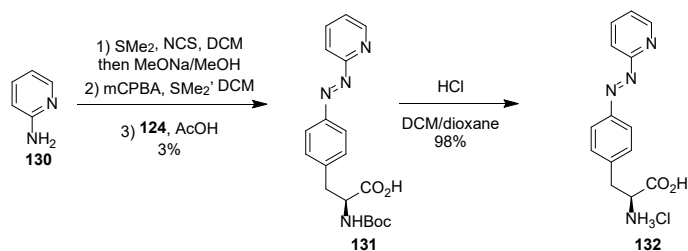
Scheme 2.3 - Synthesis of a phenazopyridine containing amino acid.

Taylor then attempted to incorporate phenazopyridine containing UAA **132** in *E. coli*. To do this, she used an identical system to that described in **Figure 2.1B**, but using a different PylRS mutant derived from *M. barkeri* (mutations Y271, L274A, N311A, C313A, Y349F).[159] The expression of sfgfp Y-151TAG-His$_{6x}$ allowed for selective purification of proteins incorporating an amino acid at the TAG codon on nickel resin. The expression was successful, but like the expression of **129**, there was background incorporation of phenylalanine (**Figure 2.2A**). This was confirmed by mass spectrometry shown in **Figure 2.2B**. In addition to the incorporation of **132** and phenylalanine, there was a third mass higher than that of incorporation of **132** that corresponded to an unknown incorporation product.
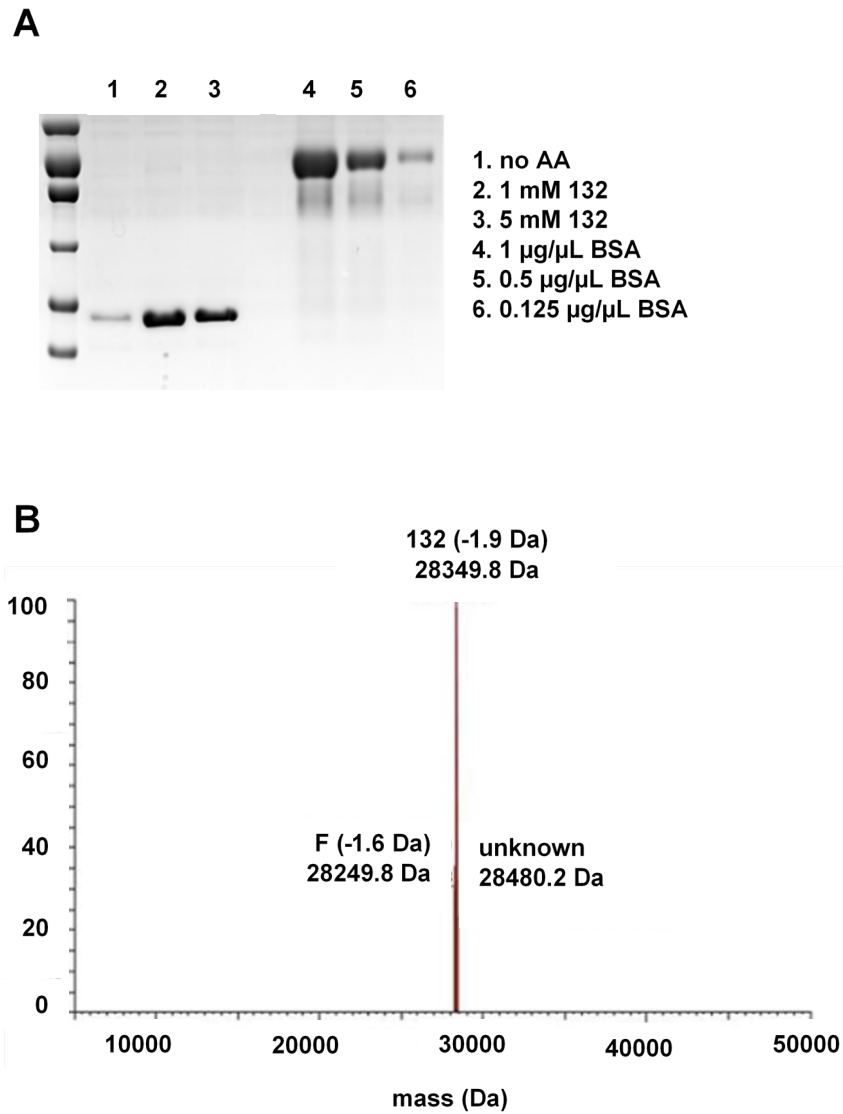
Figure 2.2 - Experiments performed by Taylor Courtney. A) Coomassie staining of nickel purified lysed *E. coli* expressing sfgfp-TAG-His$_{6x}$. B) Mass spectrometry showing the incorporation of phenylalanine.

In addition to **132**, syntheses of phenazopyridine UAAs containing a *meta* and *para* pyridinyl nitrogen were attempted, but could not be completed. To synthesize these UAAs through an analogous route would require the synthesis of 3- and 4-nitrosopyridine, but currently there is no literature precedence for either compound. Attempts to purify or use crude reaction products from the oxidations of 3- and 4-aminopyridine did not result in successful Mills reactions, likely due to the documented instability of nitroso compounds.[172] An alternative method that may circumvent the instability would be to avoid workups altogether and attempt a one pot reaction of sulfilimine oxidation to the nitroso followed by acidification and addition of **124** to transition to a Mills reaction.

2.3 Conclusions and Outlook

The syntheses of two novel photoswitching amino acids were accomplished. An arylazopyrazole-containing amino acid was incorporated into protein in mammalian cells and *E. coli*, though there was observable incorporation of another amino acid with both. A phenazopyridine-containing UAA was also incorporated in *E. coli*, but it has not been incorporated in mammalian cells. The synthesis of the nitrosopyridine used in the synthesis of the phenazopyridine UAA would benefit from optimization as the product of two consecutive reactions were used crude. The use of the amino acids beyond demonstration of incorporation, but rather to allow for reversible control of protein function has yet to be demonstrated as well. The arylazopyrazole-containing amino acid could be used in similar experiments to that of the original azobenzene UAA published by Schultz and compared for relative effects on protein activity.

Furthermore, both amino acids could be used in potentially reversible metal binding. It is common for two histidine residues to bind Zn in metzincin metalloproteases through a HEXXH sequence in the active site.[173,174] To potentially control protease activity, one of the histidine residues would need to be removed. If one of the photoswitching UAAs were introduced into the active site such that one isomer placed the heteroatomic nitrogen in proximity to the Zn ion, and the other isomer did not, this may allow for reversible control of the protease activity via reversible Zn binding.

2.4 Experimental

LED Light Sources

405 nm: LEDENGIN LZ1-10UA00-00U8 (purchased from Mouser Electronics)

415 nm: LUMILEDS LHUV-0415-0650 (purchased from Mouser Electronics)

447.5 nm: LUMILEDS LXML-PR02-A900 (purchased from Mouser Electronics)

530 nm: LUMILEDS LXML-PM01-0100 (purchased from Mouser Electronics)

General Procedures

All chemicals were obtained from commercial sources and used without further purification unless otherwise stated. All reactions were performed in flame dried glassware under nitrogen and stirred magnetically unless otherwise indicated. ^{1}H NMR spectra were obtained from a Bruker Avance III 400 MHz or Bruker Avance III 500 MHz with chemical shifts reported relative to either residual $CHCl_3$ (7.26 ppm), DMSO (2.50), or CH_3OD (3.30 ppm). Mass spectrometry was performed by University of Pittsburgh facilities.

Syntheses of **2** and **3** were conducted according to Schultz's protocol.[130]

(*S*)-2-((((9*H*-Fluoren-9-yl)methoxy)carbonyl)amino)-3-(4-(2-(2,4-dioxopentan-3-ylidene)hydrazineyl)phenyl)propanoic acid (128). Compound **127** (661 mg, 1.64 mmol, 1 eq) was suspended in acetic acid (6 mL) under air, cooled to 0 °C, and concentrated HCl (1 mL) was added dropwise. Sodium nitrite (124 mg, 1.80 mmol, 1.1 eq) was added dropwise as a solution in minimal water. After 10 minutes, a solution of 2,4-pentanedione (0.22 mL, 2.24 mmol, 1.4 eq), sodium acetate (532 mg, 6.50 mmol, 4 eq), ethanol (0.5 mL) and water (1.5 mL) was added portion wise. After 10 minutes, the solution was diluted with ethyl acetate (30 mL). The organic layer was collected and washed with a mixture of 1:1 saturated sodium bicarbonate:brine (2 x 30 mL), then with water (4 x 10 mL). The organic layer was collected, concentrated in vacuo, and the residue was purified via flash chromatography on silica gel (gradient 0% methanol in DCM → 2% methanol) to give **128** as a bright yellow solid (440 mg, 52% yield). ^{1}H NMR (500 MHz, CD_3OD) δ 7.75 (d, 2 H, J = 7.5 Hz), 7.56 (t, 2 H, J = 7.5 Hz), 7.32 (m, 8 H), 4.47 (m, 1 H), 4.34 (m, 1 H), 4.14 (t, 1 H, J = 7.5 Hz) 4.07 (t, 1 H, J = 7.5 Hz), 3.25 (m, 1 H), 2.93 (dd, 1 H, J = 14, 10 Hz), 2.50 (s, 3 H), 2.36 (s, 3 H); ^{13}C NMR (500 MHz, $CDCl_3$) δ 197.1, 196.5, 167.7, 166.3, 164.2, 157.9, 154.3, 144.2, 141.1, 130.8, 128.1, 127.5, 120.6, 116.7, 66.1, 31.6, 29.2; HRMS (ESI[+]) calcd for $C_{29}H_{26}N_3O_6$ (M+H)[+] 512.1816, found 512.1826.

(*S,E*)-2-(Chloro-λ[5]-azaneyl)-3-(4-((1,3,5-trimethyl-1*H*-pyrazol-4-yl)diazenyl)phenyl)propanoic acid (129). A suspension of **128** (193 mg, 0.38 mmol, 1 eq) in ethanol (12 mL) was created. Methylhydrazine (0.5 mL, 12.32 mmol, 32 eq) was added and the

solution was stirred under reflux for 3 hours. The solution was concentrated and the residue was purified via flash chromatography on silica gel (gradient 10% methanol in DCM → 40% methanol in DCM) to yield a yellow solid. The solid was suspended in 4 N HCl (4 mL) in dioxane, stirred for 1 hour at room temperature, and concentrated in vacuo to give **129** as a yellow solid (76 mg, 60% yield). ^{1}H NMR (500 MHz, CD$_3$OD) δ 7.84 (d, 2 H, J = 8.5 Hz), 7.48 (d, 2 H, J = 8.5 Hz), 4.31 (t, 1 H, J = 8.5 Hz), 4.00 (s, 3 H), 3.38 (m, 1 H) 3.08 (dd, 1 H, J = 14.5, 8.5 Hz), 2.72 (s, 3 H), 2.65 (s, 3 H); ^{13}C NMR (500 MHz, CD$_3$OD) δ 171.2, 152.3, 141.7, 139.6, 137.7, 134.5, 129.7, 121.8, 56.1, 36.8, 34.7, 12.4, 8.3; HRMS (ESI$^+$) calcd for C$_{15}$H$_{20}$O$_2$N$_5$ (M+H)$^+$ 302.1625, found 302.1612.

(*S*,*E*)-2-((*tert*-Butoxycarbonyl)amino)-3-(4-(pyridin-2-yldiazenyl)phenyl)propanoic acid (131). A solution of **130** (940 mg, 10 mmol, 1 eq) and dimethyl sulfide (0.8 mL, 11 mmol, 1.1 eq) in 10 mL DCM was cooled to -15 °C in an ethylene glycol/dry ice bath. A solution of *N*-chlorosuccinimide (1.33 g, 10 mmol, 1 eq) in DCM (25 mL) was added dropwise to the reaction mixture and stirred for 1 hour, then warmed to room temperature and stirred for another hour. A suspension of sodium methoxide (405 mg, 17 mmol, 1.7 eq) in methanol (7.5 mL) was added and the suspension was stirred for 10 minutes. The reaction mixture was diluted with water (15 mL) and was stirred for another hour. The organic layer was collected and the aqueous layer was extracted with DCM (2 x 5 mL). The combined organic layers were washed with water (5 mL), dried over sodium sulfate (approximately 500 mg), and concentrated in vacuo to yield 621 mg of an orange oil.

A solution of mCPBA (1.42 g, 17 mmol, 1.7 eq) in DCM (30 mL) was cooled to 0 °C and the orange oil was added slowly as a solution in DCM (6 mL). The reaction mixture was stirred for 1.5 hours. Dimethyl sulfide (0.2 mL, 2.75 mmol, 0.28 eq) was added and the reaction was stirred for 30 minutes. Saturated sodium bicarbonate (30 mL) was added and the organic layer was collected. The organic layer was washed with water (2 x 5 mL), dried over sodium sulfate (approximately 1 g), and concentrated in vacuo to yield 202 mg of an orange oil.

The orange oil and **124** (200 mg, 0.7 mmol, 0.07 eq) were dissolved in acetic acid (10 mL) and stirred at room temperature for 24 hours. The reaction mixture was diluted with ethyl acetate (20 mL) and washed with saturated sodium bicarbonate (2 x 15 mL). The organic layer was concentrated in vacuo and purified via flash chromatography on silica gel (gradient 1.5% methanol in DCM → 5% methanol in DCM) to yield **131** as a red solid (102 mg, 3% yield). ^{1}H NMR (400 MHz, CDCl$_3$) δ 8.74 (d, 1 H, J = 1.2 Hz), 7.98 (m, 3 H), 7.87 (d, 1 H, J = 8 Hz), 7.48 (m, 3 H), 5.26 (d, 1 H, J = 7.2 Hz), 4.70 (d, 1 H, J = 6.8 Hz), 3.32 (d, 2 H, J = 5.2 Hz), 1.48 (s, 9 H); ^{13}C NMR (500 MHz, CD$_3$OD) δ 169.5, 151.6, 146.1, 143.9, 142.0, 130.7, 127.6, 124.5, 117.7, 53.3, 35.9; HRMS (ESI$^+$) calcd for C20H25O4N4 (M+H)$^+$ 385.18792, found 385.18779.

(*S*,*E*)-2-(Chloro-λ^5-azaneyl)-3-(4-(pyridin-2-yldiazenyl)phenyl)propanoic acid (132).
Compound **131** (50 mg, 0.13 mmol, 1 eq) was dissolved in DCM (2 mL). The solution was diluted
with 4 N HCl in dioxane (2 mL) and stirred for 90 minutes at room temperature. The suspension
was concentrated in vacuo to yield **132** as a red solid (45 mg, 98% yield). ^{1}H NMR (400 MHz,
CD$_3$OD) δ 8.81 (d, 1 H, J = 8.4 Hz), 8.56 (s, 1 H), 8.26 (t, 1 H, J = 8.4 Hz), 8.05 (d, 2 H, J = 7.2
Hz), 7.94 (d, 1 H, J = 8.4 Hz), 7.53 (d, 2 H, J = 7.2 Hz), 4.30 (t, 1 H, J = 6.4 Hz), 3.37 (m, 1 H),
3.40 (m, 1 H); ^{13}C NMR (500 MHz, CD$_3$OD) δ 169.5, 151.6, 146.1, 143.9, 142.0, 130.7, 127.6,
124.5, 117.7, 53.3, 35.9; HRMS (ESI$^+$) calcd for C$_{14}$H$_{15}$O$_2$N$_4$ (M+H)$^+$ 271.1190, found 271.1194.

3.0 Photoswitchable Materials

3.1 Photoswitchable Monomer

3.1.1 Background

Differences in the structure of the monomer used can have a drastic effect on the properties of the bulk polymer.[175] This correlation between monomer structure and polymer properties is exemplified by the differences between *cis*- and *trans*-polybutadiene. The two polymers are structural isomers so they are quite similar, but the glass transition temperature, the temperature of transition from a hard or glassy state to a viscous, rubbery state, of *cis*-polybutadiene is nearly 20 °C lower than that of the *trans*-polybutadiene.[175] Some researchers have included light reactive chromophores into monomers allowing them to alter properties of the polymer with light.[176,177] The incorporation of photoactive chromophores has been used in many applications. The use of photoswitching groups in particular are of interest because of the reversibility of the change. Azobenzene has become a popular photoresponsive group for incorporation into polymers due to its reliable photoswitching, remarkable durability through multiple cycles of switching, and the long history of its use as a photoswitch.[178,179]

Azobenzenes have been extensively incorporated into materials to develop light-responsive actuators. Actuators are devices that convert energy into mechanical work.[180] The energy can come from a variety of inputs depending on the system. Common examples are pneumatic, hydraulic, electrical, and magnetic, but with azobenzene-containing materials, it is possible to use light as the source of energy for an actuator.[181–183] This allows for an actuator that is not physically connected to its source of energy.[184]

Researchers have also applied the use of these azobenzene-based actuators in robotics and engineering applications. Some researchers have used azobenzene-based polymers to create gels that are able to "walk" across a surface.[185] This has been further developed with the creation of entirely plastic "arms" capable of picking up and moving objects in response to light irradiation.[186] Others have used an azobenzene-based polymer to power a light driven motor based on the expansion and contraction when exposed to different wavelengths of light.[187] Shining long wavelength light on one portion of a band of the polymer induced *trans*-isomer formation leading to polymer expansion, while shining light on a different portion induced *cis*-

isomer formation that caused polymer contraction. These two processes happening simultaneously lead to a motor being powered by light.

3.1.2 Arylazopyrazole Monomer

Since arylazopyrazoles are superior photoswitches to azobenzenes in both thermal stability and photostationary states (see discussion in **1.4.1**), we collaborated with the Meenakshisundaram lab (Department of Industrial Engineering, University of Pittsburgh) to create an arylazopyrazole-based material that theoretically should have improved photoresponse over azobenzene-based photoswitching systems. Azobenzene-based materials have taken minutes to hours to fully switch in the past.[188] Similar materials containing an arylazopyrazole monomer have not been synthesized, though there have been polymers capped with arylazopyrazoles to allow for reversible cyclodextrin binding to the surface of the polymer.[125] The use of arylazopyrazoles as the photoswitching group has the potential to speed up the macroscopic response due to its improved photostationary state and quantum yield. The polymer proposed by the Meenakshisundaram lab would be a liquid crystalline polymer comprised of a mixture of both the synthesized monomer **133a** or **133b** and the commercially available, non-photoswitching monomer elvamide.

The monomer is comprised of three parts: the arylazopyrazole chromophore, the 6-atom linkers, and the acrylamides. The arylazopyrazole simply acts as the photoswitching group. The 6-atom linkers give **133a** and **133b** an overall rod-like structure, allowing it to align parallel to the elvamide in the liquid-crystal network. The placement of the oxygen in the linker should have little overall effect on the ability of **133a** or **133b** to participate in the liquid crystal network, and has only minor effects on the photoswitching of the arylazopyrazole. The variable oxygen placement in the linker was driven by synthetic ease rather than monomer properties. The acrylamides allow for the liquid crystal network to be covalently linked through a free radical mechanism to essentially lock the liquid crystal network into place.
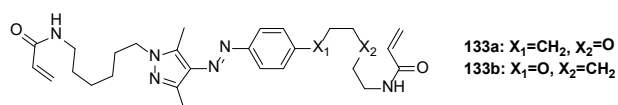

133a: $X_1=CH_2$, $X_2=O$
133b: $X_1=O$, $X_2=CH_2$

**Figure 3.1 -** Structure of the desired arylazopyrazole monomers.

We first attempted a synthesis with the monomer having only alkyl substituents attached to the chromophore (**133a**) as these arylazopyrazoles generally have longer half-lives.[124] To synthesize **133a** through a convergent pathway, we first worked on the ether containing linker (**Scheme 3.1**). Aminopropanol **134** was boc protected to yield **135**. We also converted **137** to dione **138** through a one-pot diazonium salt formation followed by attack with the enolate of 2,4-pentanedione. To form the 6-atom linker seen in **139**, alcohol **135** was converted to the triflate **136**, and after aqueous workup, was added to a solution of **138**. The mixture of the triflate **136** and the ethyl alcohol **138** did not result in formation of **139**.
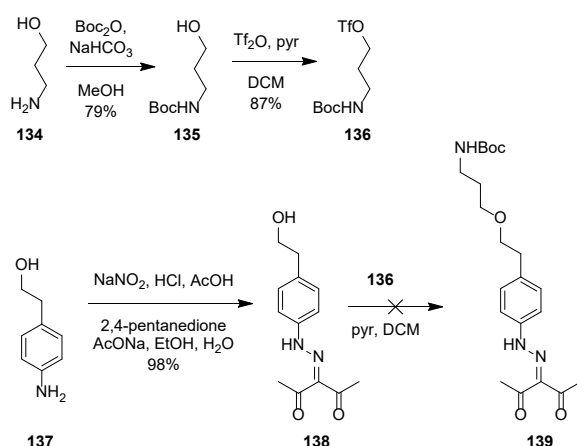
Scheme 3.1 - Attempted synthesis of arylazopyrazole monomer **133a**.

With the initial attempts to form one of the six atom linkers ineffective, other routes were explored. As shown in **Scheme 3.2**, a Mitsunobu reaction was attempted, but was unsuccessful. No product formation was observed by LCMS during the reaction. Mitsunobu reactions generally don't utilize alkyl alcohols due to their poor nucleophilicity. An additional complication may have been the superior acidity of the hydrazone NH on **138**. There is a chance it could be deprotonated and act as the nucleophile instead of the hydroxyl. A final route was tried by tosylating the alcohol of **138** to give140. After tosylation, boc-aminopropanol was deprotonated with 2 equivalents of sodium hydride and **140** was added. This also did not yield any product observable by TLC or LCMS. Since acid base reactions occur much faster than substitutions, it is possible that the

propoxide initially generated deprotonated the hydrazone of **139** rather than substitute onto the tosylated carbon.
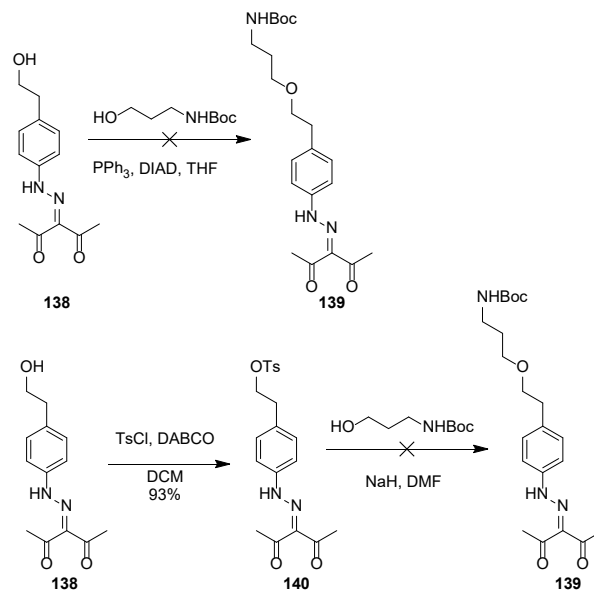
Scheme 3.2 - Alternative attempt at synthesis towards arylazopyrazole monomer **133a**.

Since formation of the alkyl ether proved difficult, we decided to go through a phenolic ether. The half-life of the *cis*-isomer of an arylazopyrazole with a phenolic ether approximately 1.3 days and 89% or better photostationary states were achieved for both isomerizations based in a literature report.[125] The synthetic route toward monomer **133b** is shown in **Scheme 3.3**.
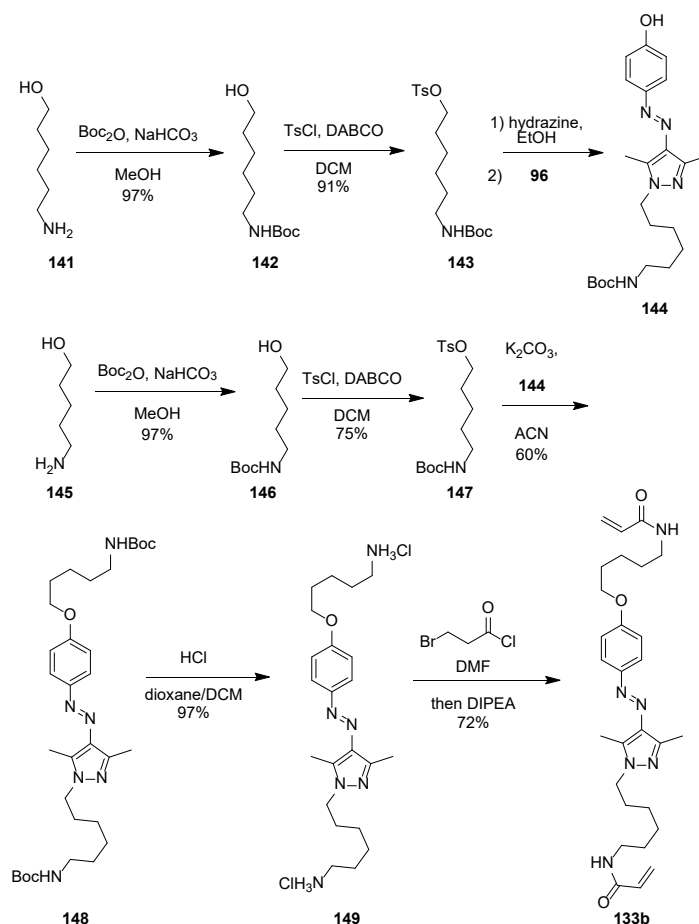
Scheme 3.3 - Synthesis of the arylazopyrazole monomer **133b**.
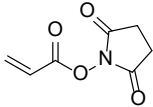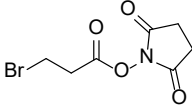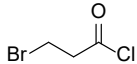
To begin the synthesis, aminohexanol **141** and aminopentanol **145** were both Boc-protected to generate **142** and **146**, respectively.[189] Alcohols **142** and **146** were tosylated under identical conditions to provide **143** and **147** in good yield.[189] These comprised the linkers between the acrylamides and arylazopyrazole in monomer **133b**. Hexyl tosylate **143** was converted into a hexyl hydrazine by heating under reflux with excess hydrazine in ethanol. Purification of the hexyl hydrazine proved difficult, so the reaction was monitored until tosylate **143** was consumed and the reaction was concentrated to remove excess hydrazine. The crude hexyl hydrazine was then refluxed with **96** to yield **144**, a phenolic arylazopyrazole with one of the six atom linkers attached. The phenol of **144** was used in an S$_N$2 reaction with tosylate **147** to generate the doubly Boc-protected monomer **148**. A deprotection was performed with 4 N HCl in dioxane diluted in DCM to yield the diammonium salt **149**. This was converted to the diacrylamide via a Schotten-

Baumann reaction followed by E2 elimination giving the target diacrylamide **133b**. Substantial optimization was required to achieve acceptable yields of **133b** in the final reaction.

Conditions attempted for the conversion of **149** to **133b** are shown in **Table 3.1** below. Initial attempts used a fourfold excess of acryloyl chloride in DCM and pyridine at 0 °C with **149** suspended in the mixture. Theoretically, once the ammonium salts were converted to acrylamides, they would be solubilized, however, after several hours, a spongy yellow mass had formed that was insoluble in a variety of solvents and was stable to acidic and basic conditions. Since the arylazopyrazole never solubilized, I decided to try using a more polar solvent to help facilitate the reaction. When switching to a DMF solvent I formed a soluble product. However, LCMS showed oligomers of 2, 3, and 4 forming. Higher oligomers were likely formed, but were out of the detectable range. The alkene of the acrylamide that was forming was being attacked by the as yet unsubstituted amines.

To avoid this, I increased the equivalents of the acryl NHS source and attempted reactions at -20 °C, -40 °C, and -80 °C. The reaction at -80 °C was run in DCM due to the higher freezing point of DMF. None of the reactions showed substantial product formation, but rather polymerization products. Surprisingly, I was only able to isolate product from the 0 °C reaction. Based on these results, it was not practical to use low temperatures to suppress the acryl alkene substitution, however, a less reactive alkene precursor had the potential to limit amine attack. The use of 3-bromopropanoate NHS ester with a delayed addition of the DIPEA base yielded a small amount of product, but the yield was still quite low and I saw substantial oligomer formation. A final effort was made to fully solubilize the diammonium salt despite its poor solubility (about 4 mg/mL DMF), and this reaction formed the diacrylamide **133b** in good yield. The polymerization was likely driven by the use of a suspension of **149** in previous experiments. Once an acrylamide formed on the surface of a solid mass of **149**, there was an artificially high concentration of unreacted amine in the proximity of the acrylamide because the acrylamide was being held close to the surface of the mass.

Table 3.1 - Conditions tested for the conversion of the ammonium salt **149** to the desired monomer **133b**. Sat. indicates a saturated solution.

Acryl Group	Acryl Eq.	Conc. of **149** / mM	Solvent	Base	Base / eq.	Temp / °C	Yield / %
(acryloyl chloride)	4	sat.	DCM	pyridine	5	0	0
(acrylate NHS ester)	3	sat.	DCM	DIPEA	4	-80	0
	10	sat.	DMF	DIPEA	5	0	5
					10	-20	0
					10	-40	0
	3	sat.	ACN	DIPEA	10	0	0
(3-bromopropanoyl NHS ester)	10	sat.	DMF	DIPEA	20	0	17
(3-bromopropanoyl chloride)	10	8.5	DMF	DIPEA	20	0	72

Once the photoswitchable monomer **133b** was successfully synthesized, it was given to Arul Clemente from the Meenakshisundaram lab to incorporate into a photoswitching polymer. Arul was able to incorporate the monomer into a liquid crystal network with the commercially available diacrylate elvamide. Liquid crystal networks are somewhat fluid mixtures of monomers that are able to flow past each other, but have general crystalline orientations of the molecules. Liquid crystal networks can be maintained as simply liquid crystals, but they can also be cross linked in the presence of an initiator to form a set polymer.[188,190,191]
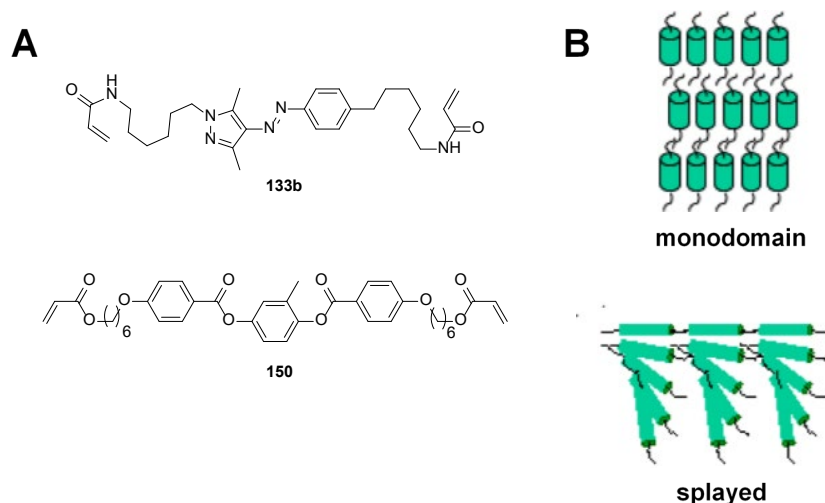
Figure 3.2 - A) Structures of monomer **133b** and elvamide **150**. B) Representation of monomers in a monodomain or splayed liquid crystal network adapted from Broer's review.[192] Adapted with permission from Liu *et al*. Liquid Crystal Polymer Networks: Preparation, Properties, and Applications of Films with Patterned Molecular Alignment. Langmuir 2014, 30 (45), 13499–13509. Copyright 2014 American Chemical Society.

Arul made a mixture of 7% **133b** and 93% **150** to create the liquid crystal network. When making the liquid crystal network, he was able to align the bulk material's components in such a way that they were parallel to one another, known as a monodomain orientation (**Figure 3.2B**). Once oriented correctly, the network was crosslinked with a photoinitiator giving a more rigid polymer and locking in the parallel orientation. When inducing *trans*-to-*cis* isomerization of many parallel components of a liquid crystal material, the material will bend since the *cis*-isomers have a shorter end-to-end distance.[193] The non-irradiated *trans*-isomers on the opposite side of the network do not isomerize, so they do not shorten, thus resulting in bending of the polymer. Given the superior photostationary states of *trans*-to-*cis* isomerization, it was believed that incorporation of **133b** into the material would cause a larger bending than an azobenzene containing material. However, the material showed a lesser bending in response to light than the azobenzene containing material. The bending achieved can be seen in **Figure 3.3**. It was believed that this could have been a result of a better quantum yield of isomerization relative to the azobenzene containing polymer. If this were the case, before the uppermost irradiated layer was able to fully isomerize and therefore shorten, the bottom layer would also begin isomerizing and shortening. Thus, the whole polymer would be shortening at a similar rate, reducing the overall bending.
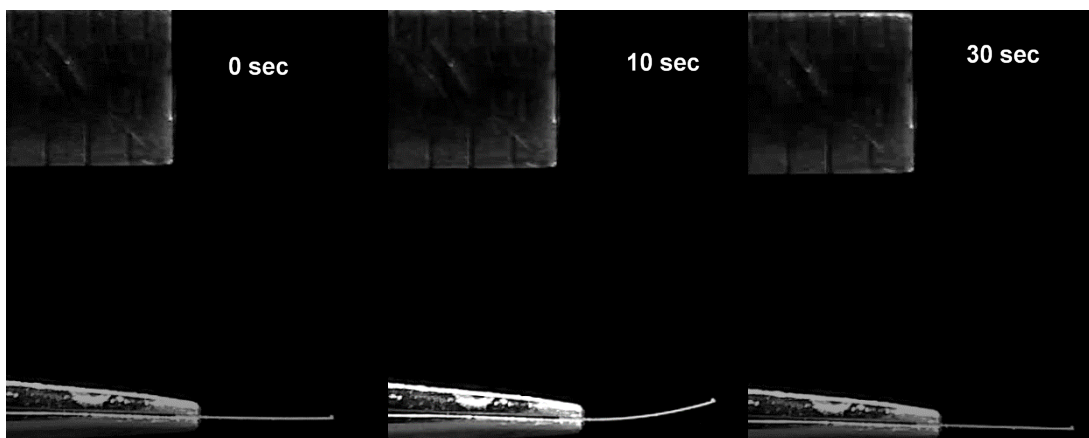
Figure 3.3 - Bending of a liquid crystal material containing monomer **150** upon irradiation with 365 nm light. The material bends vertically, then relaxes over the course of 30 seconds of irradiation.

To determine if this was the case, Arul formed a splayed liquid crystal network that would illuminate if this was the case. The splayed conformation has a layer of liquid crystal material that is parallel, but one edge of the material bends towards a perpendicular orientation (**Figure 3.2B**). In this alignment, even if all of the photoswitching units were to switch, a helical macroscopic formation should be observed since one edge of the material strip is contracting more than the other, yet this still did not show greater bending than an azobenzene liquid crystal material.

One potential reason for this lesser macroscopic response is a lesser change in distance between *cis* and *trans* isomers. Based on literature reports, this is unlikely, though in the context of a bulk material it could be the case. A second potential cause is the presence of the methyl groups on the pyrazole of **133b**. The sterics of these may be preventing isomerization in the matrix of a polymer. A final potential reason would be that there is a lower energetic force behind the *cis* isomerization in **133b** than in an analogous azobenzene, and that in a more rigid polymeric environment, less of the arylazopyrazole is actually switching. To test these hypotheses, computational studies could be performed to determine the energetic favorability of switching. Alternatively, a demethylated arylazopyrazole could be synthesized to determine the role they are playing. A nonmethylated analog was reported to have approximately a 3 year half-life and similar photostationary states making it an appropriate analog to examine the role of the methyl groups.[123]

3.2 Conclusions and Outlook

An arylazopyrazole-containing monomer was synthesized through a convergent synthesis with significant optimization of the final Schotten-Baumann reaction required. The monomer was incorporated in a liquid crystal network that was subsequently crosslinked to give a photoresponsive polymer. The arylazopyrazole polymer demonstrated a macroscopic response when irradiated, but this response was not as significant as that of azobenzene. Further synthesis of a demethylated analog could indicate the role sterics are playing in the lesser response. It is possible that in the more constrained environment of a bulk solid, the methyl groups could be reducing the favorability of switching. Computational modeling may also provide insight into the energetic favorability of the isomerization that could help rationalize the lesser response.

3.3 Experimental

General Procedures

All chemicals were obtained from commercial sources and used without further purification unless otherwise stated. All reactions were performed in flame dried glassware under nitrogen and stirred magnetically unless otherwise indicated. ^{1}H NMR spectra were obtained from a Bruker Avance III 400 MHz or Bruker Avance III 500 MHz with chemical shifts reported relative to either residual $CHCl_3$ (7.26 ppm), DMSO (2.50), or CH_3OD (3.30 ppm). Mass spectrometry was performed by University of Pittsburgh facilities.

Compounds **135**,[194] **142**,[189] **143**,[189] **146**,[189] and **147**[189] were synthesized according to literature syntheses without any modifications and obtained yields matched reported ones.

3-(2-(4-(2-Hydroxyethyl)phenyl)hydrazineylidene)pentane-2,4-dione (138). Compound **137** (1.114 g, 8.1 mmol, 1 eq) was dissolved in acetic acid (11 mL) and concentrated HCl (1.8 mL), then cooled to 0 °C. Sodium nitrite (682 mg, 9.9 mmol, 1.2 eq) was added dropwise as a solution in minimal water. After 30 minutes, a solution of acetylacetone (1.12 ml, 11 mmol, 1.4 eq) and NaOAc (2.078 g, 25 mmol, 3.1 eq) in ethanol (9.6 mL) and water (4.8 mL) was added portionwise. The reaction mixture was stirred overnight at room temperature. The reaction mixture

was diluted with ethyl acetate (20 mL), washed with excess saturated sodium bicarbonate, brine (10 mL), and then concentrated in vacuo to yield **138** as a yellow solid. (2.061 g, 98% yield). ^{1}H NMR (500 MHz, CD$_3$Cl) δ 14.78 (s, 1 H), 7.37 (d, 2 H, J = 8.5 Hz), 7.26 (d, 2 H, J = 8.5 Hz), 3.88 (q, 2 H, J = 6 Hz), 2.89 (t, 2 H, J = 6 Hz), 2.60 (s, 3 H), 2.49 (s, 3 H), 2.42 (d, 1 H, J = 6 Hz); ^{13}C NMR (500 MHz, CDCl$_3$) δ 197.9, 197.1, 140.2, 136.57, 133.2, 130.3, 116.5, 63.5, 38.6, 31.6, 26.6; HRMS (ESI$^+$) calcd for C$_{13}$H$_{17}$O$_3$N$_2$ (M+H)$^+$ 249.1234, found 249.1237.

4-(2-(2,4-Dioxopentan-3-ylidene)hydrazineyl)phenethyl 4-methylbenzenesulfonate (140). Compound **138** (100 mg, 0.4 mmol, 1 eq), tosyl chloride (92 mg, 0.48 mmol, 1.2 eq), and DABCO (67 mg, 0.6 mmol, 1.5 eq) was dissolved in DCM (3.5 mL) and stirred overnight at room temperature. The reaction mixture was diluted with ethyl acetate (10 mL) and washed with water (3 x 5 mL) and brine (5 mL). The organic layer was dried over sodium sulfate (approximately 500 mg) and concentrated in vacuo to yield the tosylate **140** as a yellow oil (151 mg, 93% yield). ^{1}H NMR (500 MHz, CD$_3$Cl) δ 14.74 (s, 1 H), 7.69 (d, 2 H, J = 8 Hz), 7.28 (m, 4 H), 7.15 (d, 2 H, J = 8 Hz), 4.21 (t, 2 H, J = 6 Hz), 2.96 (t, 2 H, J = 6 Hz), 2.60 (s, 3 H), 2.49 (s, 3 H), 2.43 (s, 3 H); ^{13}C NMR (500 MHz, CDCl$_3$) δ 198.0, 197.0, 141.7, 140.5, 134.1, 133.3, 133.1, 130.2, 130.1, 129.8, 127.8, 116.4, 70.3, 34.9, 31.6, 26.6, 21.6.

***tert*-Butyl (*E*)-(6-(4-((4-hydroxyphenyl)diazenyl)-3,5-dimethyl-1*H*-pyrazol-1-yl)hexyl)carbamate (144).** A solution of hydrazine (2.54 g, 79 mmol, 14 eq) in ethanol (25 mL) was cooled to 0 °C. Compound **143** (2 g, 5.4 mmol, 1 eq) was added to the solution and the reaction mixture was stirred overnight at 60 °C. The reaction mixture was concentrated to yield a colorless oil.

The oil was redissolved in ethanol (50 mL). Compound **96** (2.038 g, 9.3 mmol, 1.7 eq) was added and the solution was stirred overnight at 60 °C. The reaction mixture was concentrated in vacuo and the residue was purified via flash chromatography on silica gel (gradient 0% methanol in DCM → 6% methanol in DCM) to yield **144** as a yellow solid (1.004 g, 45% yield). ^{1}H NMR (400 MHz, CDCl$_3$) δ 7.71 (d, 2 H, J = 8.8 Hz), 6.91 (d, 2 H, J = 8.8 Hz), 4.58 (b, 1 H), 3.99 (t, 2 H, J = 7.2 Hz), 3.09 (q, 2 H, J = 7.2 Hz), 2.53 (s, 3 H), 2.49 (s, 3 H), 1.80 (p, 2 H, J = 7.2 Hz), 1.43 (m, 11 H), 1.32 (m, 4 H); ^{13}C NMR (500 MHz, CDCl$_3$) δ 157.7, 147.7, 142.2, 137.5, 134.7, 123.5, 115.6, 48.8, 40.4, 34.7, 31.6, 29.9, 26.3, 25.3, 22.7, 20.5, 14.1, 13.8, 15.4, 12.1; HRMS (ESI+) calcd for C$_{21}$H$_{32}$N$_5$O$_3$ (M+H)+ 402.25029, found 402.25022.

***tert*-Butyl (*E*)-(6-(4-((4-((5-((tert-butoxycarbonyl)amino)pentyl)oxy)phenyl)diazenyl)-3,5-dimethyl-1*H*-pyrazol-1-yl)hexyl)carbamate (148).** A solution of phenol **144** (1.004 g, 2.4 mmol, 1 eq) and tosylate **147** (1.004 g, 2.8 mmol, 1.2 eq) in dry acetonitrile (30 mL) was prepared. Potassium carbonate (714 mg, 5 mmol, 2 eq) was added and the reaction mixture was stirred

under reflux overnight. The reaction mixture was filtered, the filtrate was concentrated in vacuo, and the residue was purified via flash chromatography on silica gel (gradient 0% ethyl acetate in DCM → 40% ethyl acetate in DCM) to yield **148** as a yellow solid (870 mg, 60% yield). ^{1}H NMR (400 MHz, CDCl$_3$) δ 7.76 (d, 2 H, J = 8.8 Hz), 6.94 (d, 2 H, J = 9.2), 4.53 (b, 2 H), 4.00 (m, 4 H), 3.10 (m, 4 H), 2.55 (s, 3 H), 2.48 (s, 3 H), 1.82 (m, 4 H), 1.57 (m, 4 H), 1.44 (m, 20 H), 1.30 (m, 4 H); ^{13}C NMR (500 MHz, CDCl$_3$) δ 160.2, 156.0, 147.9, 142.2, 137.5, 134.8, 123.2, 114.5, 79.1, 68.0, 48.8, 40.5, 34.7, 31.6, 30.0, 29.0, 28.9, 26.3, 25.3, 23.4, 22.7, 20.7, 14.1, 13.9, 9.9; HRMS (ESI$^+$) calcd for C$_{32}$H$_{53}$O$_5$N$_6$ (M+H)$^+$ 601.4072, found 601.4052.

(*E*)-1-(6-(Chloro-λ^5-azaneyl)hexyl)-4-((4-((5-(chloro-λ^5-azaneyl)pentyl)oxy)phenyl)diazenyl)-3,5-dimethyl-1*H*-pyrazole (149). A solution of arylazopyrazole **148** (860 mg, 1.4 mmol) in dry DCM (30 mL) was prepared and then was diluted with 4 N HCl in dioxane (10 mL) and the reaction mixture was stirred for 3 hours. The reaction mixture was concentrated in vacuo to yield a yellow solid (644 mg, 97% yield) to yield **149**. ^{1}H NMR (500 MHz, CD$_3$OD) δ 7.75 (d, 2 H, J = 9 Hz), 7.00 (d, 2 H, J = 9 Hz), 4.15 (m, 2 H), 4.06 (t, 2 H, J = 6.5 Hz), 2.93 (p, 5 H, J = 6.5 Hz), 2.89 (p, 2 H, J = 6.5 Hz), 2.61 (s, 3 H), 2.49 (s, 3 H), 1.84 (m, 4 H), 1.73 (p, 2 H, J = 6.5 Hz), 1.60 (m, 4 H), 1.40 (m, 4 H); ^{13}C NMR (500 MHz, CD$_3$OD) δ 160.3, 147.6, 140.7, 134.5, 123.4, 115.3, 68.1, 49.0, 48.6, 40.5, 40.2, 39.7, 39.1, 29.5, 28.6, 27.1, 25.9, 25.8, 23.0, 14.2; HRMS (ESI$^+$) calcd for C$_{22}$H$_{37}$ON$_6$ (M+H)$^+$ 401.3023, found 401.3027.

(*E*)-1-(6-(Chloro-λ^5-azaneyl)hexyl)-4-((4-((5-(chloro-λ^5-azaneyl)pentyl)oxy)phenyl)diazenyl)-3,5-dimethyl-1*H*-pyrazole (133b). A solution of 3-bromopropionyl chloride (720 mg, 4.2 mmol, 10 eq) in dry DMF (10 mL) was cooled to 0 °C. A solution of diamine **149** (200 mg, 0.42 mmol, 1 eq) in dry DMF (50 mL) was added dropwise to the acid chloride and stirred at 0 °C for 1.5 hours. DIPEA (6 mL, excess) was added and the reaction was stirred at room temperature for 2 hours. The reaction mixture was diluted with ethyl acetate (100 mL), then washed with brine (50 mL) and water (5 x 50 mL). The organic layer was concentrated in vacuo and the residue was purified via flash chromatography on silica gel (gradient 0% methanol in DCM → 5% methanol in DCM) to yield **133b** as a yellow solid. ^{1}H NMR (500 MHz, CDCl$_3$) δ 7.76 (d, 2 H, J= 8.5 Hz), 6.93 (d, 2 H, J = 8.5 Hz), 6.27 (dd, 2 H, J = 21, 5 Hz), 6.08 (dd, 2 H, J = 22 Hz, 13 Hz), 5.74 (b, 1 H), 5.62 (m, 3 H), 4.02 (t, 2 H, J = 6.5 Hz), 3.33 (m, 4 H), 2.61 (p, 2 H, J = 6.5 Hz), 2.55 (s, 3 H), 2.48 (s, 3 H), 1.83 (m, 4 H), 1.59 (m, 2 H), 1.08 (m, 4 H); ^{13}C NMR (500 MHz, CDCl$_3$) δ 165.6, 160.2, 147.9, 142.1, 137.6, 134.8, 130.9, 126.3, 123.3, 114.5, 67.9, 53.4, 50.9, 39.5, 29.8, 26.2, 25.9, 23.5, 13.9; HRMS (ESI$^+$) calcd for C$_{28}$H$_{41}$O$_3$N$_6$ (M+H)$^+$ 509.3235, found 509.3225.

Bibliography

(1)   Ho, S. N.; Biggar, S. R.; Spencer, D. M.; Schreiber, S. L.; Crabtree, G. R. Dimeric Ligands Define a Role for Transcriptional Activation Domains in Reinitiation. *Nature* **1996**, *382* (6594), 822. https://doi.org/10.1038/382822a0.

(2)   Belshaw, P. J.; Ho, S. N.; Crabtree, G. R.; Schreiber, S. L. Controlling Protein Association and Subcellular Localization with a Synthetic Ligand That Induces Heterodimerization of Proteins. *PNAS* **1996**, *93* (10), 4604–4607. https://doi.org/10.1073/pnas.93.10.4604.

(3)   Klemm, J. D.; Beals, C. R.; Crabtree, G. R. Rapid Targeting of Nuclear Proteins to the Cytoplasm. *Current Biology* **1997**, *7* (9), 638–644. https://doi.org/10.1016/S0960-9822(06)00290-9.

(4)   Morawska, M.; Ulrich, H. D. An Expanded Tool Kit for the Auxin-Inducible Degron System in Budding Yeast. *Yeast* **2013**, *30* (9), 341–351. https://doi.org/10.1002/yea.2967.

(5)   Winter, G. E.; Buckley, D. L.; Paulk, J.; Roberts, J. M.; Souza, A.; Dhe-Paganon, S.; Bradner, J. E. Phthalimide Conjugation as a Strategy for in Vivo Target Protein Degradation. *Science* **2015**, *348* (6241), 1376–1381. https://doi.org/10.1126/science.aab1433.

(6)   Lu, J.; Qian, Y.; Altieri, M.; Dong, H.; Wang, J.; Raina, K.; Hines, J.; Winkler, J. D.; Crew, A. P.; Coleman, K.; et al. Hijacking the E3 Ubiquitin Ligase Cereblon to Efficiently Target BRD4. *Chemistry & Biology* **2015**, *22* (6), 755–763. https://doi.org/10.1016/j.chembiol.2015.05.009.

(7)   Di Stasi, A.; Tey, S.-K.; Dotti, G.; Fujita, Y.; Kennedy-Nasser, A.; Martinez, C.; Straathof, K.; Liu, E.; Durett, A. G.; Grilley, B.; et al. Inducible Apoptosis as a Safety Switch for Adoptive Cell Therapy. *New England Journal of Medicine* **2011**, *365* (18), 1673–1683. https://doi.org/10.1056/NEJMoa1106152.

(8)   Spencer, D. M.; Wandless, T. J.; Schreiber, S. L.; Crabtree, G. R. Controlling Signal Transduction with Synthetic Ligands. *Science* **1993**, *262* (5136), 1019–1024. https://doi.org/10.1126/science.7694365.

(9)   Luo, Z.; Tzivion, G.; Belshaw, P. J.; Vavvas, D.; Marshall, M.; Avruch, J. Oligomerization Activates C-Raf-1 through a Ras-Dependent Mechanism. *Nature* **1996**, *383* (6596), 181. https://doi.org/10.1038/383181a0.

(10)   Sehgal, S. N.; Baker, H.; Vézina, C. Rapamycin (AY-22,989), a New Antifungal Antibiotic. II. Fermentation, Isolation and Characterization. *The Journal of Antibiotics* **1975**, *28* (10), 727–732. https://doi.org/10.7164/antibiotics.28.727.

(11)   Yoo, Y. J.; Hwang, J.; Shin, H.; Cui, H.; Lee, J.; Yoon, Y. J. Characterization of Negative Regulatory Genes for the Biosynthesis of Rapamycin in Streptomyces Rapamycinicus and Its Application for Improved Production. *J Ind Microbiol Biotechnol* **2015**, *42* (1), 125–135. https://doi.org/10.1007/s10295-014-1546-9.

(12)   Park, S. R.; Yoo, Y. J.; Ban, Y.-H.; Yoon, Y. J. Biosynthesis of Rapamycin and Its Regulation: Past Achievements and Recent Progress. *The Journal of Antibiotics* **2010**, *63* (8), 434–441. https://doi.org/10.1038/ja.2010.71.

(13)   Kuščer, E.; Coates, N.; Challis, I.; Gregory, M.; Wilkinson, B.; Sheridan, R.; Petković, H. Roles of RapH and RapG in Positive Regulation of Rapamycin Biosynthesis in Streptomyces Hygroscopicus. *J Bacteriol* **2007**, *189* (13), 4756–4763. https://doi.org/10.1128/JB.00129-07.

(14)   Gary, D.; Joseph, G. J. J.; Anna, B.; Marshall, F. J. Anti-Tumor Activity Of Cci-779 In Papillary Renal Cell Cancer. US 8791097 B2, April 8, 2008.

(15)   Heidi, L.; Terence, O.; Marjorie, W. J. Treatment Of Solid Tumors With Rapamycin Derivatives. US 8436010 B2, February 23, 2012.

(16)   Rosborough, B. R.; Raïch-Regué, D.; Matta, B. M.; Lee, K.; Gan, B.; DePinho, R. A.; Hackstein, H.; Boothby, M.; Turnquist, H. R.; Thomson, A. W. Murine Dendritic Cell Rapamycin-Resistant and Rictor-Independent MTOR Controls IL-10, B7-H1, and Regulatory T-Cell Induction. *Blood* **2013**, *121* (18), 3619–3630. https://doi.org/10.1182/blood-2012-08-448290.

(17)   Raimondi, G.; Sumpter, T. L.; Matta, B. M.; Pillai, M.; Corbitt, N.; Vodovotz, Y.; Wang, Z.; Thomson, A. W. Mammalian Target of Rapamycin Inhibition and Alloantigen-Specific Regulatory T Cells Synergize To Promote Long-Term Graft Survival in Immunocompetent Recipients. *The Journal of Immunology* **2010**, *184* (2), 624–636. https://doi.org/10.4049/jimmunol.0900936.

(18)   Molina, L.; Yang, H.; Michael, A. O. A.; Oertel, M.; Bell, A.; Singh, S.; Chen, X.; Tao, J.; Monga, S. P. S. MTOR Inhibition Affects Yap1-β-Catenin-Induced Hepatoblastoma Growth and Development. *Oncotarget* **2019**, *10* (15). https://doi.org/10.18632/oncotarget.26668.

(19)   Seto, B. Rapamycin and MTOR: A Serendipitous Discovery and Implications for Breast Cancer. *Clinical and Translational Medicine* **2012**, *1* (1), 29. https://doi.org/10.1186/2001-1326-1-29.

(20)   Kang, C. B.; Hong, Y.; Dhe-Paganon, S.; Yoon, H. S. FKBP Family Proteins: Immunophilins with Versatile Biological Functions. *Neurosignals* **2008**, *16* (4), 318–325.

(21)   Laplante, M.; Sabatini, D. M. MTOR Signaling in Growth Control and Disease. *Cell* **2012**, *149* (2), 274–293. https://doi.org/10.1016/j.cell.2012.03.017.

(22)   Prolonged Rapamycin Treatment Inhibits MTORC2 Assembly and Akt/PKB. *Molecular Cell* **2006**, *22* (2), 159–168. https://doi.org/10.1016/j.molcel.2006.03.029.

(23)   Chen, J.; Zheng, X. F.; Brown, E. J.; Schreiber, S. L. Identification of an 11-KDa FKBP12-Rapamycin-Binding Domain within the 289-KDa FKBP12-Rapamycin-Associated Protein and Characterization of a Critical Serine Residue. *PNAS* **1995**, *92* (11), 4947–4951. https://doi.org/10.1073/pnas.92.11.4947.

(24)   Banaszynski, L. A.; Liu, C. W.; Wandless, T. J. Characterization of the FKBP·Rapamycin·FRB Ternary Complex. *Journal of the American Chemical Society* **2005**, *127* (13), 4715–4721. https://doi.org/10.1021/ja043277y.

(25)   Choi, J.; Chen, J.; Schreiber, S. L.; Clardy, J. Structure of the FKBP12-Rapamycin Complex Interacting with the Binding Domain of Human FRAP. *Science* **1996**, *273*, 239–242. https://doi.org/10.2210/pdb1fap/pdb.

(26)   Patury, S.; Geda, P.; Dobry, C. J.; Kumar, A.; Gestwicki, J. E. Conditional Nuclear Import and Export of Yeast Proteins Using a Chemical Inducer of Dimerization. *Cell Biochemistry and Biophysics* **2009**, *53* (3), 127–134. https://doi.org/10.1007/s12013-009-9044-9.

(27)   Varnai, P.; Thyagarajan, B.; Rohacs, T.; Balla, T. Rapidly Inducible Changes in Phosphatidylinositol 4,5-Bisphosphate Levels Influence Multiple Regulatory Functions of the Lipid in Intact Living Cells. *J Cell Biol* **2006**, *175* (3), 377–382. https://doi.org/10.1083/jcb.200607116.

(28)   Söhnel, A.-C.; Kohl, W.; Gregor, I.; Enderlein, J.; Rieger, B.; Busch, K. B. Probing of Protein Localization and Shuttling in Mitochondrial Microcompartments by FLIM with Sub-Diffraction Resolution. *Biochimica et Biophysica Acta (BBA) - Bioenergetics* **2016**, *1857* (8), 1290–1299. https://doi.org/10.1016/j.bbabio.2016.03.021.

(29)   Diaz, J. E.; Morgan, C. W.; Minogue, C. E.; Hebert, A. S.; Coon, J. J.; Wells, J. A. A Split-Abl Kinase for Direct Activation in Cells. *Cell Chemical Biology* **2017**, *24* (10), 1250-1258.e4. https://doi.org/10.1016/j.chembiol.2017.08.007.

(30)   Martell, J. D.; Yamagata, M.; Deerinck, T. J.; Phan, S.; Kwa, C. G.; Ellisman, M. H.; Sanes, J. R.; Ting, A. Y. A Split Horseradish Peroxidase for the Detection of Intercellular Protein–Protein Interactions and Sensitive Visualization of Synapses. *Nature Biotechnology* **2016**, *34* (7), 774–780. https://doi.org/10.1038/nbt.3563.

(31)   Wehr, M. C.; Laage, R.; Bolz, U.; Fischer, T. M.; Grünewald, S.; Scheek, S.; Bach, A.; Nave, K.-A.; Rossner, M. J. Monitoring Regulated Protein-Protein Interactions Using Split TEV. *Nature Methods* **2006**, *3* (12), 985–993. https://doi.org/10.1038/nmeth967.

(32)   Zetsche, B.; Volz, S. E.; Zhang, F. A Split-Cas9 Architecture for Inducible Genome Editing and Transcription Modulation. *Nature Biotechnology* **2015**, *33*, 139–142. https://doi.org/10.1038/nbt.3149.

(33)   Zeitlinger, J.; Stark, A. Developmental Gene Regulation in the Era of Genomics. *Developmental Biology* **2010**, *339* (2), 230–239. https://doi.org/10.1016/j.ydbio.2009.12.039.

(34)   Wright, C. W.; Guo, Z.-F.; Liang, F.-S. Light Control of Cellular Processes by Using Photocaged Abscisic Acid. *ChemBioChem* **2015**, *16* (2), 254–261. https://doi.org/10.1002/cbic.201402576.

(35)   Schelkle, K. M.; Griesbaum, T.; Ollech, D.; Becht, S.; Buckup, T.; Hamburger, M.; Wombacher, R. Light-Induced Protein Dimerization by One- and Two-Photon Activation of Gibberellic Acid Derivatives in Living Cells. *Angewandte Chemie International Edition* **2015**, *54* (9), 2825–2829. https://doi.org/10.1002/anie.201409196.

(36)   Donato, L.; Mourot, A.; Davenport, C. M.; Herbivo, C.; Warther, D.; Léonard, J.; Bolze, F.; Nicoud, J.-F.; Kramer, R. H.; Goeldner, M.; et al. Water-Soluble, Donor-Acceptor Biphenyl Derivatives in the 2-(o-Nitrophenyl)Propyl Series: Highly Efficient Two-Photon Uncaging of the Neurotransmitter γ-Aminobutyric Acid at Λ=800 Nm. *Angewandte Chemie International Edition* **2012**, *51* (8), 1840–1843. https://doi.org/10.1002/anie.201106559.

(37)   Bochet, C. G. Photolabile Protecting Groups and Linkers. *J. Chem. Soc., Perkin Trans. 1* **2002**, *0* (2), 125–142. https://doi.org/10.1039/B009522M.

(38)   Sadovski, O.; Jaikaran, A. S. I.; Samanta, S.; Fabian, M. R.; Dowling, R. J. O.; Sonenberg, N.; Woolley, G. A. A Collection of Caged Compounds for Probing Roles of Local Translation in Neurobiology. *Bioorganic & Medicinal Chemistry* **2010**, *18* (22), 7746–7752. https://doi.org/10.1016/j.bmc.2010.04.005.

(39)   Umeda, N.; Ueno, T.; Pohlmeyer, C.; Nagano, T.; Inoue, T. A Photocleavable Rapamycin Conjugate for Spatiotemporal Control of Small GTPase Activity. *J Am Chem Soc* **2011**, *133* (1). https://doi.org/10.1021/ja108258d.

(40)   Karginov, A. V.; Zou, Y.; Shirvanyants, D.; Kota, P.; Dokholyan, N. V.; Young, D. D.; Hahn, K. M.; Deiters, A. Light Regulation of Protein Dimerization and Kinase Activity in Living Cells Using Photocaged Rapamycin and Engineered FKBP. *Journal of the American Chemical Society* **2011**, *133* (3), 420–423. https://doi.org/10.1021/ja109630v.

(41)   Karginov, A. V.; Ding, F.; Kota, P.; Dokholyan, N. V.; Hahn, K. M. Engineered Allosteric Activation of Kinases in Living Cells. *Nat Biotechnol* **2010**, *28* (7), 743–747. https://doi.org/10.1038/nbt.1639.

(42)   Brown, K. A.; Zou, Y.; Shirvanyants, D.; Zhang, J.; Samanta, S.; Mantravadi, P. K.; Dokholyan, N. V.; Deiters, A. Light-Cleavable Rapamycin Dimer as an Optical Trigger for Protein Dimerization.   *Chem.   Commun.*   **2015**,   *51*   (26),   5702–5705. https://doi.org/10.1039/C4CC09442E.

(43)   Downes, C. S.; Collins, A. R.; Johnson, R. T. DNA Damage in Synchronized HeLa Cells Irradiated with Ultraviolet. *Biophys J* **1979**, *25* (1), 129–150.

(44)   Decker, E. D.; Zhang, Y.; Cocklin, R. R.; Witzmann, F. A.; Wang, M. Proteomic Analysis of Differential Protein Expression Induced by Ultraviolet Light Radiation in HeLa Cells. *Proteomics* **2003**, *3* (10), 2019–2027. https://doi.org/10.1002/pmic.200300473.

(45)   Gug, S.; Bolze, F.; Specht, A.; Bourgogne, C.; Goeldner, M.; Nicoud, J.-F. Molecular Engineering of Photoremovable Protecting Groups for Two-Photon Uncaging. *Angewandte Chemie International Edition* **2008**, *47* (49), 9525–9529. https://doi.org/10.1002/anie.200803964.

(46)   Nakad, E. A.; Bolze, F.; Specht, A. O-Nitrobenzyl Photoremovable Groups with Fluorescence Uncaging Reporting Properties. *Org. Biomol. Chem.* **2018**, *16* (33), 6115–6122. https://doi.org/10.1039/C8OB01330F.

(47)   Thuaud, F.; Rohrbacher, F.; Zwicky, A.; Bode, J. W. Photoprotected Peptide α-Ketoacids and Hydroxylamines for Iterative and One-Pot KAHA Ligations: Synthesis of NEDD8. *Helvetica Chimica Acta* **2016**, *99* (11), 868–894. https://doi.org/10.1002/hlca.201600264.

(48)   Kamps, J. H.; Hoeks, T.; Kung, E.; Lens, J. P.; McCloskey, P. J.; Noordover, B. A. J.; Heuts, J. P. A. Activated Carbonates: Enabling the Synthesis of Differentiated Polycarbonate Resins via Melt Transcarbonation. *Polymer Chemistry* **2016**, *7* (33), 5294–5303. https://doi.org/10.1039/C6PY00925E.

(49)   Heinrich, M. R.; Klisa, H. S.; Mayr, H.; Steglich, W.; Zipse, H. Enhancing the Catalytic Activity of 4-(Dialkylamino)Pyridines by Conformational Fixation. *Angewandte Chemie International Edition* **2003**, *42* (39), 4826–4828. https://doi.org/10.1002/anie.200352289.

(50)   Luker, K. E.; Smith, M. C. P.; Luker, G. D.; Gammon, S. T.; Piwnica-Worms, H.; Piwnica-Worms, D. Kinetics of Regulated Protein–Protein Interactions Revealed with Firefly Luciferase Complementation Imaging in Cells and Living Animals. *PNAS* **2004**, *101* (33), 12288–12293. https://doi.org/10.1073/pnas.0404041101.

(51)   Seyfried, P.; Eiden, L.; Grebenovsky, N.; Mayer, G.; Heckel, A. Photo-Tethers for the (Multi-)Cyclic, Conformational Caging of Long Oligonucleotides. *Angewandte Chemie International Edition* **2017**, *56* (1), 359–363. https://doi.org/10.1002/anie.201610025.

(52)   Thankachan, A. P.; Abi, T. G.; Sindhu, K. S.; Anilkumar, G. Experimental and Mechanistic Exploration of Zn-Catalyzed Sonogashira–Type Cross-Coupling Reactions. *ChemistrySelect* **2016**, *1* (13), 3405–3412. https://doi.org/10.1002/slct.201600668.

(53)   Zhou, F.; Li, C.-J. The Barbier–Grignard-Type Arylation of Aldehydes Using Unactivated Aryl Iodides in Water. *Nature Communications* **2014**, *5*, 4254. https://doi.org/10.1038/ncomms5254.

(54)   Jacobsen, Ø.; Maekawa, H.; Ge, N.-H.; Görbitz, C. H.; Rongved, P.; Ottersen, O. P.; Amiry-Moghaddam, M.; Klaveness, J. Stapling of a 310-Helix with Click Chemistry. *J. Org. Chem.* **2011**, *76* (5), 1228–1238. https://doi.org/10.1021/jo101670a.

(55)   Agarwal, H. K.; Janicek, R.; Chi, S.-H.; Perry, J. W.; Niggli, E.; Ellis-Davies, G. C. R. Calcium Uncaging with Visible Light. *J. Am. Chem. Soc.* **2016**, *138* (11), 3687–3693. https://doi.org/10.1021/jacs.5b11606.

(56)   Tai, W.; Chen, Z.; Barve, A.; Peng, Z.; Cheng, K. A Novel Rapamycin-Polymer Conjugate Based on a New Poly(Ethylene Glycol) Multiblock Copolymer. *Pharmaceutical Research* **2014**, *31* (3), 706–719. https://doi.org/10.1007/s11095-013-1192-3.

(57)   Clède, S.; Lambert, F.; Sandt, C.; Kascakova, S.; Unger, M.; Harté, E.; Plamont, M.-A.; Saint-Fort, R.; Deniset-Besseau, A.; Gueroui, Z.; et al. Detection of an Estrogen Derivative in Two Breast Cancer Cell Lines Using a Single Core Multimodal Probe for Imaging (SCoMPI) Imaged by a Panel of Luminescent and Vibrational Techniques. *Analyst* **2013**, *138* (19), 5627–5638. https://doi.org/10.1039/C3AN00807J.

(58)   Hein, J. E.; Fokin, V. V. Copper-Catalyzed Azide–Alkyne Cycloaddition (CuAAC) and beyond: New Reactivity of Copper(i) Acetylides. *Chem Soc Rev* **2010**, *39* (4), 1302–1315. https://doi.org/10.1039/b904091a.

(59)   Boinapally, S.; Huang, B.; Abe, M.; Katan, C.; Noguchi, J.; Watanabe, S.; Kasai, H.; Xue, B.; Kobayashi, T. Caged Glutamates with π-Extended 1,2-Dihydronaphthalene Chromophore: Design, Synthesis, Two-Photon Absorption Property, and Photochemical Reactivity. *J. Org. Chem.* **2014**, *79* (17), 7822–7830. https://doi.org/10.1021/jo501425p.

(60)   Wang, Z. A.; Kurra, Y.; Wang, X.; Zeng, Y.; Lee, Y.-J.; Sharma, V.; Lin, H.; Dai, S. Y.; Liu, W. R. A Versatile Approach for Site-Specific Lysine Acylation in Proteins. *Angewandte Chemie International Edition* **2017**, *56* (6), 1643–1647. https://doi.org/10.1002/anie.201611415.

(61) Campos, M. S. T.; Fialho, S. L.; Pereira, B. G.; Yoshida, M. I.; Oliveira, M. A. Kinetics Studies of the Degradation of Sirolimus in Solid State and in Liquid Medium. *J Therm Anal Calorim* **2017**, *130* (3), 1653–1661. https://doi.org/10.1007/s10973-017-6580-1.

(62) Ocain, T. D.; Longhi, D.; Steffan, R. J.; Caccese, R. G.; Sehgal, S. N. A Nonimmunosuppressive Triene-Modified Rapamycin Analog Is a Potent Inhibitor of Peptidyl Prolyl Cis - Trans -Isomerase. *Biochemical and Biophysical Research Communications* **1993**, *192* (3), 1340–1346. https://doi.org/10.1006/bbrc.1993.1563.

(63) Ruan, B.; Pong, K.; Jow, F.; Bowlby, M.; Crozier, R. A.; Liu, D.; Liang, S.; Chen, Y.; Mercado, M. L.; Feng, X.; et al. Binding of Rapamycin Analogs to Calcium Channels and FKBP52 Contributes to Their Neuroprotective Activities. *Proceedings of the National Academy of Sciences* **2008**, *105* (1), 33–38. https://doi.org/10.1073/pnas.0710424105.

(64) Umeda, N.; Takahashi, H.; Kamiya, M.; Ueno, T.; Komatsu, T.; Terai, T.; Hanaoka, K.; Nagano, T.; Urano, Y. Boron Dipyrromethene As a Fluorescent Caging Group for Single-Photon Uncaging with Long-Wavelength Visible Light. *ACS Chem. Biol.* **2014**, *9* (10), 2242–2246. https://doi.org/10.1021/cb500525p.

(65) Goswami, P. P.; Syed, A.; Beck, C. L.; Albright, T. R.; Mahoney, K. M.; Unash, R.; Smith, E. A.; Winter, A. H. BODIPY-Derived Photoremovable Protecting Groups Unmasked with Green Light. *J. Am. Chem. Soc.* **2015**, *137* (11), 3783–3786. https://doi.org/10.1021/jacs.5b01297.

(66) Slanina, T.; Shrestha, P.; Palao, E.; Kand, D.; Peterson, J. A.; Dutton, A. S.; Rubinstein, N.; Weinstain, R.; Winter, A. H.; Klán, P. In Search of the Perfect Photocage: Structure–Reactivity Relationships in Meso-Methyl BODIPY Photoremovable Protecting Groups. *J. Am. Chem. Soc.* **2017**, *139* (42), 15168–15175. https://doi.org/10.1021/jacs.7b08532.

(67) Peterson, J. A.; Wijesooriya, C.; Gehrmann, E. J.; Mahoney, K. M.; Goswami, P. P.; Albright, T. R.; Syed, A.; Dutton, A. S.; Smith, E. A.; Winter, A. H. Family of BODIPY Photocages Cleaved by Single Photons of Visible/Near-Infrared Light. *J. Am. Chem. Soc.* **2018**, *140* (23), 7343–7346. https://doi.org/10.1021/jacs.8b04040.

(68) Koziar, J. C.; Cowan, D. O. Photochemical Heavy-Atom Effects. *Accounts of Chemical Research* **1978**, *11* (9), 334–341. https://doi.org/10.1021/ar50129a003.

(69) Yogo, T.; Urano, Y.; Ishitsuka, Y.; Maniwa, F.; Nagano, T. Highly Efficient and Photostable Photosensitizer Based on BODIPY Chromophore. *Journal of the American Chemical Society* **2005**, *127* (35), 12162–12163. https://doi.org/10.1021/ja0528533.

(70) Krumova, K.; Cosa, G. Bodipy Dyes with Tunable Redox Potentials and Functional Groups for Further Tethering: Preparation, Electrochemical, and Spectroscopic Characterization. *J. Am. Chem. Soc.* **2010**, *132* (49), 17560–17569. https://doi.org/10.1021/ja1075663.

(71)   Rey, Y. P.; Abradelo, D. G.; Santschi, N.; Strassert, C. A.; Gilmour, R. Quantitative Profiling of the Heavy-Atom Effect in BODIPY Dyes: Correlating Initial Rates, Atomic Numbers, and 1O2 Quantum Yields. *European Journal of Organic Chemistry* **2017**, *2017* (15), 2170–2178. https://doi.org/10.1002/ejoc.201601372.

(72)   Oleynik, P.; Ishihara, Y.; Cosa, G. Design and Synthesis of a BODIPY-α-Tocopherol Adduct for Use as an Off/On Fluorescent Antioxidant Indicator. *J. Am. Chem. Soc.* **2007**, *129* (7), 1842–1843. https://doi.org/10.1021/ja066789g.

(73)   Rubinstein, N.; Liu, P.; Miller, E. W.; Weinstain, R. Meso-Methylhydroxy BODIPY: A Scaffold for Photo-Labile Protecting Groups. *Chem. Commun.* **2015**, *51* (29), 6369–6372. https://doi.org/10.1039/C5CC00550G.

(74)   Cimen, D.; Kursun, T. T.; Caykara, T. Synthesis and Stability of BODIPY-Based Fluorescent Polymer Brushes at Different PHs. *Journal of Polymer Science Part A: Polymer Chemistry* **2014**, *52* (24), 3586–3596. https://doi.org/10.1002/pola.27426.

(75)   Sano, Y.; Watanabe, W.; Matsunaga, S. Chromophore-Assisted Laser Inactivation – towards a Spatiotemporal–Functional Analysis of Proteins, and the Ablation of Chromatin, Organelle and Cell Function. *J Cell Sci* **2014**, *127* (8), 1621–1629. https://doi.org/10.1242/jcs.144527.

(76)   Teh, C.; Chudakov, D. M.; Poon, K.-L.; Mamedov, I. Z.; Sek, J.-Y.; Shidlovsky, K.; Lukyanov, S.; Korzh, V. Optogenetic in Vivocell Manipulation in KillerRed-Expressing Zebrafish Transgenics. *BMC Developmental Biology* **2010**, *10* (1), 110. https://doi.org/10.1186/1471-213X-10-110.

(77)   Tour, O.; Meijer, R. M.; Zacharias, D. A.; Adams, S. R.; Tsien, R. Y. Genetically Targeted Chromophore-Assisted Light Inactivation. *Nature Biotechnology* **2003**, *21* (12), 1505–1508. https://doi.org/10.1038/nbt914.

(78)   Jay, D. G. Selective Destruction of Protein Function by Chromophore-Assisted Laser Inactivation. *Proc Natl Acad Sci U S A* **1988**, *85* (15), 5454–5458.

(79)   Tkatch, T.; Greotti, E.; Baranauskas, G.; Pendin, D.; Roy, S.; Nita, L. I.; Wettmarshausen, J.; Prigge, M.; Yizhar, O.; Shirihai, O. S.; et al. Optogenetic Control of Mitochondrial Metabolism and Ca2+ Signaling by Mitochondria-Targeted Opsins. *PNAS* **2017**, *114* (26), E5167–E5176. https://doi.org/10.1073/pnas.1703623114.

(80)   Kim, K.; Lakhanpal, G.; Lu, H. E.; Khan, M.; Suzuki, A.; Kato Hayashi, M.; Narayanan, R.; Luyben, T. T.; Matsuda, T.; Nagai, T.; et al. A Temporary Gating of Actin Remodeling during Synaptic Plasticity Consists of the Interplay between the Kinase and Structural Functions of CaMKII. *Neuron* **2015**, *87* (4), 813–826. https://doi.org/10.1016/j.neuron.2015.07.023.

(81)   Berlett, B. S.; Stadtman, E. R. Protein Oxidation in Aging, Disease, and Oxidative Stress. *J. Biol. Chem.* **1997**, *272* (33), 20313–20316. https://doi.org/10.1074/jbc.272.33.20313.

(82)   Baptista, M. S.; Cadet, J.; Mascio, P. D.; Ghogare, A. A.; Greer, A.; Hamblin, M. R.; Lorente, C.; Nunez, S. C.; Ribeiro, M. S.; Thomas, A. H.; et al. Type I and Type II Photosensitized Oxidation Reactions: Guidelines and Mechanistic Pathways. *Photochemistry and Photobiology* **2017**, *93* (4), 912–919. https://doi.org/10.1111/php.12716.

(83)   Rahmanzadeh, R.; Hüttmann, G.; Gerdes, J.; Scholzen, T. Chromophore-Assisted Light Inactivation of PKi-67 Leads to Inhibition of Ribosomal RNA Synthesis. *Cell Proliferation* **2007**, *40* (3), 422–430. https://doi.org/10.1111/j.1365-2184.2007.00433.x.

(84)   Galli, F. Amino Acid and Protein Modification by Oxygen and Nitrogen Species. *Amino Acids* **2012**, *42* (1), 1–4. https://doi.org/10.1007/s00726-010-0670-8.

(85)   Ethirajan, M.; Chen, Y.; Joshi, P.; K. Pandey, R. The Role of Porphyrin Chemistry in Tumor Imaging and Photodynamic Therapy. *Chemical Society Reviews* **2011**, *40* (1), 340–362. https://doi.org/10.1039/B915149B.

(86)   Hayyan, M.; Hashim, M. A.; AlNashef, I. M. Superoxide Ion: Generation and Chemical Implications. *Chem. Rev.* **2016**, *116* (5), 3029–3085. https://doi.org/10.1021/acs.chemrev.5b00407.

(87)   Kehrer, J. P.; Robertson, J. D.; Smith, C. V. 1.14 - Free Radicals and Reactive Oxygen Species. In *Comprehensive Toxicology (Second Edition)*; McQueen, C. A., Ed.; Elsevier: Oxford, 2010; pp 277–307. https://doi.org/10.1016/B978-0-08-046884-6.00114-7.

(88)   Surrey, T.; Elowitz, M. B.; Wolf, P.-E.; Yang, F.; Nédélec, F.; Shokat, K.; Leibler, S. Chromophore-Assisted Light Inactivation and Self-Organization of Microtubules and Motors. *Proc Natl Acad Sci U S A* **1998**, *95* (8), 4293–4298.

(89)   Rajfur, Z.; Roy, P.; Otey, C.; Romer, L.; Jacobson, K. Dissecting the Link between Stress Fibres and Focal Adhesions by CALI with EGFP Fusion Proteins. *Nature Cell Biology* **2002**, *4* (4), 286–293. https://doi.org/10.1038/ncb772.

(90)   Takemoto, K.; Matsuda, T.; Sakai, N.; Fu, D.; Noda, M.; Uchiyama, S.; Kotera, I.; Arai, Y.; Horiuchi, M.; Fukui, K.; et al. SuperNova, a Monomeric Photosensitizing Fluorescent Protein for Chromophore-Assisted Light Inactivation. *Scientific Reports* **2013**, *3*, 2629. https://doi.org/10.1038/srep02629.

(91)   Lin, J. Y.; Sann, S. B.; Zhou, K.; Nabavi, S.; Proulx, C. D.; Malinow, R.; Jin, Y.; Tsien, R. Y. Optogenetic Inhibition of Synaptic Release with Chromophore-Assisted Light Inactivation (CALI). *Neuron* **2013**, *79* (2), 241–253. https://doi.org/10.1016/j.neuron.2013.05.022.

(92)   Keppler, A.; Ellenberg, J. Chromophore-Assisted Laser Inactivation of α- and γ-Tubulin SNAP-Tag Fusion Proteins inside Living Cells. *ACS Chem. Biol.* **2009**, *4* (2), 127–138. https://doi.org/10.1021/cb800298u.

(93)   Takemoto, K.; Matsuda, T.; McDougall, M.; Klaubert, D. H.; Hasegawa, A.; Los, G. V.; Wood, K. V.; Miyawaki, A.; Nagai, T. Chromophore-Assisted Light Inactivation of HaloTag Fusion Proteins Labeled with Eosin in Living Cells. *ACS Chem. Biol.* **2011**, *6* (5), 401–406. https://doi.org/10.1021/cb100431e.

(94)   Lee, J.; Udugamasooriya, D. G.; Lim, H.-S.; Kodadek, T. Potent and Selective Photo-Inactivation of Proteins With Peptoid-Ruthenium Conjugates. *Nat Chem Biol* **2010**, *6* (4), 258–260. https://doi.org/10.1038/nchembio.333.

(95)   Amat-Guerri, F.; López-González, M. M. C.; Martínez-Utrilla, R.; Sastre, R. Singlet Oxygen Photogeneration by Ionized and Un-Ionized Derivatives of Rose Bengal and Eosin Y in Diluted Solutions. *Journal of Photochemistry and Photobiology A: Chemistry* **1990**, *53* (2), 199–210. https://doi.org/10.1016/1010-6030(90)87124-T.

(96)   *Comprehensive Cytopathology: An Expert Consult Title ; Online + Print*, 3. ed.; Bibbo, M., Wilbur, D., Eds.; Saunders, Elsevier: Philadelphia, Pa, 2008.

(97)   Jakubaszek, M.; Goud, B.; Ferrari, S.; Gasser, G. Mechanisms of Action of Ru(II) Polypyridyl Complexes in Living Cells upon Light Irradiation. *Chem. Commun.* **2018**, *54* (93), 13040–13059. https://doi.org/10.1039/C8CC05928D.

(98)   Lee, J.; Yu, P.; Xiao, X.; Kodadek, T. A General System for Evaluating the Efficiency of Chromophore-Assisted Light Inactivation (CALI) of Proteins Reveals Ru(II) Tris-Bipyridyl as an Unusually Efficient "Warhead." *Mol. BioSyst.* **2007**, *4* (1), 59–65. https://doi.org/10.1039/B712307H.

(99)   Respondek, T.; Garner, R. N.; Herroon, M. K.; Podgorski, I.; Turro, C.; Kodanko, J. J. Light Activation of a Cysteine Protease Inhibitor: Caging of a Peptidomimetic Nitrile with RuII(Bpy)2. *J Am Chem Soc* **2011**, *133* (43), 17164–17167. https://doi.org/10.1021/ja208084s.

(100) Pefkianakis, E. K.; Christodouleas, D.; Giokas, D. L.; Papadopoulos, K.; Vougioukalakis, G. C. A Family of RuII Photosensitizers with High Singlet Oxygen Quantum Yield: Synthesis, Characterization, and Evaluation. *European Journal of Inorganic Chemistry* **2013**, *2013* (26), 4628–4635. https://doi.org/10.1002/ejic.201300431.

(101) Golbaghi, G.; Haghdoost, M. M.; Yancu, D.; López de los Santos, Y.; Doucet, N.; Patten, S. A.; Sanderson, J. T.; Castonguay, A. Organoruthenium(II) Complexes Bearing an Aromatase Inhibitor: Synthesis, Characterization, in Vitro Biological Activity and in Vivo Toxicity in Zebrafish Embryos. *Organometallics* **2019**, *38* (3), 702–711. https://doi.org/10.1021/acs.organomet.8b00897.

(102) Thangavel, P.; Viswanath, B.; Kim, S. Recent Developments in the Nanostructured Materials Functionalized with Ruthenium Complexes for Targeted Drug Delivery to Tumors. *International Journal of Nanomedicine* **2017**, *Volume 12*, 2749–2758. https://doi.org/10.2147/IJN.S131304.

(103) McCafferty, D. G.; Bishop, B. M.; Wall, C. G.; Hughes, S. G.; Mecklenberg, S. L.; Meyer, T. J.; Erickson, B. W. Synthesis of Redox Derivatives of Lysine and Their Use in Solid-Phase Synthesis of a Light-Harvesting Peptide. *Tetrahedron* **1995**, *51* (4), 1093–1106. https://doi.org/10.1016/0040-4020(94)01018-U.

(104) Khan, S. I.; Beilstein, A. E.; Smith, G. D.; Sykora, M.; Grinstaff, M. W. Synthesis and Excited-State Properties of a Novel Ruthenium Nucleoside: 5-[Ru(Bpy)2(4-m-4'-Pa-Bpy)]2+-2'-Deoxyuridine. *Inorg. Chem.* **1999**, *38* (10), 2411–2415. https://doi.org/10.1021/ic990067r.

(105) McClure, D. S. Triplet-Singlet Transitions in Organic Molecules. Lifetime Measurements of the Triplet State. *J. Chem. Phys.* **1949**, *17* (10), 905–913. https://doi.org/10.1063/1.1747085.

(106) Yuster, P.; Weissman, S. I. Effects of Perturbations on Phosphorescence: Luminescence of Metal Organic Complexes. *J. Chem. Phys.* **1949**, *17* (12), 1182–1188. https://doi.org/10.1063/1.1747140.

(107) Zhang, C.; Zhao, J.; Cui, X.; Wu, X. Thiol-Activated Triplet–Triplet Annihilation Upconversion: Study of the Different Quenching Effect of Electron Acceptor on the Singlet and Triplet Excited States of Bodipy. *J. Org. Chem.* **2015**, *80* (11), 5674–5686. https://doi.org/10.1021/acs.joc.5b00557.

(108) De Filippis, B.; Linciano, P.; Ammazzalorso, A.; Di Giovanni, C.; Fantacuzzi, M.; Giampietro, L.; Laghezza, A.; Maccallini, C.; Tortorella, P.; Lavecchia, A.; et al. Structural Development Studies of PPARs Ligands Based on Tyrosine Scaffold. *European Journal of Medicinal Chemistry* **2015**, *89*, 817–825. https://doi.org/10.1016/j.ejmech.2014.10.083.

(109) Redmond, R. W.; Gamlin, J. N. A Compilation of Singlet Oxygen Yields from Biologically Relevant Molecules. *Photochemistry and Photobiology* **1999**, *70* (4), 391–475. https://doi.org/10.1111/j.1751-1097.1999.tb08240.x.

(110) Żamojć, K.; Zdrowowicz, M.; Rudnicki-Velasquez, P. B.; Krzymiński, K.; Zaborowski, B.; Niedziałkowski, P.; Jacewicz, D.; Chmurzyński, L. The Development of 1,3-Diphenylisobenzofuran as a Highly Selective Probe for the Detection and Quantitative Determination of Hydrogen Peroxide. *Free Radical Research* **2017**, *51* (1), 38–46. https://doi.org/10.1080/10715762.2016.1262541.

(111) Carloni, P.; Damiani, E.; Greci, L.; Stipa, P.; Tanfani, F.; Tartaglini, E.; Wozniak, M. On the Use of 1,3-Diphenylisobenzofuran (DPBF). Reactions with Carbon and Oxygen Centered

Radicals in Model and Natural Systems. *Res Chem Intermed* **1993**, *19* (5), 395–405. https://doi.org/10.1163/156856793X00181.

(112) Wang, P.; Gao, Z.; Yuan, M.; Zhu, J.; Wang, F. Mechanically Linked Poly[2]Rotaxanes Constructed from the Benzo-21-Crown-7/Secondary Ammonium Salt Recognition Motif. *Polym. Chem.* **2016**, *7* (22), 3664–3668. https://doi.org/10.1039/C6PY00494F.

(113) Turhanen, P. A. Synthesis of Triple-Bond-Containing 1-Hydroxy-1,1-Bisphosphonic Acid Derivatives To Be Used as Precursors in "Click" Chemistry: Two Examples. *J. Org. Chem.* **2014**, *79* (13), 6330–6335. https://doi.org/10.1021/jo500831r.

(114) Beharry, A. A.; Woolley, G. A. Azobenzene Photoswitches for Biomolecules. *Chem. Soc. Rev.* **2011**, *40* (8), 4422–4437. https://doi.org/10.1039/C1CS15023E.

(115) Szymański, W.; Beierle, J. M.; Kistemaker, H. A. V.; Velema, W. A.; Feringa, B. L. Reversible Photocontrol of Biological Systems by the Incorporation of Molecular Photoswitches. *Chemical Reviews* **2013**, *113* (8), 6114–6178. https://doi.org/10.1021/cr300179f.

(116) Russew, M.-M.; Hecht, S. Photoswitches: From Molecules to Materials. *Advanced Materials* **2010**, *22* (31), 3348–3360. https://doi.org/10.1002/adma.200904102.

(117) Bandara, H. M. D.; Burdette, S. C. Photoisomerization in Different Classes of Azobenzene. *Chem. Soc. Rev.* **2012**, *41* (5), 1809–1825. https://doi.org/10.1039/C1CS15179G.

(118) Hüll, K.; Morstein, J.; Trauner, D. In Vivo Photopharmacology. *Chem. Rev.* **2018**. https://doi.org/10.1021/acs.chemrev.8b00037.

(119) Wegner, H. A. Azobenzenes in a New Light—Switching In Vivo. *Angewandte Chemie International Edition* **2012**, *51* (20), 4787–4788. https://doi.org/10.1002/anie.201201336.

(120) Goulet-Hanssens, A.; Barrett, C. J. Photo-Control of Biological Systems with Azobenzene Polymers. *Journal of Polymer Science Part A: Polymer Chemistry* **2013**, *51* (14), 3058–3070. https://doi.org/10.1002/pola.26735.

(121) Ciccone, S.; Halpern, J. Catalysis of the Cis-Trans Isomerization of Azobenzene by Acids and Cupric Salts. *Can. J. Chem.* **1959**, *37* (11), 1903–1910. https://doi.org/10.1139/v59-278.

(122) Park, J. Y.; Male, U.; Huh, D. S. Reversible Change of Wettability in Poly(ε-Caprolactone/Azobenzene) Honeycomb-Patterned Films by UV and Visible Light Illumination. *Polym. Bull.* **2017**, *74* (10), 4235–4249. https://doi.org/10.1007/s00289-017-1948-8.

(123) Weston, C. E.; Richardson, R. D.; Haycock, P. R.; White, A. J. P.; Fuchter, M. J. Arylazopyrazoles: Azoheteroarene Photoswitches Offering Quantitative Isomerization and Long Thermal Half-Lives. *J. Am. Chem. Soc.* **2014**, *136* (34), 11878–11881. https://doi.org/10.1021/ja505444d.

(124) Stricker, L.; Böckmann, M.; Kirse, T. M.; Doltsinis, N. L.; Ravoo, B. J. Arylazopyrazole Photoswitches in Aqueous Solution: Substituent Effects, Photophysical Properties, and Host–Guest Chemistry. *Chemistry – A European Journal* **2018**, *24* (34), 8639–8647. https://doi.org/10.1002/chem.201800587.

(125) Stricker, L.; Fritz, E.-C.; Peterlechner, M.; Doltsinis, N. L.; Ravoo, B. J. Arylazopyrazoles as Light-Responsive Molecular Switches in Cyclodextrin-Based Supramolecular Systems. *J. Am. Chem. Soc.* **2016**, *138* (13), 4547–4554. https://doi.org/10.1021/jacs.6b00484.

(126) Bluemmel, P.; Setaro, A.; Maity, C.; Hecht, S.; Reich, S. Tuning the Interaction between Carbon Nanotubes and Dipole Switches: The Influence of the Change of the Nanotube–Spiropyran Distance. *J. Phys.: Condens. Matter* **2012**, *24* (39), 394005. https://doi.org/10.1088/0953-8984/24/39/394005.

(127) Andersson, J.; Li, S.; Lincoln, P.; Andréasson, J. Photoswitched DNA-Binding of a Photochromic Spiropyran. *Journal of the American Chemical Society* **2008**, *130* (36), 11836–11837. https://doi.org/10.1021/ja801968f.

(128) Lukyanov, B. S.; Lukyanova, M. B. Spiropyrans: Synthesis, Properties, and Application. (Review). *Chemistry of Heterocyclic Compounds* **2005**, *41* (3), 281–311. https://doi.org/10.1007/s10593-005-0148-x.

(129) Wojtyk, J. T. C.; Wasey, A.; Xiao, N.-N.; Kazmaier, P. M.; Hoz, S.; Yu, C.; Lemieux, R. P.; Buncel, E. Elucidating the Mechanisms of Acidochromic Spiropyran-Merocyanine Interconversion. *The Journal of Physical Chemistry A* **2007**, *111* (13), 2511–2516. https://doi.org/10.1021/jp068575r.

(130) Bose, M.; Groff, D.; Xie, J.; Brustad, E.; Schultz, P. G. The Incorporation of a Photoisomerizable Amino Acid into Proteins in E. Coli. *J. Am. Chem. Soc.* **2006**, *128* (2), 388–389. https://doi.org/10.1021/ja055467u.

(131) Banghart, M.; Borges, K.; Isacoff, E.; Trauner, D.; Kramer, R. H. Light-Activated Ion Channels for Remote Control of Neuronal Firing. *Nature Neuroscience* **2004**, *7* (12), 1381–1386. https://doi.org/10.1038/nn1356.

(132) Schoenberger, M.; Damijonaitis, A.; Zhang, Z.; Nagel, D.; Trauner, D. Development of a New Photochromic Ion Channel Blocker via Azologization of Fomocaine. *ACS Chem. Neurosci.* **2014**, *5* (7), 514–518. https://doi.org/10.1021/cn500070w.

(133) Kumita, J. R.; Smart, O. S.; Woolley, G. A. Photo-Control of Helix Content in a Short Peptide. *PNAS* **2000**, *97* (8), 3803–3808. https://doi.org/10.1073/pnas.97.8.3803.

(134) Burns, D. C.; Zhang, F.; Woolley, G. A. Synthesis of 3,3′-Bis(Sulfonato)-4,4′-Bis(Chloroacetamido)Azobenzene and Cysteine Cross-Linking for Photo-Control of Protein Conformation and Activity. *Nature Protocols* **2007**, *2* (2), 251–258. https://doi.org/10.1038/nprot.2007.21.

(135) Devi, S.; Saraswat, M.; Grewal, S.; Venkataramani, S. Evaluation of Substituent Effect in Z-Isomer Stability of Arylazo-1H-3,5-Dimethylpyrazoles: Interplay of Steric, Electronic Effects and Hydrogen Bonding. *J. Org. Chem.* **2018**, *83* (8), 4307–4322. https://doi.org/10.1021/acs.joc.7b02604.

(136) Putri, R. M.; Zulfikri, H.; Fredy, J. W.; Juan, A.; Tananchayakul, P.; Cornelissen, J. J. L. M.; Koay, M. S. T.; Filippi, C.; Katsonis, N. Photoprogramming Allostery in Human Serum Albumin. *Bioconjugate Chem.* **2018**, *29* (7), 2215–2224. https://doi.org/10.1021/acs.bioconjchem.8b00184.

(137) Moldenhauer, D.; Fuenzalida Werner, J. P.; Strassert, C. A.; Gröhn, F. Light-Responsive Size of Self-Assembled Spiropyran–Lysozyme Nanoparticles with Enzymatic Function. *Biomacromolecules* **2019**, *20* (2), 979–991. https://doi.org/10.1021/acs.biomac.8b01605.

(138) Amat-Guerri, F.; Liras, M.; Carrascoso, M. L.; Sastre, R. Methacrylate-Tethered Analogs of the Laser Dye PM567—Synthesis, Copolymerization with Methyl Methacrylate and Photostability of the Copolymers¶. *phot* **2003**, *77* (6), 577–584. https://doi.org/10.1562/0031-8655(2003)077<0577:MAOTLD>2.0.CO;2.

(139) Prabakaran, S.; Lippens, G.; Steen, H.; Gunawardena, J. Post-Translational Modification: Nature's Escape from Genetic Imprisonment and the Basis for Dynamic Information Encoding: Information Encoding by Post-Translational Modification. *Wiley Interdisciplinary Reviews: Systems Biology and Medicine* **2012**, *4* (6), 565–583. https://doi.org/10.1002/wsbm.1185.

(140) Pickart, C. M.; Eddins, M. J. Ubiquitin: Structures, Functions, Mechanisms. *Biochimica et Biophysica Acta (BBA) - Molecular Cell Research* **2004**, *1695* (1), 55–72. https://doi.org/10.1016/j.bbamcr.2004.09.019.

(141) Böck, A.; Forchhammer, K.; Heider, J.; Leinfelder, W.; Sawers, G.; Veprek, B.; Zinoni, F. Selenocysteine: The 21st Amino Acid. *Molecular Microbiology* **1991**, *5* (3), 515–520. https://doi.org/10.1111/j.1365-2958.1991.tb00722.x.

(142) Atkins, J. F.; Gesteland, R. The 22nd Amino Acid. *Science* **2002**, *296* (5572), 1409–1410. https://doi.org/10.1126/science.1073339.

(143) Wang, L.; Brock, A.; Herberich, B.; Schultz, P. G. Expanding the Genetic Code of Escherichia Coli. *Science* **2001**, *292* (5516), 498–500. https://doi.org/10.1126/science.1060077.

(144) Liu, C. C.; Schultz, P. G. Adding New Chemistries to the Genetic Code. *Annu. Rev. Biochem.* **2010**, *79* (1), 413–444. https://doi.org/10.1146/annurev.biochem.052308.105824.

(145) Davis, L.; Chin, J. W. Designer Proteins: Applications of Genetic Code Expansion in Cell Biology. *Nature Reviews Molecular Cell Biology* **2012**, *13* (3), 168–182. https://doi.org/10.1038/nrm3286.

(146) Wan, W.; Tharp, J. M.; Liu, W. R. Pyrrolysyl-TRNA Synthetase: An Ordinary Enzyme but an Outstanding Genetic Code Expansion Tool. *Biochim Biophys Acta* **2014**, *1844* (6), 1059–1070. https://doi.org/10.1016/j.bbapap.2014.03.002.

(147) Dumas, A.; Lercher, L.; Spicer, C. D.; Davis, B. G. Designing Logical Codon Reassignment – Expanding the Chemistry in Biology. *Chem. Sci.* **2014**, *6* (1), 50–69. https://doi.org/10.1039/C4SC01534G.

(148) Italia, J. S.; Latour, C.; Wrobel, C. J. J.; Chatterjee, A. Resurrecting the Bacterial Tyrosyl-TRNA Synthetase/TRNA Pair for Expanding the Genetic Code of Both E. Coli and Eukaryotes. *Cell Chemical Biology* **2018**, *25* (10), 1304-1312.e5. https://doi.org/10.1016/j.chembiol.2018.07.002.

(149) Bahamonde, M. I.; Taura, J.; Paoletta, S.; Gakh, A. A.; Chakraborty, S.; Hernando, J.; Fernández-Dueñas, V.; Jacobson, K. A.; Gorostiza, P.; Ciruela, F. Photomodulation of G Protein-Coupled Adenosine Receptors by a Novel Light-Switchable Ligand. *Bioconjugate Chem.* **2014**, *25* (10), 1847–1854. https://doi.org/10.1021/bc5003373.

(150) Agnetta, L.; Kauk, M.; Canizal, M. C. A.; Messerer, R.; Holzgrabe, U.; Hoffmann, C.; Decker, M. A Photoswitchable Dualsteric Ligand Controlling Receptor Efficacy. *Angewandte Chemie International Edition* **2017**, *56* (25), 7282–7287. https://doi.org/10.1002/anie.201701524.

(151) Barber, D. M.; Liu, S.-A.; Gottschling, K.; Sumser, M.; Hollmann, M.; Trauner, D. Optical Control of AMPA Receptors Using a Photoswitchable Quinoxaline-2,3-Dione Antagonist. *Chem. Sci.* **2016**, *8* (1), 611–615. https://doi.org/10.1039/C6SC01621A.

(152) Blanco, B.; Palasis, K. A.; Adwal, A.; Callen, D. F.; Abell, A. D. Azobenzene-Containing Photoswitchable Proteasome Inhibitors with Selective Activity and Cellular Toxicity. *Bioorganic & Medicinal Chemistry* **2017**, *25* (19), 5050–5054. https://doi.org/10.1016/j.bmc.2017.06.011.

(153) Reis, S. A.; Ghosh, B.; Hendricks, J. A.; Szantai-Kis, D. M.; Törk, L.; Ross, K. N.; Lamb, J.; Read-Button, W.; Zheng, B.; Wang, H.; et al. Light-Controlled Modulation of Gene Expression by Chemical Optoepigenetic Probes. *Nature Chemical Biology* **2016**, *12* (5), 317–323. https://doi.org/10.1038/nchembio.2042.

(154) Hohsaka, T.; Sato, K.; Sisido, M.; Takai, K.; Yokoyama, S. Site-Specific Incorporation of Photofunctional Nonnatural Amino Acids into a Polypeptide through in Vitro Protein Biosynthesis. *FEBS Letters* **1994**, *344* (2–3), 171–174. https://doi.org/10.1016/0014-5793(94)00381-5.

(155) Muranaka, N.; Hohsaka, T.; Sisido, M. Photoswitching of Peroxidase Activity by Position-Specific Incorporation of a Photoisomerizable Non-Natural Amino Acid into Horseradish Peroxidase. *FEBS Letters* **2002**, *510* (1–2), 10–12. https://doi.org/10.1016/S0014-5793(01)03211-2.

(156) Nakayama, K.; Endo, M.; Majima, T. Photochemical Regulation of the Activity of an Endonuclease BamHI Using an Azobenzene Moiety Incorporated Site-Selectively into the Dimer Interface. *Chem. Commun.* **2004**, *0* (21), 2386–2387. https://doi.org/10.1039/B409844G.

(157) Hoppmann, C.; Lacey, V. K.; Louie, G. V.; Wei, J.; Noel, J. P.; Wang, L. Genetically Encoding Photoswitchable Click Amino Acids in Escherichia Coli and Mammalian Cells. *Angew Chem Int Ed Engl* **2014**, *53* (15), 3932–3936. https://doi.org/10.1002/anie.201400001.

(158) John, A. A.; Ramil, C. P.; Tian, Y.; Cheng, G.; Lin, Q. Synthesis and Site-Specific Incorporation of Red-Shifted Azobenzene Amino Acids into Proteins. *Org. Lett.* **2015**, *17* (24), 6258–6261. https://doi.org/10.1021/acs.orglett.5b03268.

(159) Luo, J.; Samanta, S.; Convertino, M.; Dokholyan, N. V.; Deiters, A. Reversible and Tunable Photoswitching of Protein Function through Genetic Encoding of Azobenzene Amino Acids in Mammalian Cells. *ChemBioChem* **2018**, *19* (20), 2178–2185. https://doi.org/10.1002/cbic.201800226.

(160) Bléger, D.; Schwarz, J.; Brouwer, A. M.; Hecht, S. O-Fluoroazobenzenes as Readily Synthesized Photoswitches Offering Nearly Quantitative Two-Way Isomerization with Visible Light. *J. Am. Chem. Soc.* **2012**, *134* (51), 20597–20600. https://doi.org/10.1021/ja310323y.

(161) Luo, J.; Torres-Kolbus, J.; Liu, J.; Deiters, A. Genetic Encoding of Photocaged Tyrosines with Improved Light-Activation Properties for the Optical Control of Protease Function. *ChemBioChem* **2017**, *18* (14), 1442–1447. https://doi.org/10.1002/cbic.201700147.

(162) Santoro, S. W.; Wang, L.; Herberich, B.; King, D. S.; Schultz, P. G. An Efficient System for the Evolution of Aminoacyl-TRNA Synthetase Specificity. *Nature Biotechnology* **2002**, *20* (10), 1044–1048. https://doi.org/10.1038/nbt742.

(163) Melançon, C. E.; Schultz, P. G. One Plasmid Selection System for the Rapid Evolution of Aminoacyl-TRNA Synthetases. *Bioorganic & Medicinal Chemistry Letters* **2009**, *19* (14), 3845–3847. https://doi.org/10.1016/j.bmcl.2009.04.007.

(164) Noro, S.; Kondo, M.; Ishii, T.; Kitagawa, S.; Matsuzaka, H. Syntheses and Crystal Structures of Iron Co-Ordination Polymers with 4,4′-Bipyridine (4,4′-Bpy) and 4,4′-Azopyridine (Azpy). Two-Dimensional Networks Supported by Hydrogen Bonding, {[Fe(Azpy)(NCS)2(MeOH)2]·azpy}n and {[Fe(4,4′-Bpy)(NCS)2(H2O)2]·4,4′-Bpy}n. *J. Chem. Soc., Dalton Trans.* **1999**, *0* (10), 1569–1574. https://doi.org/10.1039/A809523J.

(165) Zeleňák, V.; Vargová, Z.; Almáši, M.; Zeleňáková, A.; Kuchár, J. Layer-Pillared Zinc(II) Metal–Organic Framework Built from 4,4′-Azo(Bis)Pyridine and 1,4-BDC. *Microporous and Mesoporous Materials* **2010**, *129* (3), 354–359. https://doi.org/10.1016/j.micromeso.2009.11.002.

(166) Chatterjee, S.; Sanyal, A.; Hung, C.-H.; Goswami, S. Isolation of a Manganese Complex of a Tridentate Azo-Aromatic Ligand from an Unusual Mn2(CO)10 Promoted Simultaneous Reductive Azo Cleavage and Aromatic Ring Amination Reactions. *Zeitschrift für anorganische und allgemeine Chemie* **2007**, *633* (11–12), 1775–1777. https://doi.org/10.1002/zaac.200700254.

(167) Waldie, K. M.; Ramakrishnan, S.; Kim, S.-K.; Maclaren, J. K.; Chidsey, C. E. D.; Waymouth, R. M. Multielectron Transfer at Cobalt: Influence of the Phenylazopyridine Ligand. *J. Am. Chem. Soc.* **2017**, *139* (12), 4540–4550. https://doi.org/10.1021/jacs.7b01047.

(168) Green, E. D.; Zimmerman, R. C.; Ghurabi, W. H.; Colohan, D. P. Phenazopyridine Hydrochloride Toxicity: A Cause of Drug-Induced Methemoglobinemia. *Annals of Emergency Medicine* **1979**, *8* (10), 426–431. https://doi.org/10.1016/S0361-1124(79)80409-8.

(169) Song, Y.; Litao, S. Method for Preparing Chiral Gamma-Amino Acid and Derivatives Thereof. CN102249833 (A), November 23, 2011.

(170) Yamamoto, Y.; Yamamoto, H. Cataltytic Asymmetric Hetero Diels-Alder Reaction of a Heteroaromatic C-Nitroso Dienophile: A Novel Method for Synthesis of Chiral Non-Racemic Amino Alcohols. WO2005068457 (A1), July 28, 2005.

(171) Lin, W.; Gupta, A.; Kim, K. H.; Mendel, D.; Miller, M. J. Syntheses of New Spirocarbocyclic Nucleoside Analogs Using Iminonitroso Diels−Alder Reactions. *Org. Lett.* **2009**, *11* (2), 449–452. https://doi.org/10.1021/ol802553g.

(172) Novak, I. Computational Thermochemistry of C-Nitroso Compounds. *Structural Chemistry* **2016**, *27* (5), 1395–1401. https://doi.org/10.1007/s11224-016-0759-0.

(173) Hooper, N. M. Families of Zinc Metalloproteases. *FEBS Letters* **1994**, *354* (1), 1–6. https://doi.org/10.1016/0014-5793(94)01079-X.

(174) Miyoshi, S.-I.; Shinoda, S. Bacterial Metalloprotease as the Toxic Factor in Infection. *Journal of Toxicology: Toxin Reviews* **1997**, *16* (4), 177–194. https://doi.org/10.3109/15569549709016455.

(175) Ebewele, R. O. *Polymer Science and Technology*; CRC Press: Boca Raton, 2000.

(176) Jochum, F. D.; Theato, P. Temperature- and Light-Responsive Smart Polymer Materials. *Chem. Soc. Rev.* **2013**, *42* (17), 7468–7483. https://doi.org/10.1039/C2CS35191A.

(177) Yager, K. G.; Barrett, C. J. Azobenzene Polymers for Photonic Applications. In *Smart Light-Responsive Materials*; John Wiley & Sons, Ltd, 2008; pp 1–46. https://doi.org/10.1002/9780470439098.ch1.

(178) Williams, J. L. R.; Daly, R. C. Photochemical Probes in Polymers. *Progress in Polymer Science* **1977**, *5* (2), 61–93. https://doi.org/10.1016/0079-6700(77)90005-3.

(179) Eisenbach, C. D. Effect of Polymer Matrix on the Cis-Trans Isomerization of Azobenzene Residues in Bulk Polymers. *Die Makromolekulare Chemie* **1978**, *179* (10), 2489–2506. https://doi.org/10.1002/macp.1978.021791014.

(180) Zupan, M.; Ashby, M. F.; Fleck, N. A. Actuator Classification and Selection—The Development of a Database. *Advanced Engineering Materials* **2002**, *4* (12), 933–940. https://doi.org/10.1002/adem.200290009.

(181) Wie, J. J.; Lee, K. M.; Smith, M. L.; Vaia, R. A.; White, T. J. Torsional Mechanical Responses in Azobenzene Functionalized Liquid Crystalline Polymer Networks. *Soft Matter* **2013**, *9* (39), 9303–9310. https://doi.org/10.1039/C3SM51574E.

(182) Maeda, S.; Hara, Y.; Yoshida, R.; Hashimoto, S. Active Polymer Gel Actuators. *International Journal of Molecular Sciences* **2010**, *11* (1), 52–66. https://doi.org/10.3390/ijms11010052.

(183) Yu, Y.; Ikeda, T. Soft Actuators Based on Liquid-Crystalline Elastomers. *Angewandte Chemie International Edition* **2006**, *45* (33), 5416–5418. https://doi.org/10.1002/anie.200601760.

(184) Wie, J. J.; Chatterjee, S.; Wang, D. H.; Tan, L.-S.; Ravi Shankar, M.; White, T. J. Azobenzene-Functionalized Polyimides as Wireless Actuators. *Polymer* **2014**, *55* (23), 5915–5923. https://doi.org/10.1016/j.polymer.2014.06.084.

(185) Maeda, S.; Hara, Y.; Sakai, T.; Yoshida, R.; Hashimoto, S. Self-Walking Gel. *Advanced Materials* **2007**, *19* (21), 3480–3484. https://doi.org/10.1002/adma.200700625.

(186) Cheng, F.; Yin, R.; Zhang, Y.; Yen, C.-C.; Yu, Y. Fully Plastic Microrobots Which Manipulate Objects Using Only Visible Light. *Soft Matter* **2010**, *6* (15), 3447–3449. https://doi.org/10.1039/C0SM00012D.

(187) Yamada, M.; Kondo, M.; Mamiya, J.; Yu, Y.; Kinoshita, M.; Barrett, C. J.; Ikeda, T. Photomobile Polymer Materials: Towards Light-Driven Plastic Motors. *Angewandte Chemie International Edition* **2008**, *47* (27), 4986–4988. https://doi.org/10.1002/anie.200800760.

(188) Cviklinski, J.; Tajbakhsh, A. R.; Terentjev, E. M. UV Isomerisation in Nematic Elastomers as a Route to Photo-Mechanical Transducer. *The European Physical Journal E* **2002**, *9* (S1), 427–434. https://doi.org/10.1140/epje/i2002-10095-y.

(189) Otsuki, S.; Nishimura, S.; Takabatake, H.; Nakajima, K.; Takasu, Y.; Yagura, T.; Sakai, Y.; Hattori, A.; Kakeya, H. Chemical Tagging of a Drug Target Using 5-Sulfonyl Tetrazole. *Bioorganic & Medicinal Chemistry Letters* **2013**, *23* (6), 1608–1611. https://doi.org/10.1016/j.bmcl.2013.01.092.

(190) Li, M.-H.; Keller, P.; Li, B.; Wang, X.; Brunet, M. Light-Driven Side-On Nematic Elastomer Actuators. *Advanced Materials* **2003**, *15* (7–8), 569–572. https://doi.org/10.1002/adma.200304552.

(191) Finkelmann, H.; Nishikawa, E.; Pereira, G. G.; Warner, M. A New Opto-Mechanical Effect in Solids. *Phys. Rev. Lett.* **2001**, *87* (1), 015501. https://doi.org/10.1103/PhysRevLett.87.015501.

(192) Liu, D.; Broer, D. J. Liquid Crystal Polymer Networks: Preparation, Properties, and Applications of Films with Patterned Molecular Alignment. *Langmuir* **2014**, *30* (45), 13499–13509. https://doi.org/10.1021/la500454d.

(193) Yu, Y.; Nakano, M.; Ikeda, T. Photomechanics: Directed Bending of a Polymer Film by Light. *Nature* **2003**, *425* (6954), 145. https://doi.org/10.1038/425145a.

(194) Yamaguchi, T.; Asanuma, M.; Nakanishi, S.; Saito, Y.; Okazaki, M.; Dodo, K.; Sodeoka, M. Turn-ON Fluorescent Affinity Labeling Using a Small Bifunctional O-Nitrobenzoxadiazole Unit. *Chem. Sci.* **2014**, *5* (3), 1021–1029. https://doi.org/10.1039/C3SC52704B.